Annual Report (2021)

No.33
The NOVARTIS Foundation (Japan) for the Promotion of Science

2021年度

財団年報 第33号

公益財団法人 ノバルティス科学振興財団

Introduction

Kuniaki Takata, Ph.D.
Chairman of the Board of Trustees

This annual report contains the research reports of the recipients of the 33rd Novartis Research Grants. (research from April 2020 to March 2021: 37 research grants and 2 research meetings).

The COVID-19, which began in 2019, has been raging around the world, and as of this writing in early October, a cumulative total of more than 200 million people worldwide have been infected and nearly 5 million people have died, a situation that has shaken the very foundations of the world. The cumulative number of infected people in Japan has also exceeded 1.7 million, and more than 17,000 people have died. During this time, the days are far from what they were before the COVID-19 outbreak. Universities and research institutes have also been greatly affected, with campus closures and restrictions on their use. It has become difficult to hold regular conferences and we have been forced to hold webinars, cancel or postpone them. In the absence of physical human exchanges with overseas countries, researchers continue to communicate with each other on PC screens. In spite of all these difficulties, the spirit of the researchers is again evident in the way they continue to promote their research.

The NOVARTIS Foundation (Japan) for the Promotion of Science was established in 1987 with a donation of one billion yen from Ciba-Geigy AG (now Novartis AG) of Switzerland. The purpose of the Foundation is clearly stated in its Articles of Incorporation: “To contribute to the improvement of the health and welfare of the people through the promotion of science by encouraging creative research in the natural sciences. In addition, a document titled “Prospectus for the Establishment of the Foundation,” written in the year of the foundation’s establishment, states that the foundation “hopes to contribute to the welfare of mankind by promoting and subsidizing creative research in the natural sciences, which will be the axis of science in the coming 21st century. It also states that it will “provide financial support for research and opportunities for cross-border exchange. Based on this policy, our Foundation has provided financial assistance to a total of 1,854 projects over the past 34 years, amounting to approximately 2.14 billion yen. Now, in the midst of the turmoil caused by the COVID-19 disaster, our Foundation would like to return to this starting point and continue to support outstanding research.

This annual report summarizes the results of the excellent research supported by our Foundation. It is an impressive accomplishment that was achieved within the limited time frame of one year. The list of past recipients of the Foundation’s support includes many of the leading researchers in their fields, including Professor Tasuku Honjo, who was awarded the Nobel Prize in Physiology or Medicine. I hope that the recipients of these grants will use the results of their research as an opportunity to make even greater strides. I would like to express my deepest gratitude to the members of the selection committee who selected these outstanding research projects and to Novartis Pharma K.K, the donor of the donation, as well as all those who support the activities of our Foundation.

はじめに

代表理事　高田　邦昭

本年報には、第33回ノバルティス科学振興財団の研究助成金を受けられた方々の研究報告（2020年4月～2021年3月の研究：研究奨励金37件、研究集会2件）を収録しました。

2019年に始まった新型コロナウイルス（COVID-19）は世界中で猛威をふるい、この原稿を執筆している10月初旬では世界中で累計2億人以上の人が感染し、500万人近い人が亡くなるという、世界の根幹を揺るがす事態になっています。日本の累計感染者数も170万人を超え、17,000人を超える方が亡くなりました。この間、COVID-19感染が起こる前とはかけ離れた日々が続いています。大学や研究機関においても、キャンパスの閉鎖や使用の制限など大きな影響を受けてきました。通常の学会開催は困難となり、web 開催や中止・延期を余儀なくされました。海外との物理的な人的な交流ができない中で、研究者は PC 画面上で交流を続けています。このような様々な困難な状況にもかかわらず、研究者が変わりなく、あるいは一層研究を推進している様には、あらためて研究者魂を見る思いです。

本財団は1987年に、スイス、チバガイギー社（現ノバルティスファーマ社）からの10億円のご寄附をもとに設立されたものです。財団の目的は、定款に「自然科学における創造的な研究の奨励等を行うことにより、学術の振興を図り、もって国民の健康と福祉の向上に寄与する」と明記されています。また、財団設立の年に記された「財団設立の趣意」と題する文書には、財団が「来るべき21世紀の科学の軸となる自然科学の創造的研究の振興助成をはかり、以って人類の福祉に寄与できれば」とあり、「研究のための資金的な助成、並びに国境を越えた交流の場の提供」がうたわれています。このような方針のもと、34年間で総計1,854件、金額にして約21.4億円の助成を行ってきました。コロナ禍で混迷する現在こそ、財団は改めてこの原点に立ち返り、今後とも優れた研究を支援して行きたいと考えています。

この年報には本財団が支援した優れた研究の成果をまとめています。一年間という限られた時間の中で達成した立派な業績です。過去に当財団の助成を受けた方々のリストには、ノーベル医学・生理学賞を受賞した本庶佑博士をはじめ各分野をリードする研究者の名前が多数見られます。今回助成を受けた方々が、この研究成果を契機としてさらに大きく飛躍されることを祈念いたします。これらの優れた研究を選考していただいた選考委員の皆様や、出捐者であるノバルティスファーマ社をはじめとして財団の活動を支えて下さっている関係者の皆様に深く感謝いたします。

Ⅱ.

Reports from the Recipients of Novartis Research Grants

Systematic understanding of oxidative stress responses in cancer

Nobuaki Takahashi
takahashi@sbchem.kyoto-u.ac.jp
Kyoto University

Summary Abstract

Accumulating evidence has shown that cancer cells exhibit higher levels of toxic H_2O_2 compared with normal cells by through metabolic and signaling aberrations. However, there are no reports visualizing H_2O_2 levels at a single cell level in *in vivo* tumor. Here we developed a H_2O_2 probe that can be specifically accumulated in tumor cells and found that H_2O_2 levels are very heterogeneous within tumors. Interestingly, tumor cells with high levels of H_2O_2 exhibit some unique characteristics that are not observed in tumor cells with low levels of H_2O_2. These findings could provide the basis of oxidative stress beyond the role in the just toxic effects on cells in tumor biology and could be exploited for targeted cancer therapies.
Key Words : Cancer, Oxidative Stress

Introduction

Cancer cells are exposed to numerous cellular insults during tumorigenesis, leading to the generation of toxic reactive oxygen species, including H_2O_2, through metabolic and signaling aberrations[1-3]. Therefore, oxidative-stress defense programs are critically involved in tumor progression and therapy resistance and represent an “Achilles heel” or vulnerability of tumor cells. Despite the tight association between H_2O_2 and cancer cell survival, there are no reports visualizing H_2O_2 levels at a single cell level in *in vivo* tumor.

Results

In this study, we developed a H_2O_2 probe that can be specifically accumulated in tumor cells through the conjugation of a H_2O_2 probe with the antibody that binds to proteins specifically expressed in tumor cells. One important feature of this probe is that the probe allows us to know the tumor cells that experienced H_2O_2 exposure because the H_2O_2 probe irreversibly reacts with H_2O_2; therefore, this probe enables us to detect the tumor cells that experienced H_2O_2 exposure even after the isolation of tumor tissues, which is distinct from the currently used technologies for the detection of oxidative stress.

Using this innovative probe, we injected the probe to stomach cancer-carrying mice through *i.v.*, and 12-hour after administration of the probe, we dissected the tumor, prepared tumor sectioning, and assessed fluorescent signals of the probe using confocal microscopy. Notably, we uncovered that H_2O_2 levels are very heterogeneous within tumors. Heterogeneity of H_2O_2 levels was also detected in *in vivo* tumors directly observed using a two-photon microscopy without the dissection of tumors in live animals. In addition to stomach cancer, we also assess intratumor H_2O_2 levels in mice carrying breast cancer by using the H_2O_2 probe and confirmed heterogeneity of H_2O_2 levels within breast tumor cells.

While substantial evidence has shown that tumor cells overall exhibit high levels of H_2O_2 compared with normal tissue cells, our study is the first to demonstrate the heterogeneity of H_2O_2 levels at a single cell level within tumors.

We next investigated the mechanism by which specific tumor cells exhibit high levels of H_2O_2. We examined the correlation between the localization of tumor cells with high H_2O_2 levels and that of stroma cells as well as immune cells and found that tumor cells exhibit high levels of H_2O_2 are surrounded by a type of immune cells, suggesting that the enhanced H_2O_2 levels are at least in part due to the exposure of H_2O_2 or cytokines/chemokines that are produced from the immune cells. Indeed, depletion of the immune cells suppressed H_2O_2 levels in tumor cells in mice. While we found that the immune cells are critical for H_2O_2 generation within tumor, the mechanisms underlying H_2O_2 generation in the immune cells or the tumor cells are still unknown.

In order to characterize tumor cells with high levels of H_2O_2, we separated tumor cells with high levels of H_2O_2 and the cells with low levels of H_2O_2 through cell sorter and performed RNA-seq analyses. We found that tumor cells with high levels of H_2O_2 exhibit some unique characteristics, including changes in expression of extracellular matrix proteins and cytoskeletal proteins as well as signaling proteins. We show that the signaling protein is activated by H_2O_2 and regulate the expression levels of extracellular matrix proteins and cytoskeletal proteins. We are currently looking at the phenotypic changes in tumor cells with high levels of H_2O_2 in terms of tumorigenesis and metastasis.

These findings could provide the basis of oxidative stress beyond the role in the just toxic effects on cells in tumor biology and could be exploited for targeted cancer therapies.

Discussion & Conclusion

Our study reveals that tumor cells exhibit heterogeneous H_2O_2 levels within *in vivo* tumor and that the tumor cells with high levels of H_2O_2 show unique characteristics, which is distinct from tumor cells with low levels of H_2O_2.

There is now compelling evidence that oxidative-stress defense programs represent a vulnerability of tumor cells. Therefore, the development of therapies targeting oxidative-stress defense represents an attractive strategy to enhance the sensitivity of tumor cells to existing therapies. Our finding on the unique characteristics of tumor cells with high levels of H_2O_2 could be exploited for targeted cancer therapies that enhance the sensitivity of tumor cells to existing therapies.

References

1. Gorrini, C., Harris, I. S. & Mak, T. W. Modulation of oxidative stress as an anticancer strategy. *Nat. Rev. Drug Discov.* **12,** 931−947 (2013).
2. Takahashi, N. et al. Cancer Cells Co-opt the Neuronal Redox-Sensing Channel TRPA1 to Promote Oxidative-Stress Tolerance. *Cancer Cell* **33,** 985−1003 (2018).
3. Takahashi, N. et al. 3D Culture Models with CRISPR Screens Reveal Hyperactive NRF2 as a Prerequisite for Spheroid Formation via Regulation of Proliferation and Ferroptosis. *Mol. Cell* **80,** 828−844 (2020).

一般の皆様へ

かつて数十年もの間、ビタミンCやビタミンEをはじめとした抗酸化サプリメントは癌抑制効果があると信じられてきましたが、近年行われた大規模疫学調査により、抗酸化サプリメントの摂取はむしろ癌の発生率を上昇させることが明らかにされました。

癌細胞は、正常細胞が本来存在している場所を逸脱して生存・増殖することが知られていますが、近年の研究により、このようなニッチの逸脱は高いレベルの酸化ストレスにさらされることになり、抗酸化を含めた強固な酸化ストレス防御機能の獲得が癌化および癌の成長過程において必須であることが分かってきました。実際、放射線治療や一部の癌化学療法は酸化ストレスを亢進させることで癌細胞を攻撃することが知られており、癌細胞は正常細胞に比べて酸化ストレスに対して脆弱であるといえます。

このように、癌と酸化ストレスとの間には密接な関連性がありますが、腫瘍内1細胞レベルで酸化ストレスを可視化した例はこれまで存在しませんでした。

本研究では腫瘍内酸化ストレスの度合いを1細胞レベルで検出することに成功し、また強い酸化ストレスにされされているがん細胞は他とは違う特徴的な性質を有することが明らかになりました。

本研究による成果は、酸化ストレス防御を標的とした新しいがん治療薬の開発につながることが期待できます。

Elucidation of the molecular mechanism of phytochrome-regulated alternative promoter selection

Tomonao Matsushita
mat@gr.bot.kyoto-u.ac.jp
Kyoto University

Summary Abstract

It is widely believed that the plant photoreceptor phytochrome regulates the transcription of light-responsive genes by modulating the activity of several transcription factors. However, we recently found that phytochrome controls not only transcription, but also alternative promoter selection, to allow plants to adapt to light environment in Arabidopsis. In order to reveal the molecular mechanism of phytochrome-regulated alternative promoter selection, we conducted a forward genetic screen and isolated several mutants with aberrant patterns of light-responsive changes in alternative promoter selection. Moreover, we also performed cis element analysis and found that some non-G-box motif was enriched in the promoters of the target genes.

Key Words : phytochrome, alternative promoter, gene expression, light signaling, Arabidopsis

Introduction

Our group has found that phytochrome controls not only transcription, but also alternative splicing, at a similar genomic scale to mediate light responses in *Arabidopsis* (Shikata et al., ***PNAS*** 2014). Recently, we found that phytochromes also directly induce the selection of alternative promoters in more than 2,000 genes in *Arabidopsis*, resulting in light-dependent production of protein isoforms with different subcellular localizations (Ushijima et al. ***Cell*** 2017). Moreover, we physiologically demonstrated that this mechanism indeed allows plants to respond metabolically to fluctuating light conditions for more efficient photosynthesis (Ushijima et al. ***Cell*** 2017). The purpose of this research is to reveal the molecular mechanism of how phytochrome regulates alternative promoter selection without affecting total amount of mRNA in each target gene.

Results

One of the target genes, *GLYCERATE KINASE* (*GLYK*), encodes proteins that show light-dependent changes in subcellular localization through phytochrome-mediated alternative promoter selection. The T-DNA insertion null mutant of *GLYK* was transformed with the *GLYK* genomic DNA fragment fused with GFP at its 3' end. Then, after confirming that the mutant phenotype was complemented and that the GFP subcellular localization pattern exhibited light-dependent alterations, this transgenic line was mutated with EMS and a forward genetic screen was conducted in the M2 population. As a result, we isolated several mutants with aberrant patterns of light-responsive changes in GFP subcellular localization. Then, we identified candidate responsible genes for each mutant after high-

throughput mapping by re-sequencing of genomic DNA using next-generation sequencer. Further analysis of these candidate responsible genes will lead to the identification of trans-acting factors required for phytochrome-regulated alternative promoter selection.

Phytochrome is known to regulate transcription by inhibiting basic helix-loop-helix transcription factors PIFs, which specifically bind to some DNA sequence motif called G-box both in vitro and in vivo. Consistently, G-box motif is shown to be overrepresented in the promoters of those genes whose mRNA levels are regulated by phytochrome. Therefore, cis element analysis was performed to see whether G-box motif is also enriched in the promoters of the genes under the control of phytochrome-mediated alternative promoter selection. If the G-box motif is enriched in these target genes, it is most likely that PIFs are also involved in phytochrome-mediated alternative promoter selection. However, surprisingly, certain cis element other than G-box motif was identified in the analysis, suggesting that trans-acting factors other than PIFs are involved in this regulatory mechanism. As some particular trans-acting factor can be inferred from the nucleotide sequence of the identified cis element, the following experiments are now being conducted. 1) 5' RACE experiments will be performed to see if red light-responsive changes in alternative promoter patterns of some target genes are impaired in the mutants deficient in the trans-acting factor. 2) Direct interaction between the inferred trans-acting factor and DNA fragments containing the non-G-box motif will be examined in the AlphaScreen system. 3) ChIP analysis will be performed to examine whether the trans-acting factor bind to the non-G-box motifs in vivo. 4) the non-G-box element will be mutated in the context of genomic DNA fragments and these mutated constructs will be introduced into wild-type plants to see if the non-G-box motif is required for the binding of the trans-acting faoctor and for phytochrome-mediated alternative promoter control.

Discussion & Conclusion

enerality and biological impact of alternative promoter control has been somewhat underestimated. However, given that alternative promoter changes of a similar scale could be potentially induced, not only by phytochrome but also by any kinds of signals, alternative promoters are likely to represent another universal aspect of gene expression regulation in eukaryotes. Therefore, the mechanistic elucidation of phytochrome-regulated alternative promoter selection would not only reveal novel mechanism of light signaling in plants, but also force us to reconsider the general concept of gene expression regulation in eukaryotes.

References

Shikata H, Hanada K, Ushijima T, Nakashima M, Suzuki Y, and Matsushita T. Phytochrome controls alternative splicing to mediate light responses in *Arabidopsis*.
Proc Natl Acad Sci USA 111: 18781-18786 (2014)

Ushijima T, Hanada K, Gotoh E, Yamori W, Kodama Y, Tanaka H, Kusano M, Fukushima A, Tokizawa M, Yamamoto YY, Tada Y, Suzuki Y, and Matsushita T. Light controls protein localization through phytochrome-mediated alternative promoter selection.
Cell 171: 1316-1325 (2017)

一般の皆様へ

同規模の転写開始点変化は、フィトクロムシグナルに限らず、ありとあらゆるシグナル・事象に伴って、真核生物において共通の分子機構で起こるものである可能性が高いと考えられるため、その分子機構が本研究により解明されれば、1 つの遺伝子から機能の異なる複数のタンパク質を生み出す普遍的な仕組みを世界に先駆けて明らかにすることとなり、生物学上の大きな進歩となることは間違いないと考えられます。

Carbon beam induced upregulation of cardiac gap junction proteins and prevention of sympathetic nerve sprouting in hypercholesterolemic rabbits, leading to reduction of arrhythmia vulnerability

Mari Amino
mariam@is.icc.u-tokai.ac.jp
Department of Cardiology, Tokai University, Isehara, Japan
National Institute for Quantum and Radiological Science and Technology, Inage, Japan

Summary Abstract

Development of noninvasive cardiac radioablation therapy for ventricular tachycardia attracts scientific attention as a novel antiarrhythmic method. To examine the effects of targeted heavy ion irradiation (THIR) in hypercholesterolemia (HC) rabbits with gap junctional remodeling and nerve sprouting. A single 15-Gy THIR was applied to eight rabbits with high fat/cholesterol chow (HC+THIR group). Another eight rabbits who did not undergo THIR were used as controls (HC group). THIR reduced the vulnerability to atrial/ventricular tachyarrhythmias by improving cardiac conductivity. This mechanism may be attributed to the upregulation of gap junction proteins and, partly, to sympathetic growth suppression.
Key Words : radioablation therapy, late potential, growth-associated protein 43, tyrosine hydroxylase, sympathetic denervation

Introduction

A single 25-Gy X-ray application for patients with refractory ventricular tachycardia (VT) using stereotactic body radiation therapy markedly reduced the VT burden.[1,2] A recent review on previous animal experiments reported that the antiarrhythmic effect occurred with not only depend on the replacement with fibrosis but other radiobiological changes.[3] We previously reported that targeted heavy ion irradiation (THIR; 15 Gy) to rabbit or canine hearts with myocardial infarction (MI) caused connexin 43 (Cx43) upregulation in the ventricles 2 weeks thereafter.[4,5,6] However, changes in atrial vulnerability, Cx40 levels, or relation with the autonomic nervous system remain unknown. We aimed to examine the effects of THIR on in-vivo electrophysiology and vulnerability to atrial/ventricular tachyarrhythmias in aged hypercholesterolemia (HC) rabbits, which were reported as the model of electrical- and neural-remodeling involved in proarrhythmic propensities,[7,8] with gap junctional remodeling and nerve sprouting.

Results

Animals and Serum cholesterol levels

Sixteen 3-year-old rabbits were fed with high fat/cholesterol chow for 14 weeks. A single 15-Gy THIR was applied to eight rabbits (HC+THIR group) using a heavy ion medical accelerator. Eight rabbits who did not undergo THIR were used as controls (HC group). In the serum cholesterol levels, there was no significant difference in the cholesterol levels between the two groups.

Signal averaged ECGs (SAECGs), UCGs, and 12-lead ECGs

The atrial late potentials (LPs) were characterized by RMS20ms increase in HC+THIR rabbits compared to HC rabbits (n=4 for both groups, $p<0.01$). There was no significant difference in the fPd between the two groups. The ventricular LP in HC+THIR rabbits was characterized by a decrease in the fQRSd and LAS40μV, and an increase in the RMS40ms, compared to the HC group ($p<0.05$). Regarding the hemodynamic status estimated by UCG, LV systolic and diastolic functions were not different between the two groups. There were no differences in the ECG parameters, including RR and PQ intervals and QRS durations. The QT interval was prolonged moderately in the HC+THIR group, but QTc was unaffected.

In-vivo electrophysiology

Sustained AT (≥60 s) was elicited spontaneously in the absence of ACh infusion in 2/4 HC rabbits. In the remaining 2, sustained AT or AF was induced by programmed stimulation or burst stimulation in the presence of ACh infusion. AT or AF lasting for ≥60 sec was terminated by direct current shock application. The incidence rate and average duration of the HC group were 100% and 62.4 s, respectively, while in the HC+THIR group, the mean duration was very short (5.1 s). AT was induced only in one rabbit by burst stimulation in the presence of ACh infusion. Atrial arrhythmia inducibility and durations were higher and longer in the HC+THIR group than in the HC group ($p<0.05$).

Non-sustained or sustained VT was elicited spontaneously in two HC rabbits in the absence of NE infusion. Additionally, VF was induced by programmed LV stimulation or LSS in the remaining two rabbits. Sustained VT or VF lasting for ≥30 s was terminated by direct current shock application. The incidence rate and average duration in the HC group were 100% and >30 s, respectively, while in the HC+THIR group, the mean duration was very short (2.2 s). NST was induced in one rabbit by LSS in the presence of NE infusion. Ventricular arrhythmia inducibility and durations were higher and longer in the HC+THIR group than in the HC group ($p<0.05$).

Cardiac gap junction proteins

The cardiac gap junction protein expressions were examined in four rabbits of the HC and HC+THIR groups, respectively. Cx40 formed clusters of brown punctate immunoreacted domains at the periphery of atrial myocytes in abutment with neighbor myocytes. The total cell area proportion occupied by Cx40 signals indicated that THIR resulted in an increase by 59.7% and 43.6% in the RA and LA, respectively, compared with the HC group ($p<0.01$). Cx43 formed clusters of brown punctate immunoreacted domains at the periphery of ventricular myocytes; some of them were confined to intercalated disks running perpendicular to the longitudinal axis, and others were on the lateral cell abutment. THIR resulted in an increase by 48.1% and 40.3% in the RV and LV, respectively, compared with the HC group (all $p<0.01$).

Sympathetic nerve sprouting

Immunolabeling of the growth-associated protein 43 and tyrosine hydroxylase (GAP43- and TH-) positive nerves in four rabbits of the HC and HC+THIR groups, respectively. In the tissue sections of HC+THIR rabbits, the GAP43 positive nerves were less prominent. The proportion of total area indicated that the irradiation resulted in a reduction of the GAP43-immunopositive nerve density by 56.0%, 62.8%, 68.3%, and 70.6% in the RA, LA, RV and LV, respectively, compared with the HC group ($p<0.01$). Contrarily, the TH-immunopositive

domains were less abundant in the HC+THIR rabbits. The irradiation resulted in a reduction of the TH-immunopositive nerve density by 29.1%, 61.0%, 66.1%, and 64.8% in the RA, LA, RV and LV, respectively, compared with the HC group ($p<0.01$).

Discussion & Conclusion

We examined the electrophysiological effects of radiation in terms of gap junction and neural remodeling using HC rabbits. In hypotheses that the arrhythmogenic substrate of HC rabbits could be ameliorated by 15-Gy THIR. We found that SAECG showed better atrial/ventricular LPs, electrophysiological study resulted in lower inducibility of atrial/ventricular arrhythmias, and immunohistochemistry indicated higher Cx40 and Cx43 expressions and lower sympathetic nerve densities.

THIR may improve cardiac conductivity in favor of reduction of vulnerability to AT/AF and VT/VF. Moreover, we showed that this antiarrhythmic effect is attributed to gap junction protein upregulation and, in part, to sympathetic denervation.

To our knowledge, our work was the first to identify the suppression of atrial/ventricular arrhythmias with the underlying mechanism of suppression efficacy by using heavy ion beams. Next steps will be required to investigate these proposed mechanisms in humans, using LP assessment by SAECGs and functional evaluation for sympathetic/vagus nerves by nuclear medicine study or heart rate variability analysis.

References

1. Cuculich PS, Schill MR, Kashani R, et al. Noninvasive cardiac radiation for ablation of ventricular tachycardia. N Engl J Med 2017;377:2325-2336.
2. Robinson CG, Samson PP, Moore KMS, et al. Phase I/II trial of electrophysiology-guided noninvasive cardiac radioablation for ventricular tachycardia. Circulation 2019;139:313-321.
3. van der Ree MH, Blanck O, Limpens J, et al. Cardiac radioablation-A systematic review. Heart Rhythm 2020;17:1381-1392.
4. Amino M, Yoshioka K, Tanabe T, et al. Heavy ion radiation up-regulates Cx43 and ameliorates arrhythmogenic substrates in hearts after myocardial infarction. Cardiovasc Res 2006;72:412-421.
5. Amino M, Yoshioka K, Fujibayashi D, et al. Year-long upregulation of connexin43 in rabbit hearts by heavy ion irradiation. Am J Physiol Heart Circ Physiol 2010;98:1014-1021.
6. Amino M, Yoshioka K, Furusawa Y, et al. Inducibility of ventricular arrhythmia 1 year following treatment with heavy ion irradiation in dogs with myocardial infarction. Pacing Clin Electrophysiol 2017;40:379-390.
7. Lee KT, Hsieh CC, Tsai WC, et al. Characteristics of atrial substrates for atrial tachyarrhythmias induced in aged and hypercholesterolemic rabbits. Pacing Clin Electrophysiol 2012;35:544-552.
8. Liu YB, Wu CC, Lu LS, et al. Sympathetic nerve sprouting, electrical remodeling, and increased vulnerability to ventricular fibrillation in hypercholesterolemic rabbits. Circ Res 2003;92:1145-1152.

一般の皆様へ

体幹部定位放射線治療などの放射線技術を“難治性致死性心室不整脈（心室頻拍）”に対して応用する発想により、「X 線を体外から照射して不整脈基質をわずか15分で焼灼する」という新しい治療法が2017年にワシントン大学にて実施され、その成果は瞬く間に循環器領域のトップニュースとなりました（NEJM，2017）。東海大学でも2019年11月、日本人で第一例目となる臨床治療を実施し（jRCTs032190041）、その効果につき論文報告を行っています（Heart Rhythm Case Reports 2021）。しかし、なぜ放射線が不整脈治療に有効であるかの理由は十分に明らかではありません。我々は世界に先駆けて1997年より「重粒子線（放射線のなかで健常組織への影響が少ない）を利用し、心臓に及ぼす電気生理学的効果について」基礎研究を実施してきました（放射線医学総合研究所との共同研究）。放射線による抗不整脈作用の主要なメカニズムは、「ギャップ結合蛋白コネキシン43（Cx43）の亢進による興奮伝導の回復」に起因することを発見しましたが、今回の研究ではさらに、「心表面の過剰な交感神経増生の除神経作用を呈する」可能性を明らかにしました。現在は重粒子以外に X 線についても基礎実験を施行し、放射性臓器障害を最小限にとどめつつ、最大効果を得るためのデータを蓄積中です。

Evolution of membrane morphogenesis in Asgard archaea

Yosuke Senju
yosuke.senju@okayama-u.ac.jp
Okayama University

Summary Abstract

Metagenomic analysis of the novel superphylum Asgard archaea, considered phylogenetically close to eukaryotes, has revealed genes that encode protein homologs to those in eukaryotes that regulate morphological changes of cell membrane. We propose solving this novel protein's three-dimensional structure and elucidate its function by combining biophysical and cell biology methods. We will show that membrane properties such as membrane curvature and tension are essential, evolutionarily conserved features that can trigger downstream signals and maintain cell morphogenesis and biological functions. Additionally, we will elucidate further insights into the origin of life in prokaryotes by identifying any conserved eukaryotic-like cellular functions.

Key Words : membrane, cytoskeleton, evolution, liposome, structural biology

Introduction

Cells are defined as the basic units of life. A key function is to compartment cellular contents from their surroundings by cell membranes. Besides this, morphological changes in cell membranes are essential for biological functions, including cell motility, cell division, and differentiation, which are pathologically relevant in cancer cell invasion and metastasis (1).

How are signal transduction mechanisms that originate with changes in cell membrane morphology acquired and selected during evolution? Recently, metagenomic reconstruction of Asgard archaea superphylum, considered closely related to eukaryotes, revealed several genes that encode proteins with eukaryotic homologs (2-4). These include proteins that control changes in cell membrane morphology, actin cytoskeleton, and regulators of actin polymerization, previously thought to be absent in prokaryotes.

Results

This study elucidates how the ability to facilitate and respond to morphological changes in the cell membrane of a representative biological system has evolved by solving the crystal structures of novel proteins found in Asgard archaea

Based on metagenomic analysis results, novel proteins with eukaryotic homologs have been identified in Asgard archaea, suggesting that a mechanism for altering membrane morphogenesis is conserved in both prokaryotes and eukaryotes. Asgard archaea may have obtained this mechanism by phagocytosis of a bacterium with these novel proteins and actin polymerization.

We are pursuing the following six lines of research.

Line 1

We have identified novel proteins in Asgard archaea using bioinformatics and created a

molecular evolutionary phylogenetic tree (unpublished). Genes have been synthesized for these and are for further studies.

Line 2

We have successfully expressed and purified the novel proteins. Crystals were obtained by screening for protein crystallization conditions (Fig.1), and a 2.9-Å resolution diffraction dataset has been collected at Spring-8 (unpublished). We are now introducing selenomethionine to determine its phase.

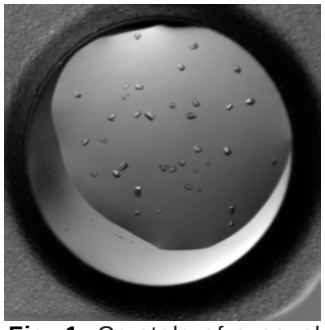

Fig. 1. Crystals of a novel protein from Asgard archaea (unpublished)

Line 3

X-ray crystal structure analysis will be attempted using the beamlines of the Spring-8 synchrotron radiation facilities. From the XRD data, we will elucidate the three-dimensional structures of the proteins and compare them with those of known eukaryotic proteins to predict intracellular functions. Additionally, we will examine the conservation of amino acid residues necessary for phospholipid binding.

Line 4

Purified archaeal proteins will be labeled with fluorescent dyes and applied to giant unilamellar vesicles (GUVs) to clarify whether they can deform cell membranes.

Line 5

We will express Asgard archaeal proteins fused with green fluorescent protein (GFP) in cells to determine whether they can deform cell membranes and identify their subcellular localizations.

Line 6

Correlative light and electron microscopy (CLEM) has allowed us to identify protein functions and elucidate morphology, and high spatial resolution fluorescence and electron microscopy have revealed structure information (unpublished).

The laboratory in which the applicant is currently working has published remarkable accomplishments in protein purification, crystallization, and structural analyses and has accumulated significant knowledge and resources. Additionally, the applicant has sufficient experience in biophysics using GUVs, and cell biological experiments, and has already prepared samples and equipment (5-6).

From the above series of studies, we will further elucidate whether the regulation of Asgard archaeal proteins in cell morphogenesis are essential for maintaining biological systems preserved throughout evolution.

Discussion & Conclusion

Functional analysis of proteins that regulate cell membrane morphogenesis has been performed mainly in eukaryotic endocytosis and filopodia formation studies. Recent metagenomic studies have shown that Asgard archaea contain protein homologs involved in cell membrane morphogenesis, including cytoskeletal actin and regulators of actin polymerization. A professor in the applicant's laboratory has succeeded in X-ray crystallographic analysis of complex actin and Asgard profilin, an actin-binding protein regulating actin polymerization (7). Interestingly, Asgard profilins bind to actin and regulate

actin polymerization. Thus, actin polymerization is essential for life and is conserved throughout the evolutionary process from prokaryotes to eukaryotes. According to this background, we are convinced that we can find in Asgard archaea how the functions of proteins in cell morphogenesis have been conserved and developed during evolution.

References

1: Senju Y, Kalimeri M, Koskela EV, Somerharju P, Zhao H, Vattulainen I, Lappalainen P. Mechanistic principles underlying regulation of the actin cytoskeleton by phosphoinositides. Proc Natl Acad Sci U S A. 2017 Oct 24;114(43):E8977-E8986.
2: Spang A, Saw JH, Jørgensen SL, Zaremba-Niedzwiedzka K, Martijn J, Lind AE, van Eijk R, Schleper C, Guy L, Ettema TJG. Complex archaea that bridge the gap between prokaryotes and eukaryotes. Nature. 2015 May 14;521(7551):173-179.
3: Zaremba-Niedzwiedzka K, Caceres EF, Saw JH, Bäckström D, Juzokaite L, Vancaester E, Seitz KW, Anantharaman K, Starnawski P, Kjeldsen KU, Stott MB, Nunoura T, Banfield JF, Schramm A, Baker BJ, Spang A, Ettema TJ. Asgard archaea illuminate the origin of eukaryotic cellular complexity. Nature. 2017 Jan 19;541(7637):353-358.
4: Imachi H, Nobu MK, Nakahara N, Morono Y, Ogawara M, Takaki Y, Takano Y, Uematsu K, Ikuta T, Ito M, Matsui Y, Miyazaki M, Murata K, Saito Y, Sakai S, Song C, Tasumi E, Yamanaka Y, Yamaguchi T, Kamagata Y, Tamaki H, Takai K. Isolation of an archaeon at the prokaryote-eukaryote interface. Nature. 2020 Jan;577(7791):519-525.
5: Senju Y, Zhao H. Fluorescence Assays to Study Membrane Penetration of Proteins. Methods Mol Biol. 2021;2251:215-223.
6: Senju Y, Lappalainen P, Zhao H. Liposome Co-sedimentation and Co-flotation Assays to Study Lipid-Protein Interactions. Methods Mol Biol. 2021;2251:195-204.
7: Akıl C, Robinson RC. Genomes of Asgard archaea encode profilins that regulate actin. Nature. 2018 Oct;562(7727):439-443.

一般の皆様へ

真核生物に近い系統と考えられている、アスガルドと命名された新規古細菌のメタゲノム解析から、細胞膜の形態変化を制御するタンパク質をコードする遺伝子が発見された。本研究課題では、アスガルド古細菌の新規タンパク質の立体構造を解き、生物物理的手法と細胞生物学を組み合わせてその機能を解明する。さらに、原核生物にも保存された真核生物と同様な細胞機能を見いだしていくことで、生命の起源の一端を解明していく。

Quantum beam analysis on structure formation of glucuronosyltransferase catalyzing drug metabolism

Eiichi Mizohata
mizohata@chem.eng.osaka-u.ac.jp
Osaka University

Summary Abstract

Glucuronosyltransferase plays a central role in detoxification of toxic insoluble compounds by promoting their removal from the body. This study elucidated the interaction of glucuronosyltransferase and GroEL by observing the binary complex structure using cryo-EM single particle analysis at 3 Å resolution.
Key Words : glucuronosyltransferase; cryo-electron microscopy; protein folding

Introduction

Glucuronosyltransferase catalyzes the transfer of UDP-glucuronic acid as a donor substrate to insoluble compounds such as bilirubin as an acceptor substrate. Determination of the structure of the enzyme and understanding of its structure-function relationship are important for future medical applications. However, structural studies of the enzyme have been difficult because it has never been functionally isolated and purified using any recombinant protein expression system. I attempted to purify a mutant enzyme by expressing it in *E. coli*, and succeeded in isolating a complex of the enzyme and *E. coli* GroEL. The aim of this study is to elucidate the mechanism of interaction of glucuronosyltransferase and GroEL by observing the complex structure using cryo-EM.

Results

1.2 million particle images from 2,951 micrographs were processed using the RELION software package and successfully classified into 38 reference-free 2-dimensional classes with multiple particle orientations with flexible substrate densities clearly visible in the side view in the ring cavity. Scrutiny of these particle images resulted in an asymmetric reconstruction of two GroEL complexes containing bound glucuronosyltransferase substrates with a resolution of 3 Å, evaluated at the criterion of FSC = 0.143. The modeling of the individual subunits was done by rigid fitting of the atomic coordinates of the previously solved structure to the EM density map using COOT and final refinement of the map model in Phenix. As in previous studies, the density of glucuronosyltransferase is found to be localized in the hydrophobic substrate-binding helix of the apical domain covering the folding chamber cavity. It is conspicuously in contact with 2-3 subunits on one side of the ring.

The capture of non-native substrates by GroEL is performed by exposed hydrophobic residues covering the open cavity of the seven-membered ring. Such non-specific binding of non-native polypeptides is required for the folding protein of GroEL, which requires contact with the apical domains of the 2-3 contiguous subunits that make up the ring. Previous

studies of non-native polypeptide binding have revealed several structures detailing the essential residues of GroEL binding, various low-energy substrate binding conformational states, hydrophobic and amphiphilic binding motifs, and the initial substrate binding state. In complete agreement with these studies, the substrate density was formed around two or three subunits in the ring. Based on previous biochemical and structural studies, this study developed a new approach to 3-dimensional classification using a signal mask to confirm this observation. A tailor-made masking strategy was created, combining a cylindrical volume containing a cavity region and specific residues of the apical domains of the three subunits (two adjacent and one laterally opposite in the ring).

Focused classification (masked 3D classification) on the refined map allowed to separate the particle images from the 3 Å consensus map based on compositional and conformational heterogeneities contained only in the masked regions, while maintaining the orientation of the original particle images.

The analysis resulted in a three-dimensional volume that accounted for 96% of the total particle image. This volume clearly showed the density formed between the two tip domains, while very little was present in the tip domain across the cavity.

Unexpectedly, this method resulted in a classified volume (about 2% of the particle image) where the density in the cavity was not visible. When the mask was removed and the rings with and without substrate were compared, it was found that the ring cavity had expanded by about 4 Å as the substrate bound to it. Closer examination of the results revealed that the conformation of the seven-membered ring was different at the domain level of the subunit.

Discussion & Conclusion

This study demonstrated that there are 2-3 consecutive subunit binding motifs in the seven-membered ring, which explains the unexpected ring cavity extension in the ring occupied by glucuronosyltransferase.

Furthermore, the study analyzed the single-ring (sR) and double-ring (dR) complexes and were able to model the continuous movement of subunits upon substrate binding.

These data provide an *in vivo* and near-atomic resolution snapshot of the early stages of the GroEL-glucuronosyltransferase folding reaction cycle.

This allows us to reveal the recognition and occupancy of non-native substrates by GroEL, as well as to annotate intramolecular changes.

一般の皆様へ

生物の細胞はタンパク質でできています。タンパク質は様々な構造をもち、この構造はGroELと呼ばれる巨大なタンパク質の中で形づくられます。今回、体内の有毒物質や薬剤の解毒を担うタンパク質であるグルクロン酸転移酵素が、GroELにどのように認識されて構造が形成されるのか、そのメカニズムの一端を、クライオ電子顕微鏡を用いて可視化することができました。将来、がんや黄疸などの病気の治療につながる成果です。

Novel molecular basis of intracellular cholesterol trafficking in endothelial cells

Masashi Maekawa
masashim@m.ehime-u.ac.jp
Proteo-Science Center, Ehime University

Summary Abstract

Endothelial cells lining along inside vessels receive a variety of stimulations leading to their patho-physiological responses (*e.g.* angiogenesis). Cholesterol is an essential lipid for cell survival including endothelial functions. In this study, we identified a ubiquitin ligase complex, cullin-3 (CUL3)/BTBP/substrates, that requires both localization of cholesterol at the plasma membrane and angiogenesis.

Key Words : Endothelial cells, Cholesterol, Cullin-3, BTBP

Introduction

Cholesterol is an essential component of cell membranes. Although angiogenesis of human umbilical endothelial cells (HUVECs) requires plasmalemmal cholesterol (ref 1), the molecular mechanisms for the determination of proper cholesterol localization at the plasma membrane remain unclear. Cullin-3 (CUL3) is a scaffold protein for a RING-type ubiquitin E3 ligase complex. The CUL3-mediated ubiquitination requires recruitment of target substrates through its recognition by substrate recognition receptors, BTBPs. Human genome encodes 183 BTBPs and the repertoire of BTBP exerts various cellular functions of the CUL3 system. We have found that CUL3 knockdown inhibited angiogenesis as well as dissociation of D4H, a cholesterol biosensor (ref 2), from the plasma membrane. These data suggest the existence of BTBP/substrates axes that are essential for cholesterol trafficking to the plasma membrane leading to proper angiogenesis. This study aims to identify the BTBPs and ubiquitinated substrates in the CUL3 system, which regulate cholesterol trafficking in endothelial cells.

Results

Identification of a BTBP that is responsible for plasmalemmal localization of cholesterol in HUVEC

To identify BTBPs that regulate cholesterol localization at the plasma membrane, we silenced 183 BTBP genes in HUVECs using BTBP siRNA library (ref 3). The mCherry-tagged D4H cholesterol biosensor was expressed in HUVECs. As a readout, we observed D4H localization at the plasma membrane by an A1R confocal microscopy. As a result, we identified one BTBP (BTBP-X), by which knockdown caused the disappearance of D4H from the plasma membrane (unpublished data). Importantly, knockdown of BTBP-X in HUVECs drastically inhibited tube formation that mimics angiogenesis *in vitro*. These data suggest that BTBP-X is essential for cholesterol trafficking and angiogenesis.

A screen of BTBP-interacting proteins by AlphaScreen using human protein arrays

We next sought to identify the ubiquitinated substrate by the CUL3/BTBP-X axis. To this aim, we made use of AlphaScreen that detects the direct protein-protein interactions *in vitro*. The human protein array (approximately 20,000 of FLAG-GST tagged proteins) was produced by wheat germ extracts. We also prepared biotinylated BTBP-X. As a result, we identified approximately 100 proteins that interact with BTBP-X (unpublished data).

Discussion & Conclusion

We still need to assess candidate substrates of the CUL3/BTBP-X axis. First, we will prepare siRNA library for the candidate substrates (~100 genes). Genes by which knockdown exhibits mislocalization of D4H at the plasma membrane as well as inhibition of angiogenesis could be target substrates the CUL3/BTBP-X axis. Second, we will validate the CUL3/BTBP-X-dependent ubiquitination of the substrates by *in vitro* ubiquitination assay. We have recently identified novel molecular machineries that regulates endothelial functions (ref. 4, 5). The crosstalk of the CUL3/BTBP-X/substrate complex with other pathways should be examined. In future, inhibitors of the formation of CUL3/BTBP-X/substrate complex would be novel anti-angiogenic drugs. Since the agents do not target VEGF pathways, the combination with existing anti-VEGF drugs would promise better anti-angiogenic efficacy.

References

(1) Fang *et al*., Nature. 498 (7452). 118-122. 2013

(2) Maekawa and Fairn. J. Cell Sci. 128 (7). 1422-1433. 2015.

(3) Maekawa *et al*., Biol. Open. 6 (11). 1707-1719. 2017.

(4) Kovacevic *et al.*, J. Cell Biol. 217 (3). 1015-1032. 2018.

(5) Tanigawa, Maekawa *et al*., 234 (10). 17280-17294. 2019.

一般の皆様へ

全身に行き渡る血管は人体最大の臓器の一つです。血管の内側に存在し、血流と直に接する血管内皮細胞は炎症反応や血管新生等の生理機能発揮に重要な役割を持ちます。近年の研究で、血管内皮細胞内でコレステロールが細胞膜に適切に存在する事が血管内皮細胞の機能に重要である事が分かってきました。一方で、血管内皮細胞内のコレステロールを適材適所に配置させる仕組みは良く分かっていません。本研究では、この仕組み（= コレステロールの細胞内輸送）の分子機構の一端を解明する事に成功しました。今後は当該分子機構を標的とする新しい医薬品（血管新生阻害剤等）開発への応用が期待されます。

Study of the mechanistic dissection of cancer incidence caused by aging-associated dysfunction of cell competition in intestinal cells

Shunsuke Kon
kon44@rs.tus.ac.jp
Tokyo University of Science

Summary Abstract

In this study, we exploited the cell competition mouse model and examined how sequential accumulation of gene mutations which mimic the aging-associated genomic alteration affects the function of cell competition. The directionality of cellular extrusion of RasV12-transformed cells in the Wnt-activated background conferred by APC ablation or β-catenin activation is reversed, and the transformed cells were outcompeted to basal side through non-cell autonomous MMP21 upregulation. Furthermore, we found that the increased production of MMP21 was mediated at least, in part, via NF-κB signal, and hampering NF-κB signal restored apical elimination of transformed cells. Collectively, these results demonstrate that Wnt activation promotes diffuse invasion of transformed cells through malfunctional cell competition.

Key Words : Cell competition, multi-sequential carcinogenesis, diffuse invasion,

Introduction

Living organisms implement the self-defense systems to fight against cancer, with cell competition being one of tumor-surveillance systems to remove the newly emerging transformed cells. In general, the progressive accumulation of genetic aberrations by aging is strongly associated with onset of tumorigenesis. This prompted us to investigate whether the sequential genetic mutations affect the behavior of transformed cells in the competitive environment. We herein engineer the mice to sustain infrequent somatic activation of *Ras* in the background of *APC* silencing in a manner reminiscent of human familial adenomatous polyposis and examine the cell fates of transformed cells.

Results

1.Aberrant Wnt-activation disturbs apical extrusion of RasV12-transformed cells and induces non-cell autonomous diffuse invasion.

To examine the effects of APC-deficiency on efficiency of cell competition, we exploited APCmin mice harboring heterozygous loss-of-functional mutation in *APC* gene and crossed with the cell competition mouse model where RasV12-transformed cells are mosaically pro-

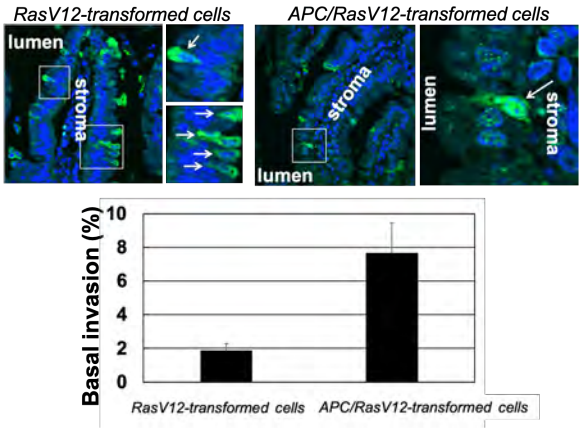

Figure 1. Frequency of basal invasion

duced by administration of the low dose tamoxifen (1). The substantial number of RasV12-expressing cells surrounded by normal cells were apically eliminated in single RasV12-mutated mice, while tiny fraction of transformed cells appeared basally extruded. We then found that number of basally extruded cells in APC/RasV12-mutated mice were significantly higher than single RasV12-mutated mice. This suggests that Wnt activation leads to malfunction of cell competition, resulting in promotion of basal extrusion of RasV12-transformed cells (Figure 1). At 28 days after tamoxifen administration, APC/RasV12-transformed cells were confined in the stroma of the upper villi. Yet, microscopically detectable deformities to the tissue architecture in the form of benign tumors were not observed in surrounding tissues, indicating that cancer cells were directly generated from normal mucous membrane through diffuse invasion of transformants.

2. MMP21 regulates the non-cell autonomous basal invasion of β-cat ΔN/RasV12 cells *in vitro*.

With the aim of understanding molecular mechanism underlying the non-cell autonomous basal extrusion of transformed cells, we established MDCK or MDCK pTR-RasV12 cells stably expressing a mcherry-conjugated β-catenin mutant (β-catΔN) to mimic Wnt-induced basal extrusion of RasV12 cells *in vitro.* When β-catΔN/RasV12-transformed cells were co-cultured with β-cat ΔN cells at a ratio of 50:1, a sizeable fraction of β-cat ΔN/RasV12 cells were basally invaded into the collagen matrix over time, successfully recapitulating the salient feature of non-cell autonomous basal extrusion of APC/RasV12 cells *in vitro*. To reveal the underlying molecular mechanism whereby Wnt activation promotes the diffuse invasion of RasV12-transformed cells, we conducted a microarray analysis to search for molecules whose expression is changed in β-cat ΔN/RasV12 cells co-cultured with β-cat ΔN cells. Among the top listed highly expressing genes, we found one member of matrix metalloproteases (MMPs) superfamily named MMP21 was highly upregulated. Furthermore, MMP21 knockout prevented the basal extrusion of β-catΔN/RasV12 cells, highlighting an active role for MMP21 in non-cell autonomous basal invasion of transformed cells.

3. NF-κB signal regulates the upregulation of MMP21.

A gene-set enrichment analysis (GSEA) revealed that NF-κB pathway was activated in β-cat ΔN/RasV12 cells co-cultured with β-cat ΔN cells. Accordingly, the reporter assay using the plasmid in which luciferase expression is under the control of tandem repeats of the NF-κB transcriptional response element showed the non-cell autonomous activation of NF-κB signal. To study functional relevance of NF-κB signal in MMP21-mediated diffuse invasion of transformed cells, we treated cells with inhibitor of NF-κB, BAY11-7082. As a result, addition of BAY 11-7082 substantially diminished the non-cell autonomous upregulation of MMP21, suggesting that NF-κB signal functions as an upstream regulator for enhancing the MMP21 expression. Furthermore, inhibition of NF-κB signal profoundly suppressed the basal extrusion of β-cat ΔN/RasV12 cells co-cultured

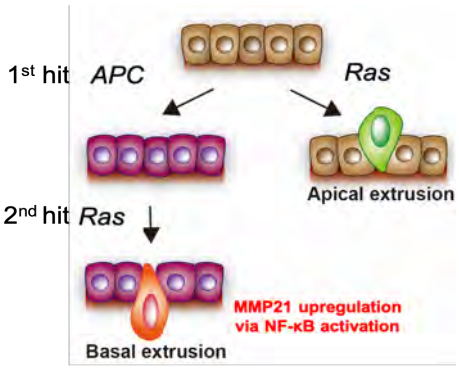

Figure 2. Summary of this study

with β-cat ΔN cells, or even enhanced apical elimination of them. These results suggest that NF-κB signal plays a central role for redirecting transformed cells to basal invasion via MMP21 upregulation (Figure 2).

Discussion & Conclusion

In this study, we found the aberrant activation of Wnt signaling altered the balance in cell competition-induced cellular extrusion, turning RasV12-transformed cells to invade basally. The basal invasion of RasV12 cells was induced, at least partly, by MMP21 activity intrinsic to the translocating cells, and involved NF-κB signal. The diffuse-type cancers generated in the digestive tract are hardly treatable due to inconspicuous early symptoms, highly invasive characters of cancer cells. Therefore, it is of clinical significance to delineate the nature of pathogenesis of diffuse-type cancer, and there is a requirement for sensitive novel treatments. The present study is indicative of NF-κB-MMP21 axis as a novel therapeutic target for the treatment of diffuse-type carcinoma. This study also points to NF-κB signal as one of key determinants of switching the predominant direction of extrusion from apical to basal. Yet, it remains elusive which factor(s) determine the divergent fate or APC/RasV12-transfomed mutants. It needs to be addressed in the future how the molecular landscape is profoundly remodeled to rewire the direction of extrusion by Wnt activation, which could be harnessed for therapeutic applications.

References

1) Kon, S., Ishibashi, K., Katoh, H., *et al*. 2017. Cell competition with normal epithelial cells promotes apical extrusion of transformed cells through metabolic changes. Nat Cell Biol 19:530-541.

一般の皆様へ

本研究成果より、細胞競合の機能変容によって、がん変異細胞が基底膜へとびまん性に浸潤する分子機構の一端を明らかにすることができました。具体的には、Wnt シグナルの活性化によって、細胞非自律的に NF-κB シグナルが活性化され、さらにマトリックスメタロプロテアーゼである MMP21の発現が増加することにより、がん細胞が基底膜浸潤能を獲得することが分かりました。びまん性の悪性腫瘍は一般的に予後が悪く、革新的な治療法が希求されているため、本研究により明らかとなった NF-κB-MMP21経路が治療標的となることが今後期待されます。

Identification of premalignant gastric glands in chronic gastritis mucosa and prophylactics for gastric cancer development.

Takahiro Shimizu
shimy@kuhp.kyoto-u.ac.jp
Kyoto University Hospital

Summary Abstract

To explore the susceptibility of pure gastric intestinal metaplasia (IM) to cancer development, we investigated the landscape of genetic alterations in gastric single glands. Whole exome sequencing of gastric single glands revealed significantly high accumulation of somatic mutations in various genes within IM glands compared with non-IM glands. Targeted capture deep sequencing and copy number analyses in gastric clustered glands showed that IM glands polyclonally expanded to aggregates, which commonly had copy number aberrations (CNAs) similar to those of intramucosal gastric carcinoma (IGC). These results suggest that in the gastric mucosa inflamed with *Helicobacter pylori* (*H. pyl*ori) infection, IM glands expand via acquisition of CNAs comparable to those of gastric cancer, contributing to field cancerization.

Key Words : gastric cancer, intestinal metaplasia, copy number aberration

Introduction

Gastric IM is considered a risk factor for gastric cancer in gastric mucosa with *H. pylori* infection. However, whether IM is a true precursor lesion or just a confounding factor for gastric cancer remains unknown. To explore the susceptibility of pure gastric IM to cancer development, we investigated the landscape of genetic alterations in gastric single glands with IM.

Results

We isolated 42 single glands with or without IM in inflamed gastric mucosa from 11 patients with IGC and in non-inflamed gastric mucosa from 3 people. Then, we performed whole-exome sequencing (WES) of each single gland after the whole amplification process. The mean number of mutations in single normal glands was 18.5, whereas those in single non-IM glands and single IM glands were 32.2 and 81, respectively. Somatic mutations in single normal glands and single non-IM glands were within the range predicted to be acquired spontaneously in normal cells of various tissues, whereas single IM glands had more spontaneous mutations than those predicted in normal cells. In addition, mutation signature analysis of single glands revealed that C to T substitutions at the CpG site, or signature 1, was clearly dominant in single IM glands, suggesting that increased cell turnover could be related to the induction of mutations in IM glands. Intramucosal gastric carcinoma with microsatellite stability phenotype in the same cases had averages of 89.65 mutations. Limited to cancer-related genes, single IM glands showed 3.8 non-synonymous mutations on average, whereas single non-IM glands and normal glands showed 1.2 and

1.0 non-synonymous mutations on average, respectively. However, no mutations were detected in the driver genes crucial for gastric cancer development, such as *TP53*, *ARID1A*, *APC*, *CDH1* and *RHOA*. Phylogenetic analyses of IM aggregates showed that IM glands expand to form clusters sharing some mutations.

Next, we performed targeted-capture deep sequencing in 96 gastric-clustered glands. The number of somatic mutations in targeted genes was similar between clustered IM glands and clustered non-IM glands (1.92 vs 1.67 on average, respectively, $P = 0.60$). Regarding cancer-related genes, clustered IM glands had more mutations than did clustered non-IM glands, but the difference was not significant (0.27 vs 0.13 per sample, respectively, $P = 0.39$). No mutations were detected in crucial driver genes, including *TP53*, *ARID1A*, *APC*, *CDH1* and *RHOA*.

Furthermore, we performed autosomal CN analyses in 96 clustered glands of inflamed gastric mucosa. CNAs were identified in 33 of 72 clustered IM glands, whereas only 2 glands among 24 clustered non-IM glands had CNAs. The CNA score revealed that clustered IM glands had significantly broader CN gain than did clustered non-IM glands (BCS 1.62 vs 0.17, $P = 0.0121$), whereas no difference was observed between clustered IM and non-IM glands in terms of CN loss (BCS 0.11 vs 0, $P = 0.61$. FCS 0.51 vs 0, $P = 0.757$) and focal CN gain (FCS 0.56 vs 0, $P = 0.535$). To compare the CNAs of IM or non-IM glands with those of gastric cancer, we calculated the autosomal CNA score for 41 IGC from our previous study, and of 10 submucosal gastric carcinoma at Stage IA and 34 gastric adenocarcinoma at Stage IB from TCGA database. Broad CNAs showed similar trends between IM and IGC and were significantly increased in submucosal gastric carcinoma and stages that are more progressive. On the contrary, focal CNAs were increased in IGC compared to those in IM glands. CNAs frequently observed in clustered IM glands showed broad gains of chr 2, 8 and 20. The distribution of CN gain in IM glands was quite similar to that in IGC and more progressive stages. CN loss was frequently observed in Stage IA and IB gastric carcinoma, whereas it was rarely observed in gastric IM glands and non-IM glands. These results suggest that broad CN gains, including gain of chr 8 and 20, were acquired by IM before malignant transformation, and that focal CNAs and broad CN loss emerged from the early stage of gastric cancer.

Discussion & Conclusion

We demonstrated that gastric IM is susceptible to somatic mutations and CNAs and that it expands multi-focally with acquisition of CNAs commonly found in gastric cancer. This suggests that the chronic inflamed stomach has a number of small fields where IM glands with CNAs expand, resulting in field cancerization. In addition, the similarity of CNA patterns and the number of mutations in gastric IM and gastric cancer in the early stage indicated that most intestinal-type gastric cancers might originate from IM glands. These findings could be a clear evidence that gastric cancer risk exists, especially, in people with gastric IM even after eradication of *H pylori*. Thus, to prevent gastric cancer development, *H pylori* eradication should be performed early before the development of IM. For people with gastric IM, the IM region should be evaluated carefully during short-interval endoscopy as surveillance for cancer development. To determine approaches for further prevention of gastric cancer development, it would also be important to unveil the mechanism by which IM develops during chronic gastric inflammation and to develop therapeutic and preventive

approaches targeting IM specifically.

References

Shimizu T, Marusawa H, Matsumoto Y, et al. Accumulation of somatic mutations in TP53 in gastric epithelium with Helicobacter pylori infection. Gastroenterology 2014;147:407–17. e3.

Huang KK, Ramnarayanan K, Zhu F, et al. Genomic and Epigenomic Profiling of High-Risk Intestinal Metaplasia Reveals Molecular Determinants of Progression to Gastric Cancer. Cancer Cell 2018;33:137-150.e5.

Kakiuchi N, Yoshida K, Uchino M, et al. Frequent mutations that converge on the NFKBIZ pathway in ulcerative colitis. Nature 2020;577:260–265.

一般の皆様へ

H.pylori 感染による慢性胃炎粘膜に発生する腸上皮化生は前癌病変であるのか傍癌病変であるのかは議論の分かれるところである。そこで、本研究では、慢性胃炎粘膜から腸上皮化生と非腸上皮化生を取り分け、網羅的なゲノム解析を行うことで、その点を明らかにしようとした。腸上皮化生には、早期胃癌とほぼ同じ数の遺伝子変異を認め、また早期胃癌でよく見られるコピー数異常も認めた。本研究の結果は、腸上皮化生から胃癌が発生することを直接証明したわけではないが、腸上皮化生が前癌病変である可能性を示唆する結果であった。腸上皮化生の発生予防や、腸上皮化生をターゲットとした治療に向けて現在研究を継続中である。

Mechanism of inflammatory memory in hematopoietic stem cells using informatics unifying multidimensional single cell data

Hitoshi Takizawa
htakizawa@kumamoto-u.ac.jp
International Research Center for Medical Sciences, Kumamoto University

Summary Abstract

Inflammation is the cardinal immune response for defense against pathogens and for facilitating tissue repair. Long-lived hematopoietic stem cells (HSCs) are maintained in adult bone marrow (BM) with little immune reactions upon immunological challenges, and produce all blood and immune cells. This project aims at understanding how HSCs can memorize inflammation, and if it is possible to enhance HSC function by modulating its inflammatory memory.

Key Words : Hematopoietic stem cells, Inflammatory memory, single cell data

Introduction

Adult bone marrow (BM) had been long thought to be an immune-privileged organ and thus, to form an advantageous environment to preserve long-lived hematopoietic and immune cells. However, recent studies indicate that the BM is in fact an active site of various types of immunological and inflammatory reactions which largely influence quiescent blood-forming hematopoietic stem cells (HSCs). We have previously shown that systemic bacterial infection modulates BM-resident HSC identity through innate immune signal activation in a HSC-intrinsic and -extrinsic (niche-dependent) manner.

Results

Recent works have proposed that innate immunity is sensitized (“trained”) upon infection and immune cells are epigenetically inscribed with innate immune memory to resist future infectious insults (Netea MG, Science 2016). Likewise, HSC and their progenitor can also memorize infection by changing their metabolism and epigenetics (Sezaki M, Front Immunol 2020). Our study has previously shown with bacterial infection models, that gram negative bacterial infection activates HSCs to proliferation but eventually impairs their hematopoietic repopulating ability through direct activation of innate immune signaling (Takizawa H, Cell Stem Cell 2017).

Since microorgansims coexist in our body, we studied how hematopoiesis responds to microbial signals upon their infiltration to the body, by using inflammatory bowel disease mouse model. We have found that intestinal tissue damage activates early hematopoiesis in BM via microbial signals and direct early hematopoietic progenitors to inflamed mesenteric lymph node to locally produce myeloid cells and promote tissue repair, suggesting cross-organ communication-driven tissue repair (unpublished data). However, chronic tissue invasion impinges on lifelong hematopoietic repopulation without disturbance of daily hematopoiesis, and decreased their responsiveness to immunological challenges.

To understand the mechanism by which microbial signals regulate HSC function toward tissue repair, we performed single cell RNA-/ATAC-sequencing with HSCs that had been in vivo pre-stimulated with lipopolysaccharide (LPS), a gram-negative bacterial component, and a microbacterial species (Bac). Although the analysis is still ongoing, a preliminary result showed innate immune signal activation as a control, metabolic regulators, and many genes involved in immune activation and epigenetics. We also performed a mass cytometer to analyze a number of epigenetic marks like histon H3 K27 acetylation, and found some histon marks got activated at 16 hours after the stimulation and stayed active even at 1 month after, indicating that the innate immune signals imprint on HSCs. To confirm this chromatin change and its impact on locus specific gene regulation, we will do cut-tag sequencing, an alternative of ChIP-seq for smaller cell number, and see what genes are regulated by the specific epigenetic marks found here. We are still on the way to develop a bioinformatics analytic pipeline that unifies all three single cell data set to predict key factors that control inflammatory memory in HSCs. Given successful selection of those candidate genes, we will overexpress or knockdown the genes of our interest in HSCs and transplant the genetically modified HSCs to lethally irradiated mice, to reconstitute hemato-immune system and test immune activation in response to infection re-challenge.

Discussion & Conclusion

How long-lived tissue stem cells as HSCs respond to hematopoietic challenges, and how the response relates to the functional alteration of hemato-immune system and hematopoietic abnormalities (e.g. aplasia/neoplasis) is a focus of ongoing research. Emerging evidences have demonstrated that in response to tissue invasion such as infection, inflammation, HSCs and their progenies are activated to migrate, proliferate and differentiate via immune cell-secreted cytokine- or pathogen-associated molecule pattern signaling. We have shown that tissue-insulting bacteria or LPS directly cause functional attenuation, while commensal bacteria, i.e, microbiota instructs hematopoiesis to promote tissue repair. Thus, Uncovering the molecular mechanism by which hematopoietic adaptation is formed and maintained in early hematopoietic cells, which reside at the apex of hemato-immune system, will dissociate beneficial signals from unwanted ones.

The project will converge to the development of a new strategy for vaccination against existing and emerging infection, or for regenerative medicine, especially for infants or elderly who have reduced tissue function. Adequate management of the hematopoiesis-niche cross-talk during tissue invasion is a key to success in treating patients with chronic inflammatory diseases, autoimmunity, and cancer, which incidence increase with age (Kovtonyuk LV, Front Immunol 2016).

References

1. Netea MG, Joosten LA, Latz E, Mills KH, Natoli G, Stunnenberg HG, O'Neill LA, Xavier RJ. Trained immunity: A program of innate immune memory in health and disease. ***Science***. 2016 Apr 22;352(6284):aaf1098. doi: 10.1126/science.aaf1098. Epub 2016 Apr 21.
2. Sezaki M, Hayashi Y, Wang Y, Johansson A, Umemoto T, **Takizawa H.** Immuno-modulation of hematopoietic stem and progenitor cells in inflammation, ***Front Immunol***.,

2020 Nov 24;11 doi: 10.3389/fimmu.2020.585367
3. **Takizawa H**, Fritsch K, Kovtonyuk LV, Saito Y, Yakkala C, Jacobs K, Ahuja AK, Lopes M, Hausmann A, Hardt WD, Gomariz Á, Nombela-Arrieta C and Manz MG. Pathogen-induced TLR4-TRIF innate immune signaling in hematopoietic stem cells promotes proliferation but reduces competitive fitness. ***Cell Stem Cell***., 2017 Aug 3;21(2):225-240
4. Kovtonyuk LV, Fritsch K, Feng X, Manz MG, **Takizawa H.** Inflamm-Aging of Hematopoiesis, Hematopoietic Stem Cells and the Bone Marrow Microenvironment. ***Front Immunol***., 2016, Nov 14;7;502

一般の皆様へ

炎症は病原体に対する生体防御および組織修復を促進するための主要な免疫応答です。骨髄はほとんど免疫応答が起こらない免疫特権臓器の一つとして、長命の血液細胞および免疫細胞を保存するのに有利な環境を形成すると考えられてきました。しかしながら、近年、骨髄では実に活発で多様な免疫応答が行われており、血液の源泉である血液幹細胞の機能特性に多大な影響を及ぼすことが分かりつつあります。本研究では、炎症が血液幹細胞機能を適応させ、感染症、炎症および血液悪性腫瘍などに対してより応答性のある血液・免疫系を構築するという“血液幹細胞の炎症記憶”という概念を検証します。得られる知見は、様々な感性症に対するワクチン戦略や老化に伴い増加する炎症疾患の制御や治療に対して非常に有用な知見をもたらすものと期待されます。

Molecular mechanisms of mycobacterial effector protein for the development of novel anti-TB drugs

Giichi Takaesu
takaesug@comb.u-ryukyu.ac.jp
Tropical Biosphere Research Center, University of the Ryukyus

Summary Abstract

A mycobacterial virulence factor, Zn^{2+} metalloprotease 1 (Zmp1), is known to suppress IL-1β production by inhibiting caspase-1 resulting in phagosome maturation arrest. However, the molecular mechanism of caspase-1 inhibition by Zmp1 remains obscure. In this study, we identified GRIM-19 (also known as NDUFA13), an essential subunit of mitochondrial respiratory chain complex I, as a novel Zmp1-binding protein. Using CRISPR/Cas9-mediated gene knockout cells, we found a previously unrecognized role of GRIM-19 as an essential regulator of NLRP3 inflammasome and a molecular mechanism underlying Zmp1-mediated suppression of IL-1β production during mycobacterial infection.
Key Words : Tuberculosis, Inflammasome, Mitochondrial respiratory complex I

Introduction

Mycobacterium tuberculosis (Mtb), a causative agent of human tuberculosis, is an intracellular pathogen that primarily infects macrophages. Macrophages cultured in the presence of anti-IL-1β neutralizing antibody lose control of intracellular Mtb replication. Conversely, the addition of recombinant IL-1β in the macrophage culture restricts the intracellular Mtb replication, indicating the critical role of IL-1β for the bactericidal activity of macrophages against Mtb[1,2]. It has been shown that the mycobacterial *Rv0198c* gene that encodes Zmp1 is required for phagosome maturation arrest and intracellular survival of Mtb in macrophages by inhibiting IL-1β production[3]. However, the molecular mechanisms underlying the inhibition of IL-1β production by Zmp1 are currently unclear.

Results

To investigate the molecular mechanisms of the Zmp1-mediated inhibition of IL-1β production, we performed yeast two-hybrid screening using the full-length Zmp1 as a bait and isolated a cDNA encoding the C-terminal portion (86-144 amino acids) of murine GRIM-19. The interaction of Zmp1 with GRIM-19 in mammalian cells was confirmed by immunoprecipitation assay using cell extracts of HEK293T cells transfected with T7-tagged GRIM-19 and FLAG-tagged Zmp1. Since GRIM-19 functions as an accessory subunit of mitochondrial respiratory chain complex I[4-7], we examined the subcellular localization of Zmp1 in macrophages. We found that endogenous GRIM-19 is mainly expressed in mitochondria, and colocalization of Zmp1 with GRIM-19 was detected in mouse bone marrow-derived macrophages infected with BCG. Collectively, these data indicate that Zmp1 interacts with GRIM-19 in mitochondria during mycobacterial infection.

It is currently unclear whether GRIM-19 is involved in IL-1β production. To understand

the role of GRIM19 in macrophages, we generated *Grim-19*-deficient J774.1 mouse macrophage cells using the CRISPR/Cas9 system. IL-1β production was barely detected when J774.1 cells were infected with wild-type BCG, but it was significantly increased when these cells were infected with Δ*zmp1* BCG, confirming that Zmp1 suppresses IL-1β production in BCG-infected J774.1 cells. The IL-1β production induced by Δ*zmp1* BCG infection was abolished in *Grim-19*-deficient cells, suggesting that GRIM-19 plays an essential role in IL-1β production in macrophages upon mycobacterial infection. We also confirmed that Δ*zmp1* BCG-induced IL-1β production was dependent on NLRP3 since pretreatment of these cells with MCC950 blunted the production of IL-1β upon Δ*zmp1* BCG infection.

Next, we analyzed the mechanism of GRIM-19-mediated regulation of the NLRP3 inflammasome. Wild-type and *Grim-19*-deficient J774.1 cells were primed with LPS to induce expression of pro-IL-1β and treated with ATP or nigericin to activate the NLRP3 inflammasome. We found that mature IL-1β protein was detected in culture supernatants of wild-type, but not *Grim-19*-deficient, cells treated with ATP or nigericin. Pro-IL-1β protein was detected from the cell lysates of both wild-type and *Grim-19*-deficient cells stimulated with LPS. We observed a 10-kDa fragment of caspase-1, which is generated upon activation of caspase-1, in the culture supernatant of wild-type cells treated with ATP or nigericin. This fragment was almost completely diminished in *Grim-19*-deficient cells. Since the components of the NLRP3 inflammasome, NLRP3, pro-Caspase-1, and ASC were expressed in *Grim-19*-deficient cells to a similar extent to wild-type cells, it is suggested that GRIM-19 is required for activation of the NLRP3 inflammasome.

Because mitochondria-derived reactive oxygen species (mtROS) is known to induce NLRP3 inflammasome activation[8], we next examined whether GRIM-19 is involved in the production of mtROS. The level of mtROS was significantly increased when LPS-primed wild-type J774.1 cells were treated with ATP, whereas the level of mtROS was not increased in *Grim-19*-deficient cells under the same condition. We also examined the activity of mitochondrial respiratory complex I in these cells and found that the complex I activity was markedly reduced in *Grim-19*-deficient cells compared to wild-type cells. These results indicate that GRIM-19 is necessary for mtROS production, and the diminished mtROS production in *Grim-19*-deficient cells is most likely due to the impaired complex I activity.

An intact mitochondrial respiratory chain generates mitochondrial membrane potential (ΔΨm). Wild-type and *Grim-19*-deficient J774.1 cells were stained with a cell-permeable fluorescent probe, JC-1, and analyzed by fluorescence microscopy. We found that the fluorescence ratio of red/green (JC-1 aggregates/monomer) was significantly lower in the *Grim-19*-deficient cells than in wild-type cells, suggesting that GRIM-19 is essential for maintaining ΔΨm in macrophages. We also found that a transient expression of Zmp1 in HEK293T cells decreased the ΔΨm to a similar extent as the cells treated with rotenone, a selective inhibitor of the mitochondrial respiratory chain complex I, implying that Zmp1 decreases ΔΨm presumably by modulating the complex I activity.

Discussion & Conclusion

In this study, we identified GRIM-19, an essential accessory subunit of mitochondrial respiratory chain complex I, as a novel Zmp1-interacting host protein. CRISPR/Cas9-

mediated gene knockout of *Grim-19* in a murine macrophage cell line revealed that GRIM-19 is required for IL-1β production during mycobacterial infection. Further analysis suggested that GRIM-19 is critically involved in NLRP3 inflammasome activation via the production of mtROS. Either loss of GRIM-19 or expression of Zmp1 resulted in a significant decrease in mitochondrial membrane potential. Collectively, our results indicate that Zmp1 inhibits IL-1β production, presumably by targeting GRIM-19 which is necessary for NLRP3 inflammasome activation. Our work provides new insight into the mechanism underlying the activation and modulation of the NLRP3 inflammasome during mycobacterial infection. The development of a drug that blocks the interaction between Zmp1 and GRIM-19 could potentially be a novel host-directed therapeutic option for tuberculosis treatment. In addition, our study also provides clues to enhance the effect of trained immunity, leading to the development of novel drugs for infectious diseases.

References

1 Jayaraman, P. *et al.* IL-1β promotes antimicrobial immunity in macrophages by regulating TNFR signaling and caspase-3 activation. *J Immunol* **190**, 4196-4204 (2013).

2 Jayaraman, P. *et al.* Tim3 binding to galectin-9 stimulates antimicrobial immunity. *J Exp Med* **207**, 2343-2354 (2010).

3 Master, S. S. *et al.* Mycobacterium tuberculosis prevents inflammasome activation. *Cell Host Microbe* **3**, 224-232 (2008).

4 Fearnley, I. M. *et al.* GRIM-19, a cell death regulatory gene product, is a subunit of bovine mitochondrial NADH:ubiquinone oxidoreductase (complex I). *J Biol Chem* **276**, 38345-38348 (2001).

5 Huang, G. *et al.* GRIM-19, a cell death regulatory protein, is essential for assembly and function of mitochondrial complex I. *Mol Cell Biol* **24**, 8447-8456 (2004).

6 Stroud, D. A. *et al.* Accessory subunits are integral for assembly and function of human mitochondrial complex I. *Nature* **538**, 123-126 (2016).

7 Guerrero-Castillo, S. *et al.* The Assembly Pathway of Mitochondrial Respiratory Chain Complex I. *Cell Metab* **25**, 128-139 (2017).

8 Zhou, R., Yazdi, A. S., Menu, P. & Tschopp, J. A role for mitochondria in NLRP3 inflammasome activation. *Nature* **469**, 221-225 (2011).

一般の皆様へ

本研究では、結核菌（Mycobacterium tuberculosis）が産生する炎症抑制因子の作用機序の解明を目的として、まず宿主側標的タンパク質を同定し、その遺伝子を破壊した細胞を作製して、この宿主タンパク質が炎症誘導に重要な役割を果たす新規制御因子であることを見出しました。本研究の成果は、宿主免疫応答を増強するタイプの新たな抗結核薬、新しい結核ワクチン、さらには近年注目されている「訓練免疫」を増強することによる感染症の治療法や予防法の創出に繋がるものと期待されます。

Functional mechanisms and dynamics of oxytocin in autism spectrum disorder

Teruhiro Okuyama
okuyama@iqb.u-tokyo.ac.jp
The University of Tokyo

Summary Abstract

The ability to recognize familiar individuals is essential for social animals including humans, and an impairment of this ability is a hallmark of autism spectrum disorders (ASDs). We previously showed that neurons in the ventral CA1 (vCA1) of the hippocampus store social memory for familiar individuals. However, how neural activities of vCA1 neurons are coordinated for social memory formation remained unclear. Here, we found that social memory in the vCA1 is replayed during sleep period, which is disrupted in autism-model mice.

Key Words : Autism spectrum disorder, social memory, hippocampus, Oxytocin, physiology

Introduction

Autism spectrum disorder (ASD) is a developmental disability that can cause significant difficulties with social communication and interaction and may also exhibit restricted, repetitive behaviors and interests. To understand the molecular basis underlying ASD, large-scale genetic screenings of ASD-related genes have been vigorously conducted [1], and a large number of genes, including shank3 and neuroligin, were identified. Most of these genes are involved in forming the dendritic spine and synapse, which function as a physical scaffold for neurons to process information [2]. However, the essential question of which brain region(s) and neural circuit(s) were impaired in ASD remains unanswered.

Results

Along with social communication impairment, clinical studies have reported that autistic patients also exhibit social memory impairment, which is the inability to remember others accurately [3]. This evidence came up with the idea that the information processing abnormalities in the neurons involved in social memory itself, or the social neurons located upstream or downstream of those neurons, may cause autism symptoms.

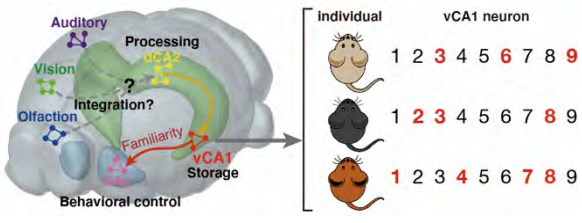

On the other hand, we previously showed that ventral CA1 neurons in the hippocampus store social memory (Okuyama et al., Science 2016). Using the microendoscopy to detect the neural activity of ventral CA1 neurons during social behavior, we found that a particular population of ventral CA1 neurons is enormously excited only when recalling a specific memorized individual. However, how neural activities

of this social memory ensemble are coordinated remained unclear. Here, we found that social memory in the vCA1 is replayed during sleep period, which is disrupted in autism-model mice.

Our *in vivo* electrophysiological recordings allow us to compare neural activities during awake social behavior and during high-frequency oscillations called sharp-wave ripples (SPW-Rs) observed during sleep periods with high temporal resolution. In this study, we showed that vCA1 social memory neurons, characterized by enhanced activity in response to memorized individuals, were preferentially reactivated during sharp-wave ripples. Also, we revealed that these features are impaired in autism-associated Shank3 mutant mice [4].

Discussion & Conclusion

These results suggest that SPW-R-mediated sequential reactivation of memory ensembles is a general mechanism for coordinating hippocampus-dependent social memories and spatial memory. Importantly, we found that its disruption may underlie the pathophysiology of ASD-related social memory defects. Our findings provide a first-ever neuroscientific answer to the question of why autistic patients are unable to exhibit social familiarity, which is expected to provide a breakthrough in the therapeutic development of ASDs.

References

[1] A de novo convergence of autism genetics and molecular neuroscience. Niklas Krumm, Brian J O'Roak, Jay Shendure, Evan E Eichler. Trends in Neurosci. 37:95(2014)

[2] Progress toward treatments for synaptic defects in autism. Richard Delorme, Elodie Ey, Roberto Toro, Marion Leboyer, Christopher Gillberg, Thomas Bourgeron. Nat. Med.19:685 (2013)

[3] Face identity recognition in autism spectrum disorders: a review of behavioral studies. Sarah Weigelt, Kami Koldewyn, Nancy Kanwisher. Neurosci. Biobehav. Rev. 36:1060 (2012)

[4] Disrupted social memory ensembles in the ventral hippocampus underlie social amnesia in autism-associated Shank3 mutant mice. Kentaro Tao, Myung Chung, Akiyuki Watarai, Ziyan Huang, Mu-Yun Wang, Teruhiro Okuyama. bioRxiv (2021)

一般の皆様へ

自閉症スペクトラムは、社会性コミュニケーションなどに異常を示す発達障害で、その病態神経メカニズムの解明は喫緊の課題の一つです。私たちの研究では、自閉症を引き起こす事が既に報告されている自閉症関連遺伝子の一つであるShank3遺伝子に注目し、脳内のどのような神経回路がどのように変容することで自閉症病態を引き起こすのかを明らかにしました。

Fasting Specific Metabolic Regulation by the Circadian Clock

Kenichiro Kinouchi
ken-k@keio.jp
Keio University School of Medicine

Key Words : Circadian rhythms, Fasting, Metabolism, Epigenetics, Circadian clock

Introduction

Circadian rhythms are organismal innate oscillation to preserve homeostasis in an anticipation of day-night cycle. The intrinsic rhythms are driven by the circadian clock, which orchestrates daily rhythms of metabolism, physiology, and behavior. Feeding-fasting rhythms entrain peripheral circadian clocks, emphasizing the notion that temporal patterns of nutrient availability impact clock functions. While a number of molecular mechanisms are responsible for clock integration of metabolic states, it remains to be defined whether clock-mediated transcriptional regulation is altered by fasting.

Results

To explore whether the circadian clock impinges on genomic response to fasting, 8-12 weeks-old, male clock deficient (*Bmal1*$^{-/-}$) mice and control mice were subjected to ad libitum feeding (FED) or 24hr fasting (FAST) under a 12hr/12hr light-dark condition. Liver, skeletal muscle, and serum were collected at two different time points (at zeitgeber time (ZT) 8 and 20, wherein light turns on at ZT0 and off at ZT12). qPCR revealed differentially expressed transcripts in the liver and skeletal muscle between FED and FAST conditions (Figure 1). Ablation of *Bmal1* has been first validated. We previously demonstrated that genomic response to fasting is categorized into three groups: Class I, BMAL1 target and repressed by fasting; Class II, BMAL1 target and induced by fasting; Class III, non-BMAL1 target and induced by fasting [1]. Consistent with the previous study, expression of hepatic *Dbp* gene was repressed by fasting and virtually abolished in *Bmal1*$^{-/-}$ mice (Class I). Hepatic *Por* expression was induced by fasting and attenuated in *Bmal1*$^{-/-}$ mice (Class II). Hepatic *Fgf21* expression was induced by fasting and this induction was comparable between WT and *Bmal1*$^{-/-}$ mice (Class III). Similarly, expression of skeletal muscle *Dbp* gene was repressed by fasting and virtually abolished in *Bmal1*$^{-/-}$ mice (Class I). Skeletal muscle *Per1* expression was induced by fasting and attenuated in *Bmal1*$^{-/-}$ mice (Class II). Thus, distinct classes of genes display differential genomic response to fasting.

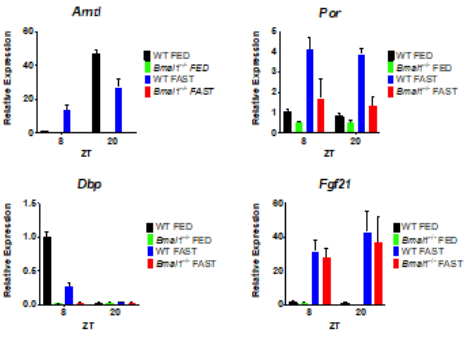

Figure 1

Circadian gene expression is controlled by rhythmic activation of clock and non-clock, nutrient-sensitive transcription factors (metabolic clock) such as SREBP, PPAR, and CREB[2]. Fasting-specific gene regulation is achieved by cyclic coordination of circadian and

metabolic clocks. To advance our understanding of underlying transcriptional mechanisms, high-throughput transcriptomic analysis was performed by RNA sequencing (RNA-seq). After the process of mapping, alignment, annotation and quantitation, differentially expressed genes were identified using CyberT analysis[3]. BMAL1 target genes were defined by genes whose expression was repressed by BMAL1 ablation. 816 and 879 genes were identified as the class I gene in the liver and skeletal muscle, respectively. 269 and 221 genes were found as the class II gene in the liver and skeletal muscle, respectively. 2293 and 2981 genes in the class III were discovered in the liver and skeletal muscle, respectively. 96 genes in the class I, 20 genes in the class II, and 879 genes in the class III were in common between liver and skeletal muscle, respectively. This observation likely represents tissue specificity of the clock regulation upon fasting. KEGG (Kyoto Encyclopedia of Genes and Genomes) pathway analysis revealed that pentose and glucuronate interconversions is enriched in the hepatic class I genes, AMPK signaling, FoxO signaling pathways in the hepatic class II genes, and Proteasome, PPAR signaling pathway in the hepatic class III genes. Meanwhile, PI3K-Akt signaling pathway are overrepresented in the muscle class I genes, circadian rhythm in the muscle class II genes, Proteasome in the muscle class III genes. Thus fasting seems to induce a transcriptional switch of the circadian clock, whereby achieving different classes of fasting-specific gene regulation in the liver and skeletal muscle.

Discussion & Conclusion

Circadian transcription is subject to temporal patterns of nutrient availability. There are a number of underlying mechanisms which contribute to such receptivity of the clock machinery to nutritional states. For instance, feeding drives *Per2* gene expression through insulin signaling, while fasting induces *Per1* gene activation by glucagon and glucocorticoid via phosphorylated CREB and GR, respectively. Although it becomes more evident that clock components are subject to regulation or modification by nutrient sensing pathways, it remains to be clarified whether changes in chromatin landscape by nutritional states dictate clock-mediated transcription in concert with nutrient sensitive transcription factors. Preliminary results from our study suggest that fasting imparts a switch to clock-mediated transcription both in the liver and skeletal muscle. Future experiments will define how clock transcription factors are conditioned by fasting at the chromatin level.

References

1 Kinouchi, K. *et al.* Fasting Imparts a Switch to Alternative Daily Pathways in Liver and Muscle. *Cell reports* **25**, 3299-3314 e3296 (2018).
2 Vollmers, C. *et al.* Time of feeding and the intrinsic circadian clock drive rhythms in hepatic gene expression. *Proceedings of the National Academy of Sciences of the United States of America* **106**, 21453-21458 (2009).
3 Kayala, M. A. & Baldi, P. Cyber-T web server: differential analysis of high-throughput data. *Nucleic acids research* **40**, W553-559 (2012).

一般の皆様へ

体内時計は昼夜の明暗の変化に予測して適応する分子であり、光や食事で時刻合わせをします。本研究では、体内時計がどのように空腹に対する応答を調節することで、臓器間の代謝協調性に寄与するのかを研究目的としています。これまでの検討で、肝臓や筋肉の絶食に対する応答は体内時計で調節されていることが明らかになっています。今後詳細な分子機序を検討することで、空腹によって分泌されるホルモンの効果が、ホルモン分泌の日内変動に加えて、効き目にも日内変化が存在し、それが体内時計によって調節されている可能性を明らかにしていきたいと考えています。

Cell senescence effects on transcriptional regulation and differentiation in beige preadipocytes

Kenji Ikeda
kikeda.mem@tmd.ac.jp
Department of Molecular Endocrinology and Metabolism,
Tokyo Medical and Dental University

Summary Abstract

Beige fat was induced by thermal stress adaptation and increase energy expenditure as heat. Aging, obesity, cell senescence strongly inhibits the induction of beige adipocytes. Still, how cell senescence regulate differentiation of beige adipocytes remain incompletely understood. The complicated reasons to study their mechanism, because beige adipocytes are heterogeneity.

Here, we analyzed single cells with adipose tissue in young and aging mice using single cell RNA sequencing. We identified new cell populations of subtype of preadipocytes. These findings provides understanding the beige adipocytes differentiation in aging.

Key Words : Beige adipocytes, Senescence, cell differentiation

Introduction

Beige fat was induced by thermal stress adaptation and increase energy expenditure as heat. Aging, cell senescence strongly inhibits the induction of beige adipocytes. Still, how cell senescence regulate differentiation of beige adipocytes remain incompletely understood. The complicated reasons to study their mechanism, because beige adipocytes are heterogeneity.

Recently our study reveals a new subtype of beige adipocytes and preadipocytes . This new subtype is distinct from conventional beige fat in developmental origin and regulation and cell function.

We analyzed single cell RNA sequencing with adipose tissue in young and aging mice with cold simulation. We identified new cell populations of subtypes of preadipocytes.

Results

1. Aging mice showed cell senescent in inguinal adipose tissue.

To examine aging effects in inguinal adipose tissue, we analyzed young and old mice in inguinal adipose tissue. Old mice showed higher mRNA expression of several cell senescent marker genes, *p19* and *p16*(Figure1).

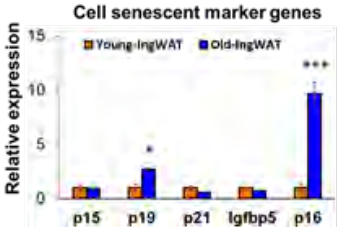

Figure1. Aging mice showed cell senescent in inguinal adipose tissue.

2. Aging mice showed impaired beige fat induction.

Next, we investigated the beige fat induction in old mice at cold exposure. Old mice showed a significantly decrease beige fat induction at cold exposure(Figure2).

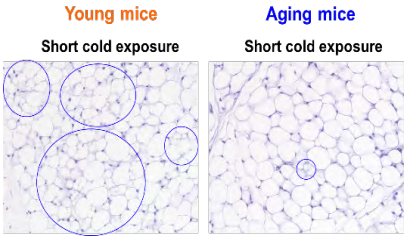

Figure2. Aging mice showed impaired beige fat induction.

3. Chronic cold exposure induced beige fat in old mice.

In contrast to this, longer cold stimulation can induce beige fat induction in aging mice.

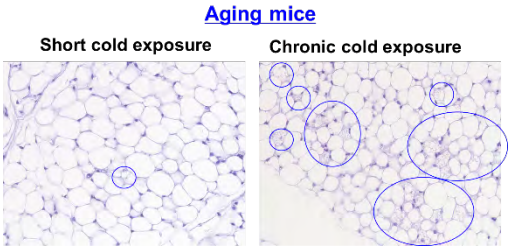

Figure3. Chronic cold exposure induced beige fat in old mice.

4. Identification and Characterization of inguinal adipose tissue by scRNA-seq.

Given the differences in beige fat induction in inguinal adipose tissue between young and aged mice.We next explored the inguinal adipose tissue, we run scRNA-seq analysis. We isolated single cell suspension in inguinal adipose tissue by collagenase digestion as previously described(1). Next, single cell cDNA libraries were generated using 10X Genomics platform to run scRNA-seq in inguinal adipose tissue from young mice and old mice housed room temperature (RT) or Cold. To classify the cell types in the inguinal adipose tissue, we performed uniform manifold approximation and projection(UMAP) analysis using Seurat.

We identified 40 cell clusters, which are displayed using UMAP dimension reduction technique after integration datasets. Clusters were annotated based on canonical genes, for example adipocytes progeneitor, preadipocytes(Pdgfra) We identify preadipocytes are multiple cluster and subpopulations (Figure4).

We compared to clusters among datasets, notably we identified cell clusters specifically in cold exposure (Figure5).

Cluster 23 and 30 are expressed preadipocytes marker *Pdgfra* and uniquely enriched in cold exposure condition, it suggest that these cell cluster are associated with beige fat induction even in aging condition.

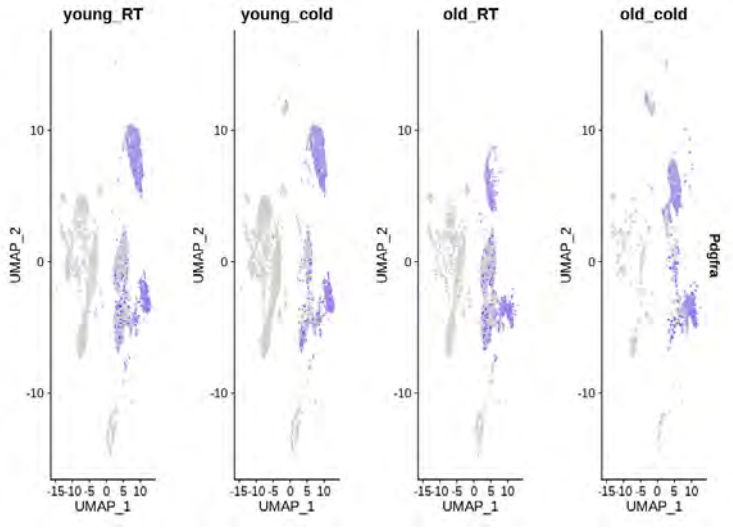

Figure4. Single cell RNA sequencing identifies preadipocytes cell cluster (Pdgfra expressed) in adipose tissue.

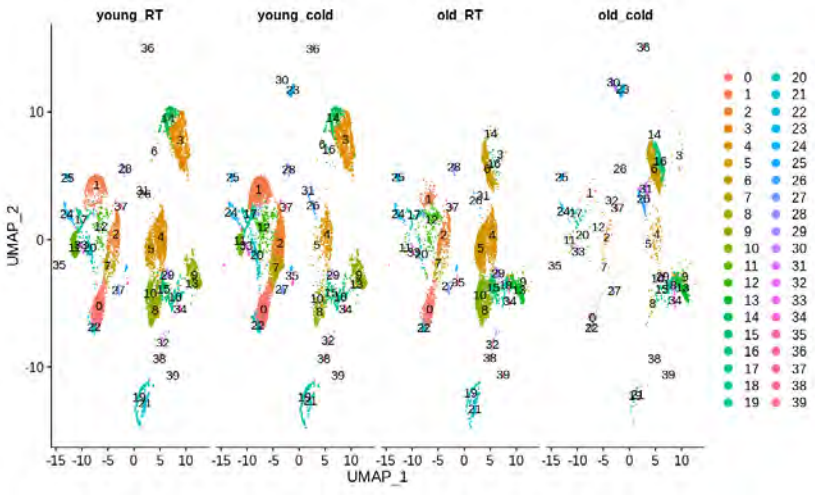

Figure5. Single cell RNA sequencing identifies cell clusters in adipose tissue.

Discussion & Conclusion

Cell senescent impairs beige fat induction[2]. Obese condition cause cell senescence in adipose tissue. Aging and Obesity storongly inhibit beige induction.

However, our findings suggest that even in aging mice, chronic cold stimulation can induce beige adipocytes. Aging mice have potential beige fat induction.

Recently our study reveals a new subtype of beige adipocytes and preadipocytes[3] . These findigs suggest that subtypes of beige adipocytes are different under aging conditions. By single-cell analysis in inguinal adipose tissue, we identified new cell populations in cold stimulation. These new cell populations are likely associated with beige fat induction in cell senescence. Future work will further elucidate the role of the new cell population in beige fat induction, even in aging and obesity.

References

1. Ikeda K, Kang Q, Yoneshiro T, Camporez JP, Maki H, Homma M, et al. UCP1-independent signaling involving SERCA2b-mediated calcium cycling regulates beige fat thermogenesis and systemic glucose homeostasis. Nat Med. 2017;23(12):1454-65.
2. Berry DC, Jiang Y, Arpke RW, Close EL, Uchida A, Reading D, et al. Cellular Aging Contributes to Failure of Cold-Induced Beige Adipocyte Formation in Old Mice and Humans. Cell Metab. 2017;25(1):166-81.
3. Chen Y, Ikeda K, Yoneshiro T, Scaramozza A, Tajima K, Wang Q, Kim K, Shinoda K, Sponton CH, Brown Z, Brack A, Kajimura S.
Thermal stress induces glycolytic beige fat formation via a myogenic state. *Nature. 2019;*565:180-185.

一般の皆様へ

熱産生脂肪組織であるベージュ脂肪組織は、エネルギー消費量を増やし抗糖尿病、抗肥満作用を示すことから肥満症や2型糖尿病への治療開発が期待されています。ベージュ脂肪組織は、長期の寒冷暴露や運動などの刺激によって誘導されることが特徴です。ベージュ脂肪細胞は肥満や老化に伴い、その誘導が低下することが知られておりますが、その仕組みはこれまで明らかになっておりません。ベージュ脂肪細胞は脂肪前駆細胞から分化することが知られておりますが、その詳細は未だ不明な点が多いです。最近になってベージュ脂肪細胞、前駆細胞には様々なサブタイプが存在することがわかってきました。本研究では、ベージュ脂肪細胞の誘導機構を一細胞毎に調べることで、その仕組みを明らかにし、加齢や肥満状態でもエネルギー消費量を亢進する肥満症・2型糖尿病に対する新しい治療法開発に繋げることを目指します。

Identification of molecular network between mitochondria and nucleus underlying mitochondrial biogenesis

Atsushi Hoshino
a-hoshi@koto.kpu-m.ac.jp
Kyoto Prefectural University of Medicine

Summary Abstract

Mitochondrial degradation and biogenesis are coordinately regulated to maintain mitochondrial homeostasis. Genome-wide CRISPR library screen and subsequent perturb-sequence identified p53 and RREB1 as novel regulators for mitochondrial biogenesis after mitophagy.

Key Words : mitochondrial biogenesis, heart failure

Introduction

Mitochondria play a critical role in energy production, redox and calcium metabolism and apoptosis, all of which are involved in cardiac hypertrophy and fibrotic change during heart failure progression. Mitochondria are dynamic organelle, repeating fission and fusion and damaged ones are degraded by autophagy machinery, called “mitophagy”. Usually, mitophagy are coupled with biogenesis to maintain mitochondrial content. We and other groups reported that mitophagy was down-regulated by p53 and others and mitochondrial biogenesis was also impaired subsequently in heart failure. The dysregulated balance between degradation and biogenesis induced low mitochondrial content, energy compromise, oxidative stress and impaired homeostasis. In this study, we aim to reveal mitochondria-nucleus signal network to maintain the balance of mitochondrial degradation and biogenesis.

Results

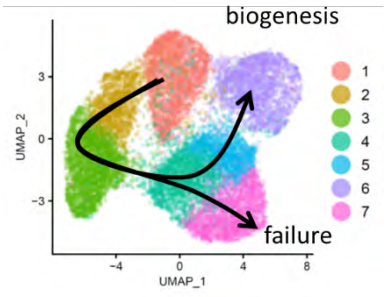

We employed the mitochondrial biogenesis in response to forced mitophagy in cultured C2C12 cells. At first, we performed CRISPR library screening to identify key players in mitophagy-mediated mitochondrial biogenesis. Lentivirus based GeCKO library was transduced to Parkin expressing cells. Mitophagy was induced by CCCP or OXPHOS inhibitor cocktail treatment. Mitochondrial content was analyzed by MitoTracker Green. High or low MitoTracker signal population was sorted and then analyzed by deep sequencing. This screening identified TNFα-NFkB pathway including Traf3, Traf2, Birc2, RBCK1, ubiquitin-related genes and nuclear protein-coding genes including Rreb1, p53, Bmi1, Atxn7l3 as positive regulators for mitochondrial biogenesis after mitochondrial degradation. Based on these regulators, single cell CRISPR screening was performed in the Perturb-seq platform. gRNAs targeting 9 genes as well as non-targeting

control were transduced to Parkin expressing cells. Samples were harvested 4 time points before and after mitophagy induction with parkin overexpression and CCCP treatment. Single cell analysis was performed by 10X Genomics platform. After quality control filtering, we obtained 16,616 cells from 4 time points around mitophagy induction. In the clustering analysis, there were seven clusters with two fate directions; successful mitochondria biogenesis (cluster 6) and failure of biogenesis (cluster 7). Cluster 6 was characterized by gene ontology of mitochondrial respiratory electron transport chain, whereas cluster 7 had upregulated genes in related with p53-mediated transduction and cell cycle arrest. Among the perturbed genes, Rreb1 knockout shifted the population from cluster 6 to 7, and p53 knockout decreased cluster 6 with increased cluster 4. These results indicated that Rreb1 knockout failed mitochondrial biogenesis, whereas p53 knockout just delayed biogenesis.

ATAC sequence was performed to analyze the epigenetic alteration in mitochondrial biogenesis after mitophagy induction. High accessibility was associated with regulation of transcription, cell differentiation, and regulation of ion transmembrane transport. In contrast, low accessibility was related with DNA methylation, DNA replication, positive regulation of gene expression, and nucleosome assembly. In the motif analysis, SP1, SP2, Sp3, Sp8, KLF5, KLF16, RREB1, and ZNF 740 motifs become more accessible in the phase of mitochondrial biogenesis. These results indicated that RREB1 binding site becomes open and contributes to mitochondrial biogenesis.

As the downstream of RREB1, RREB1 motif binding peak was analyzed with RNA sequence data. There were about 50 genes matched with ATAC-seq peaks annotated as promoter. Among them, several genes including ESR1 ware involved in mitochondrial biogenesis and functional maturation.

PGC1a is well-known master regulator of mitochondrial biogenesis. Its expression level was elevated and partially involved in biogenesis after mitophagy. To find upstream of PCG-1a expression, we also performed CRISPR library screening using PGC-1a reporter cells. P2A-mCherry fragment was knocked-in in the front of stop codon. Several COMM (copper metabolism gene MURR1) domain containing genes were identified to positive regulator for PGC-1a expression. Together with mitochondrial biogenesis regulators screening, autophagy-related gene, AMBRA1 and cell cycle-related gene, PPP1R15A were common hit genes in both PGC-1a expression and biogenesis, indicating that AMBRA1 and PPP1R15A were promoted biogenesis through PGC-1a expression.

Discussion & Conclusion

Our current impressive result is that RREB1 was identified in both CRIPR library screening and ATAC sequence. RREB1 is responsible for mitochondrial biogenesis and its binding site becomes more accessible after mitophagy. Single cell RNA sequence with perturbed genes also suggested RREB1 knockout failed to promote mitochondrial biogenesis after mitochondrial degradation. One of the candidates of downstream is estrogen receptor to drive biogenesis. RREB1 seemed to regulate other mitochondrial genes. To obtain more convincing data, we are now setting to perform Cut&Tag. This method can provide direct evidence of RREB1 binding sites. And RREB1-flox mouse is under generation to analyze the physiological and pathological importance of RREB1 in associated with mitochondrial biogenesis.

一般の皆様へ

ミトコンドリアは細胞のエネルギー産生の中心であるとともに酸化ストレスや慢性炎症、細胞死の制御に関連しておりその機能は細胞の恒常性維持に非常に重要です。不良ミトコンドリアはオートファジーによる分解され、新たなミトコンドリアが合成されますが、それらがどのようにして協調的に制御されているかはよく分かっていません。本研究では多面的オミクス解析で RREB1という転写因子がミトコンドリア分解後の生合成に重要であることが分かりました。今後さらにミトコンドリアと RREB1をつなぐ因子の同定に取り組んでいきます。

Development of Planar Chiral Cyclic (Amino) (ferrocenyl) carbene Ligands for Medicinal Chemistry

Kazuhiro Yoshida
kyoshida@faculty.chiba-u.jp
Chiba University

Summary Abstract

New cyclic (amino)(ferrocenyl)carbene (CAFeC) ligand containing the $C_5(Ph)_5$ group has been developed as a modification of their prototype Cp version. The new carbene was generated from a salt by simple deprotonation with a strong base and identified by a carbene trapping experiment with sulfur.

Key Words : asymmetric synthesis, chiral N-heterocyclic carbene (NHC), planar chirality

Introduction

Chiral N-heterocyclic carbenes (NHCs) have received much recent attention for their importance as asymmetric organocatalysts and chiral ligands in transition metal catalysis. Very recently, we developed a new type of planar chiral cyclic (amino)(ferrocenyl)carbene (R_p)-**1**. The purpose of this study was to develop Cp(Ph)$_5$ version (R_p)-**2** in order to create a more attractive chiral environment than **1** as chiral ligands because of the bulkiness of the $C_5(Ph)_5$ group.

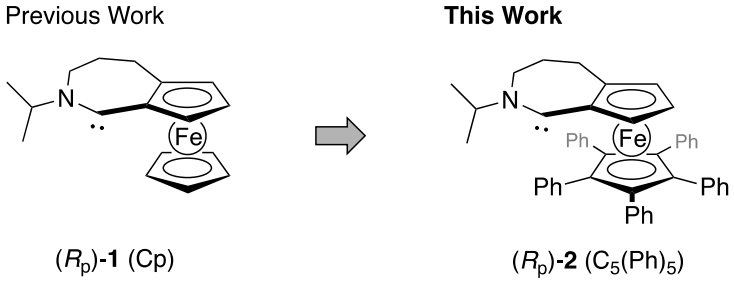

With the aim to increase steric hindrance

Results

Scheme 1.

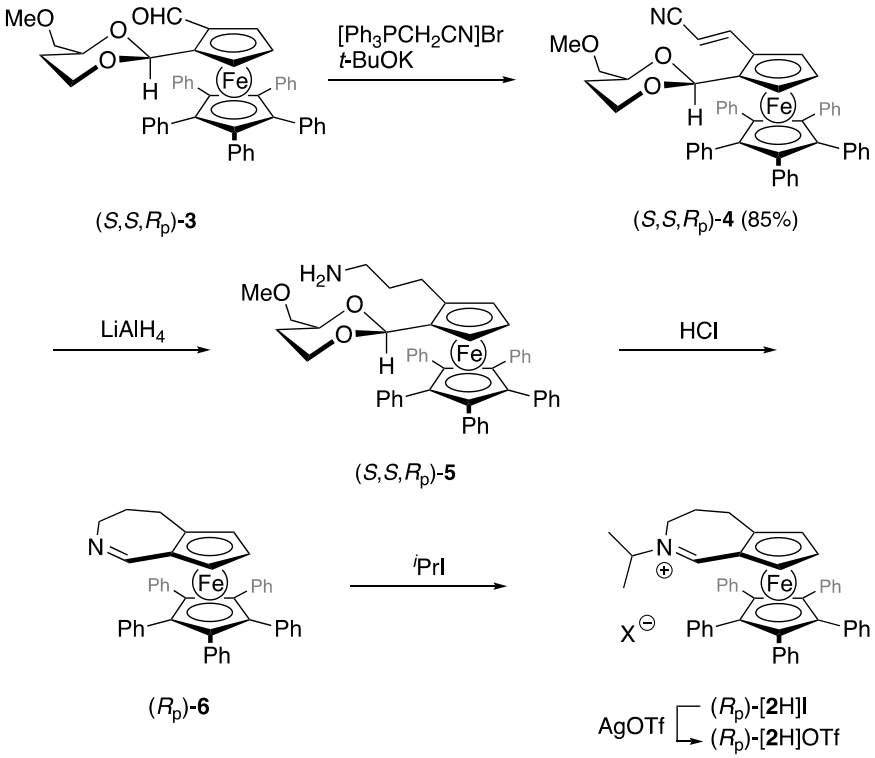

The synthetic route to carbene precursor (R_p)-[**2**H]OTf is shown in Scheme 1. Here, the same strategy as that established by us for prototype ligand (R_p)-**1** was employed. First, known chiral formylferrocene **3**, which was obtained by a diastereoselective *ortho*-functionalization strategy, was subjected to the Wittig reaction with $[Ph_3PCH_2CN]Br$ to form **4**. Then, resulting **4** was treated with $LiAlH_4$ to give primary amine **5**. Then, **5** was treated with hydrochloric acid for acetal hydrolysis, and this was followed by a spontaneous intramolecular cyclization reaction to yield aldimine **6**. Desired iminium salt (R_p)-[**2**H]OTf was obtained by reacting **6** with isopropyl iodide, followed by an anion exchange with AgOTf.

Because it was confirmed that CAFeC **1** was not isolable and decomposed into a mixture even at low temperature, the generation of **1** was indirectly confirmed by carbene trapping experiments with sulfur in our previous study. The same trapping experiment was also conducted to confirm the generation of **2**. As a result, the addition of LiHMDS as a base to a mixture of iminium salt (R_p)-[**2**H]OTf and sulfur in THF gave desired sulfur adduct (R_p)-**7** in 26% yield (Scheme 2).

Scheme 2.

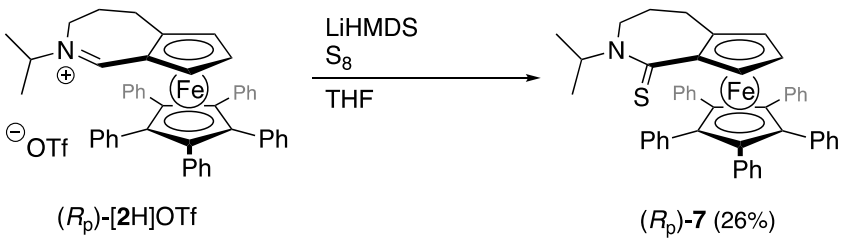

Discussion & Conclusion

We have developed novel CAFeC ligand **2** with $C_5(Ph)_5$ group by the modification of its prototype version, **1**. The existence of the carbene at low temperature was confirmed by a carbene trapping experiment with sulfur. Encouraged by these results, we are now preparing its metal complexes to apply this novel ligand in asymmetric reactions.

References

1. Planar Chiral Cyclic (Amino)(ferrocenyl)carbene as Ligand for Transition Metals *Adv. Synth. Catal.* **2017**, *359,* 255-259. Risa Yasue, Masaru Miyauchi, and Kazuhiro Yoshida
2. Coordination Behavior of a Planar Chiral Cyclic (Amino)(Ferrocenyl)Carbene Ligand in Iridium Complexes *Chem. Eur. J.* **2017**, *23*, 16806-16812. Yuta Shikata, Risa Yasue, and Kazuhiro Yoshida
3. A Planar Chiral Six-Membered Cyclic (Amino)(Ferrocenyl)Carbene and Its Sulfur Adduct *Tetrahedron: Asymmetry* **2017**, *28*, 824-829. Risa Yasue, Masaru Miyauchi, and Kazuhiro Yoshida
4. Planar-Chiral Ferrocene-Based N-Heterocyclic Carbene Ligands *Chem. Eur. J.* **2018**, *24*, 18575-18586. Kazuhiro Yoshida and Risa Yasue
5. Synthesis and Application of Planar Chiral Cyclic (Amino)(ferrocenyl)carbene Ligands Bearing FeCp* Group *Organometallics* **2019**, *38*, 2211-2217. Risa Yasue and Kazuhiro Yoshida
6. Development of Planar Chiral Five-membered Cyclic (Amino)(ferrocenylene)carbene Ligand and Its Iridium Dicarbonyl Complex *Bull. Chem. Soc. Jpn.* **2020**, *92*, 200-204. Waka Takagaki, Risa Yasue, and Kazuhiro Yoshida

一般の皆様へ

中心不斉や軸不斉を持つことにより、その鏡像と重ね合わすことのできない化合物は鏡像異性体と呼ばれています。鏡像異性体は互いにその生物活性を異にするため、これらを区別して合成することは医薬化学及び有機合成化学における重要課題となっています。本研究は、このような鏡像異性体を作り分ける技術の中で、最も理想的とされている「触媒的不斉合成（微量の不斉源より大量の光学活性化合物の合成を可能とする技術）」分野における研究です。将来の産業に役立つ、力量ある触媒の開発を目指しています。

Regulation of gene expression network and cell death by microRNAs during viral infection

Tomoko Takahashi
takahas@mail.saitama-u.ac.jp
Saitama University

Summary Abstract

RNA silencing is a posttranscriptional gene silencing mechanism directed by endogenous small non-coding RNA, microRNAs (miRNAs). By contrast, the type-I interferon (IFN) system is an innate immune system activated by exogenous RNA such as viral RNAs. RNA silencing and IFN system are considered as independent pathways previously. We found that the crosstalk between RNA silencing and IFN system regulates gene expression network and functions as an antiviral defense system in mammalian cells.
Key Words : microRNA, IFN system, antiviral immunity

Introduction

RNA silencing is a posttranscriptional gene silencing mechanism directed by endogenous small non-coding RNAs called microRNAs (miRNAs). The human genome encodes > 2,000 miRNAs, and the deletion or mutation, as well as upregulation or downregulation, of miRNA causes serious diseases including cancer, neurodegenerative diseases, and diabetes. By contrast, the type-I interferon (IFN) system is an innate immune system activated by exogenous RNAs, such as viral RNAs.

Results

During viral infection, viral RNAs are detected by virus sensor proteins, including Toll-like receptors (TLRs) and retinoic acid-inducible gene I (RIG-I)-like receptors (RLRs) in the endosome and cytoplasm, respectively. The activated sensor proteins transfer signals to the downstream molecules to induce IFN production. Secreted IFN induces hundreds of IFN-stimulated genes (ISGs), which represses viral replications.

Among RLRs, RIG-I recognizes 5'-triphosphate- or 5'-diphosphate RNA and small RNA duplexes, and MDA5 recognizes long RNA duplexes as exogenous RNAs. They transfer signals to downstream molecules through their caspase recruitment domains (CARDs). LGP2 is a member of the RLRs, but does not have a CARD, rendering it incapable of transferring signals downstream. We identified that LGP2 modulates RNA silencing by interacting with the RNA silencing enhancer, TRBP. LGP2 interacts with TRBP via the dsRNA-binding sites of TRBP through competition with TRBP-bound pre-miRNAs. This competitive binding inhibits the binding of 40 types of pre-miRNAs with TRBP in HeLa cells, as well as the maturation of those miRNAs by Dicer/TRBP, and their subsequent RNA silencing activities.

To identify the spe- cific structural characteristics of TRBP-bound and -non- bound pre-miRNAs, we calculated the base-pairing prob- ability (BPP), which provides the probability for each base- pair with respect to an ensemble of RNA secondary struc- tures for predict-

ing accurate RNA secondary structure. The mean BPP values at stem regions of all pre-miRNAs, TRBP-bound and non-bound pre-miRNAs were calculated using the max values of fluctuating BPPs at each nucleotide, calculated by CentroidFold. The results clearly distinguished be- tween pre-miRNA that preferably bound to TRBP and pre- miRNA not bound to TRBP in the context of miRNA sec- ondary structures. The stem region of TRBP-bound pre- miRNA had tight base-pairing, while that of TRBP-non- bound pre-miRNA had weak base-pairing.

Thus, LGP2 has been demonstrated to inhibit RNA silencing directed by TRBP-bound miRNAs and upregulate expression of their target genes. However, the biological implications of this activity remained unclear. We generated TRBP or LGP2 knock-out cell lines using CRISPR/Cas9 genome engineering. The Gene expression profiling using these cell lines revealed that apoptosis regulatory genes were upregulated during SeV infection: caspases-2, -8, -3 and -7, four cysteine proteases with key roles in apoptosis, were upregulated directly or indirectly through the repression of a typical TRBP-bound miRNA, miR-106b. LGP2 upregulated apoptosis regulatory genes by inhibition of TRBP-bound pre-miRNA maturation by competitive binding with TRBP, and enhanced apoptosis during Sendai virus (SeV) infection. SeV is a single-stranded RNA virus recognized by RIG-I, and its infection induces IFN production, which strongly induces LGP2 expression. Induced LGP2 protein interacted with TRBP and reduced RNA silencing directed by a typical TRBP-bound miRNA, miR-106b, resulting in upregulation of its target genes, including initiator or executioner caspases, directly or indirectly.

We showed that caspase-2 is a direct target of miR-106b. Although we could not clarify whether caspase-8 is a direct or indirect target gene of miR-106b, caspase-2 is reported to be activated along with caspase-8 in response to multiple triggers including DNA damage, heat shock, endoplasmic reticulum stress, and oxidative stress. The initiator caspases, caspases-2 and -8, form a complex with Fas-associated protein with death domain (FADD), and this interaction induces the downstream activation of executioner caspase-3, and finally induces apoptosis. Thus, LGP2 may efficiently enhance apoptosis by regulating initiator caspase(s).

Discussion & Conclusion

The function of one of RLRs, LGP2, was controversial. We revealed that LGP2 functions as a modulator of RNA silencing by interacting with an RNA silencing enhancer, TRBP. The biological implication of modulation of RNA silencing by LGP2 induction during viral infection was unclear in previous reports, but we found that LGP2 upregulates apoptosis regulatory genes mediated by the repression of TRBP- bound miRNAs and enhances apoptosis during SeV infection. Our finding showed that the crosstalk between RNA silencing, which is directed by endogenous miRNAs, and IFN system, which is activated by exogenous viral RNAs, functions to induce apoptosis as an antiviral defense system in mammalian cells.

References

Takahashi T, Ui-Tei K.
Mutual regulation of RNA silencing and the IFN response as an antiviral defense system in mammalian cells.
Int. J. Mol. Sci. 21, E1348 (2020)
aTakahashi T, Nakano Y, Onomoto K, Yoneyama M, Ui-Tei K.
LGP2 virus sensor enhances apoptosis by upregulating apoptosis regulatory genes through TRBP-bound miRNAs during viral infection.
Nucleic Acids Res. 48, 1494-1507. (2019)

Takahashi T, Nakano Y, Onomoto K, Murakami F, Komori C, Suzuki Y, Yoneyama M, Ui-Tei K. LGP2 virus sensor regulates gene expression network mediated by TRBP-bound microRNAs. Nucleic Acids Res., 46, 9134-9147. (2018)

一般の皆様へ

ウイルスが細胞に感染すると、生体を防御するための免疫応答が誘導されます。我々は、細胞内ウイルスセンサータンパク質のひとつであるとされながらも機能が不明であった「LGP2」がRNA サイレンシングの促進因子である「TRBP」と相互作用することで、TRBP が結合する特定のマイクロ RNA の成熟過程を阻害し、ウイルス感染細胞の細胞死を促進することを明らかにしました。

LGP2と TRBP によるマイクロ RNA を介した細胞死の制御は、ウイルス感染細胞における新しい生体防御機構として機能していると考えられ、抗ウイルス治療や核酸医薬開発への応用が期待されます。

Functional analysis of the paraventricular nucleus of the thalamus involved in social behavior

Kazuhiko Yamamuro
muro@naramed-u.ac.jp
Department of Psychiatry, Nara Medical University

Summary Abstract

Whether oxytocin neurons in posterior paraventricular thalamus (pPVT) are related to sociability are poorly understand. Chemogenetic suppression of oxytocin neurons in pPVT activity in adulthood was sufficient to induce sociability deficits without affecting anxiety-related behaviors. However, optogenetic activation of oxytocin neurons in pPVT activity in adulthood did not increase sociability. Our study identifies oxytocin neurons in pPVT activity required for sociability.

Key Words : Posterior paraventricular thalamus, Oxytocin, Sociability

Introduction

My previous study showed 2 weeks of social isolation immediately following weaning leads to a failure to activate medial prefrontal cortex neurons projecting to the posterior paraventricular thalamus (mPFC→pPVT) during social exposure in adulthood[1)]. However, whether oxytocin neurons in posterior paraventricular thalamus (pPVT) are related to sociability are poorly understand. Here, we sought to identify the specific types of neurons in pPVT that requires sociability.

Results

To examine the extent to which activity of oxytocin neurons in pPVT activity is necessary for sociability, we chemogenetically suppressed the activity of oxytocin neurons in pPVT expressing inhibitory DREADD (iDREADD). Cre-dependent iDREADD or mCherry vector were injected into the pPVT, respectively, to express iDREADD in pPVT neurons in oxtr mice. Suppression of oxytocin neurons in pPVT activity through clozapine N-oxide dihydrochloride (CNO) treatment in adult mice reduced sociability in the three-chamber test ((two-way repeated-measures (RM) ANOVA, drug (CNO or SAL) × stimulus (social or object) interaction $F_{1,24} = 12.900$, $^{**}P = 0.001$; effect of drug $F_{1,24} = 1.905$, $P = 0.180$; effect of stimulus $F_{1,24} = 0.419$, $P = 0.524$), with no impact on motor activity or measurements of anxiety-related behavior (Left, two-tailed paired *t*-test, $t_{12} = 0.005$, $P = 0.996$, Middle, two-tailed paired *t*-test, $t_{12} = 0.864$, $P = 0.405$, Right, two-tailed paired *t*-test, $t_{12} = 0.368$, $P = 0.719$). Moreover, we found reduced social contact in suppression of oxytocin neurons in pPVT activity through AR-LABO (Animals Behavior Observing-system). CNO injection in mCherry-expressing control mice produced no significant differences in behavior compared with saline (SAL) injection in sociablity(two-way RM ANOVA, drug (CNO or SAL) × stimulus (social or object) interaction $F_{1,18} = 0.428$, $P = 0.415$; effect of light $F_{1,18} = 0.204$, $P = 0.657$; effect of stimulus $F_{1,18} = 6.135$, $P = 0.023$) and motor activity or anxiety-related behaviors (Left: two-tailed

paired *t*-test, $t_9 = 0.796$, $P = 0.447$, Middle: two-tailed paired *t*-test, $t_9 = 1.267$, $P = 0.237$, Right: two-tailed paired *t*-test, $t_9 = 0.255$, $P = 0.804$)..

To examine whether oxytocin neurons in pPVT activity is sufficient to increase sociability in adult mice, we optogenetically activated oxytocin neurons in pPVT virally expressing channelrhodopsin (ChR2) under the CaMKII promotor by wirelessly illuminating a blue LED implanted over the pPVT while mice performed the three-chamber test. CaMKII-ChR2 AAV1 was injected into the pPVT and a wireless blue LED was inserted above the pPVT in oxtr mice. However, we did not find that optogenetic activation of oxytocin neurons in pPVT within the social-interaction chamber led to an increase in sociability (two-way RM ANOVA, light (ON or OFF) × stimulus (social or object) interaction $F_{1,18} = 0.428$, $P = 0.415$; effect of light $F_{1,18} = 0.204$, $P = 0.657$; effect of stimulus $F_{1,18} = 6.135$, $P = 0.023$). On the other hand, optogenetic activation of oxytocin neurons in pPVT in one of two empty corral interaction zones was sufficient to increase time spent in that zone (ChR2+ mice with optogenetic stimulation showed real-time preference to the stimulation zone (S) over the nonstimulation zone (N) as indicated by increased discrimination score (calculated as (S − N)/(S + N), two-tailed paired *t*-test, $t_9 = 3.197$, $^*P = 0.011$) as well as investigation time (two-way RM ANOVA, time (OFF, ON) × zone (stimulation zone or nonstimulation zone) interaction $F_{1.18} = 8.500$, $^{**}P = 0.009$; effect of time $F_{1.18} = 3.185$, $P = 0.091$; effect of zone $F_{1.18} = 2.879$, $P = 0.107$).

Discussion & Conclusion

Overall, our study identifies oxytocin neurons in pPVT activity required for normal adult sociability. Given that the paraventricular thalamus (PVT) projects to various reward-associated areas including the nucleus accumbens, the bed nucleus of the stria terminalis and the central amygdala through collateralized projections[2)3)]. In contrast to other mPFC projections that have been reported to reduce sociability upon activation, such as the projections to the lateral habenula (located in close proximity to the PVT), activation of mPFC→PVT projections promotes sociability[4)5)]. Future studies are warranted to reveal how different populations of mPFC projection neurons influence subcortical networks that control social behavior and are impacted by previous social experience.

References

1) Yamamuro K et al. A prefrontal–paraventricular thalamus circuit requires juvenile social experience to regulate adult sociability in mice. Nature Neuroscience volume 23, pages1240–1252 (2020)
2) Kirouac, G. J. Placing the paraventricular nucleus of the thalamus within the brain circuits that control behavior. Neurosci. Biobehav. Rev. 56, 315–329 (2015).
3) Dong, X., Li, S. & Kirouac, G. J. Collateralization of projections from the paraventricular nucleus of the thalamus to the nucleus accumbens, bed nucleus of the stria terminalis, and central nucleus of the amygdala. Brain Struct. Funct. 222, 3927–3943 (2017).
4) Benekareddy, M. et al. Identification of a corticohabenular circuit regulating socially directed behavior. Biol. Psychiatry 83, 607–617 (2018).
5) Murugan, M. et al. Combined social and spatial coding in a descending projection from the prefrontal cortex. Cell 171, 1663–1677.e16 (2017).

一般の皆様へ

オキシトシンが社会行動に関わることが知られているが、その機序はいまだに不明のままである。私達は前頭全皮質－視床室傍核の神経回路が者かい行動に関わることを報告した。その視床室傍核にはオキシトシン受容体が発現している神経細胞が豊富にあることが知られており、今回は視床室傍核のオキシトシン受容体が発現している神経細胞が社会行動に関わることを明らかにした。今後はさまざまな精神疾患に関わる社会行動への薬物治療への応用が期待される。

Identification of precursor memory B cells and mechanistic characterization of memory B cell generation

Takeshi Inoue
inoue@ifrec.osaka-u.ac.jp
Immunology Frontier Research Center, Osaka University

Summary Abstract

Memory B cells and long-lived plasma cells are the critical components of humoral immune memory. In this study, we analyzed the memory B cells differentiation mechanisms during germinal center reaction using single cell RNA-seq techniques. These results may contribute to the understanding how immunological memory establishes in our body during infection or vaccination.

Key Words : memory B cell, vaccine, single cell RNA-seq

Introduction

"Immunological memory" is the ability of the immune system of our body to quickly and specifically recognize the previously encountered antigens, such as viruses and bacteria. Memory B cells and long-lived plasma cells are the cellular components which have central roles in humoral immune memory. In this study, we have tried to identify and characterize precursor memory B cells during germinal center B cell selection using single cell RNA-seq techniques.

Results

During germinal center (GC) reaction, light zone B cells are selected to differentiate into memory B cells, plasma cells, or to re-enter into dark zone. We have previously identified and characterized a small GC population of precursor memory B cells, and found that GC B cells with lower mTORC1 activity resulted from weak T cell help and higher survival signal from surface B cell receptors favor a memory B cell fate (Fig. 1) (Inoue et al., ***J Exp Med***, 2021).

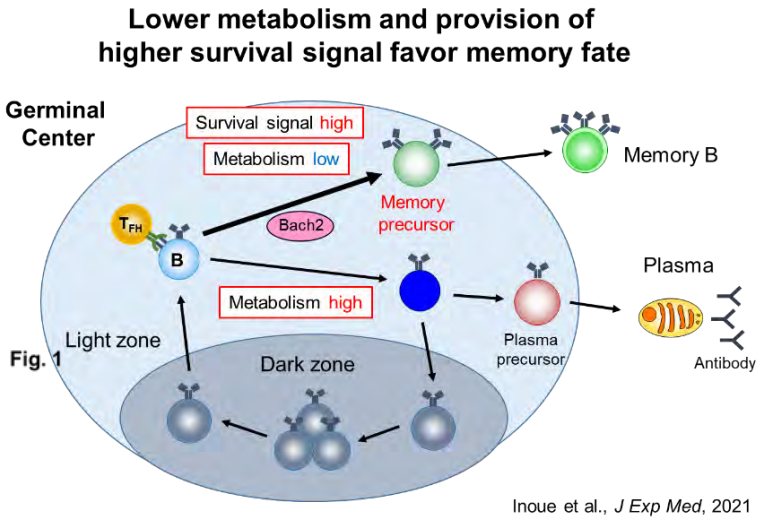

Fig. 1

To further clarify the detailed trajectory path of the GC B cell differentiation into memory B cell, I first performed a high throughput droplet-based single cell RNA-seq (scRNA-seq) analysis on sorted splenic murine B cells after T cell dependent antigen (protein) immunization using the 10x Genomics Chromium platform. After quality control, 9,972 cells with 2,086 median genes per cell were retained. Unsupervised clustering revealed 14 clusters on t-SNE plot, which were assigned to each B cell subsets (GC light zone, dark zone, plasma cells, memory B cells, and naïve B cells) using known landmark genes (*Cd38*, *Bcl6*, *Zeb2*, *Cd83*, *Sdc1*, and *Hmmr*) (Fig. 2). Validation of this assignment was achieved by comparing the results with bulk RNA-seq data we obtained before (Inoue et al., ***J Exp Med***, 2021).

Fig. 2

scRNA-seq analysis of samples prepared as above was also performed using micro-well based BD Rhapsody platform, which provided a comparable or a slightly better throughput and sensitivity than with 10x Chromium. These results showed that scRNA-seq analysis of murine activated B cells has been successfully set up with two independent platforms. Interestingly, these scRNA-seq data identified putative dying GC B cells (not dead cells) which could not be observed in the conventional flow cytometry analysis, suggesting the possibility of the existence of GC B cell-specific population which failed to receive appropriate T cell help and therefore are destined to apoptosis and to be outcompeted during selection. Differential gene expression analysis to identify the specific genes in this apoptosis-prone GC population is now under investigation.

Discussion & Conclusion

scRNA-seq analysis of primary immune cells, such as B cells and T cells, is generally difficult due to their extremely low mRNA abundance, resulted in only few studies published so far (Laidlaw et al., ***Nat Immunol***, 2020). In this study, I have successfully obtained scRNA-seq data using ex vivo murine GC B cells and assigned each clusters to known B cell subsets and also identified uncharacterized dying GC B cells. Clarifying the heterogeneity in GC B cells will be a key to elucidate the memory B cell generation from the GC.

Given the importance of memory B cells in protecting us against re-infection, understanding how memory B cells are produced will provide us the basal information required for novel vaccine design against Influenza infection or COVID-19. Our studies may contribute better understanding how immunological memory against these viruses or vaccines establishes in our body.

References

Inoue T, Shinnakasu R, Kawai C, Ise W, Kawakami E, Sax N, Oki T, Kitamura T, Yamashita K, Fukuyama H, Kurosaki T. Exit from germinal center to become quiescent memory B cells depends on metabolic reprograming and provision of a survival signal. ***J Exp Med.*** 218(1):e20200866, 2021

Laidlaw BJ, Duan L, Xu Y, Vazquez SE, Cyster JG. The transcription factor Hhex cooperates with the corepressor Tle3 to promote memory B cell development. ***Nat Immunol.*** 21(9):1082-93, 2020

一般の皆様へ

免疫記憶応答はワクチン療法の根幹となる免疫反応であり、記憶 B 細胞の産生、活性化原理の解明は、インフルエンザ・新型コロナウイルスなどに対する効果的なワクチン開発において重要な課題である。我々は様々なマウスモデルを駆使して記憶 B 細胞の分化メカニズムの解明に注力し、エネルギー代謝や生存シグナルの獲得など記憶 B 細胞への分化運命決定に必要な様々な細胞特性を明らかにしてきた。このような基礎研究による知見の蓄積が新規ワクチン開発戦略に貢献できれば幸いである。

Rhodium(I)-catalyzed enantioselective hydroacylation through dynamic kinetic resolution

Yoshihiro Oonishi
oonishi@pharm.hokudai.ac.jp
Faculty of Pharmaceutical Sciences Hokkaido University

Summary Abstract

Rhodium(I)-catalyzed enantioselective intermolecular hydroacylation of an alkyne through a dynamic kinetic resolution was investigated. It was found that the reaction of a racemic aldehyde having a sulfur atom in the tether with an alkyne gave the α,β-unsaturated ketone in good yield with moderate ee.

Key Words : rhodium, hydroacylation, enantioselective, alkyne, aldehyde

Introduction

Transition metal-catalyzed hydroacylation is one of the most promising methods for the synthesis of ketones from an aldehyde and a C-C multiple bond.[1] In particular, rhodium-catalyzed intermolecular hydroacylation of an alkyne has been received much attention from chemists because various α,β-unsaturated ketones can be prepared by using it.[1] However, there is only one report on the enantioselective variant through a *kinetic resolution* so far.[2] In this context, I investigated rhodium(I)-catalyzed enantioselective intermolecular hydroacylation of an alkyne through a *dynamic kinetic resolution*.

Results

Initially, the reaction of racemic aldehyde **1a** having a sulfur atom in the tether with alkyne **2a** was investigated (Table 1). The reaction was carried out in the presence of 10 mol% of $[Rh(cod)_2]ClO_4$ and (*R,R*)-Me-duphos at 0 °C in acetone, and the desired α,β-unsaturated ketone **3aa** showed moderate yield and low ee (entry 1). Next, the effects of the reaction temperature and additives were examined. As a result, it was found that when the reaction was carried out at -20°C, the yield of **3aa** was improved to 78%, albeit with 10% ee (entry 2). On the other hand, the use of alcohol and phenol derivative as an additive showed the improvement of the ee of **3aa** (entries 3-6). On the basis of these results, the reaction was carried out using various ligands. When (*R,R*)-Et-duphos was used as a ligand, the reaction proceeded to give **3aa** in 43% yield with 60% ee (entry 7). On the other hand, when biary-type ligands were employed in this reaction, both yield and ee of **3aa** were decreased (entries 8,9).

Table 1. Condition Screening.

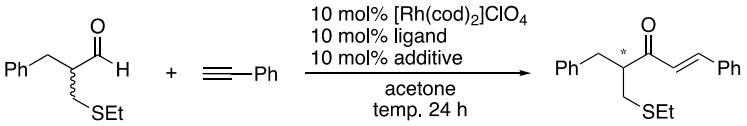

1a (*racemic*) **2a** **3aa**

entry	temp. (°C)	ligand	additive	**3aa** yield (%)	**3aa** ee (%)
1	0	(*R,R*)-Me-duphos	none	59	8
2	-20	(*R,R*)-Me-duphos	none	78	10
3	-20	(*R,R*)-Me-duphos	1-propanol	61	43
4	-20	(*R,R*)-Me-duphos	phenol	71	40
5	-20	(*R,R*)-Me-duphos	BHT	55	56
6	-20	(*R,R*)-Me-duphos	(*R*)-BINOL	53	43
7	-20	(*R,R*)-Et-duphos	phenol	43	60
8	-20	(*R*)-binap	phenol	18	17
9	-20	(*R*)-segphos	phenol	24	20

Next, the reaction of **1a** with various alkyne using (*R,R*)-Me-duphos as a ligand was examined (Scheme 1). As a result, it was found that alkyne **2b** having an alkyl moiety (R = *n*-Bu) at the terminus afforded **3ab** in 49% yield with 65% ee. When alkyne **2c** having *t*-Butyl moiety was used, the yield of **3ac** was decreased to 19%. On the other hand, the use of the internal alkyne **2d** gave α,β-unsaturated ketone **3ad** in 45% yield with 20% ee. These results suggest that the steric and electric property of alkyne **2** is influenced on the reactivity in this hydroacylation.

Scheme 1. Reaction of **1a** with various alkynes.

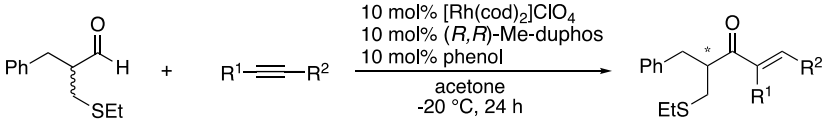

1a (*racemic*)

2b (R^1 = H, R^2 = *n*-Bu)
2c (R^1 = H, R^2 = *t*-Bu)
2d (R^1 = R^2 = Et)

3ab: 49%, 65% ee
3ac: 19%, N.D.
3ad: 45%, 20% ee

Furthermore, the reaction of aldehyde **1b** having an aromatic ring at the α-position with alkyne **2a** was employed in this hydroacylation (Scheme 2). The reaction proceeded to give α,β-unsaturated ketone **3ba** in 79% yield with 26% ee.

Scheme 2. Reaction of **1b** with **2a**.

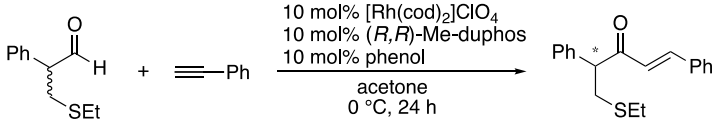

1b (*racemic*) **2a** **3ba**: 79%, 26% ee

Discussion & Conclusion

I investigated rhodium(I)-catalyzed enantioselective intermolecular hydroacylation of an alkyne. As a result, it was found that this hydroacylation proceeded smoothly even at -20 °C, giving the α,β-unsaturated ketone in good yield with moderate ee when phenol was used as an additive. At this stage, this reaction cannot be expanded to the enantioselective hydroacylation through a dynamic kinetic resolution. Further investigation of improvement of the ee is in progress.

References

1. (a) Willis M. C. *Chem. Rev.* **2010**,*110*, 725. (b) Davison, R. T.; Dong, V. M. *Acc. Chem. Res.* **2021**, *54*, 1236.
2. Gonzalez-Rodriguez, C.; Parsons, S. R.; Thompson, A. L.; Willis, M. C. *Chem*. *Eur. J*. **2010**, *16*, 10950.

一般の皆様へ

ロジウム触媒を用いた分子間ヒドロアシル化反応は、アルデヒドとアルキンから不飽和ケトンを合成する効率的な手法です。しかしながら、この方法を利用して光学活性な不飽和ケトンを合成した報告はわずか一例しかありません。そこで、本研究では、動的速度論的光学分割を利用して、この反応を不斉合成へと応用すべく検討しました。その結果、フェノールを添加剤として用いると、ラセミ体のアルデヒドとアルキンから良好な収率及び中程度の不斉収率で不飽和ケトンが得られることがわかりました。不斉収率は未だ満足するものではありませんが、フェノールのような弱酸性の物質を添加すると、ヒドロアシル化反応に大きく影響を与えるという現象を初めて見出しました。

Molecular mechanism underlying development of memory-like Group 2 innate lymphoid cells

Takashi Ebihara
tebihara@med.akita-u.ac.jp
Department of Medical Biology, Akita University Graduate School of Medicine

Summary Abstract

Group 2 innate lymphoid cells (ILC2s) are tissue-resident cells that contribute to the pathogenesis of allergy by producing innate type 2 cytokines. Allergy-experienced ILC2s can live long and exhibit memory-like features upon second allergen challenge. However, it is not clear what activated ILC2s differentiate into memory-like ILC2s or die due to over-activation. Here, our new fate-mapping mice demonstrated that ILC2s extremely activated during chronic allergic airway inflammation express Tigit and are destined to die either in the middle of chronic allergy or in the convalescent phase of allergy. We here show the first evidence of activation-induced cell death of ILC2s during chronic allergy.
Key Words : memory-like ILC2, trained ILC2, Tigit, activation-induced cell death

Introduction

Group 2 innate lymphoid cells (ILC2s) are responsible for innate allergic inflammation[1]. ILC2s can proliferate well in vitro for over a year. However, physiological conditions do not allow ILC2s to grow forever. There should be a machinery of cell death caused by overactivation. We previously showed that activated ILC2s successively express an inhibitory receptor PD-1, an inhibitory cytokine IL-10, and an inhibitory receptor Tigit, and that highly activated ILC2s express all these molecules[2-4]. However, as expression of Tigit by ILC2s is not so high, it is hard to isolate Tigit+ ILC2s for research. In addition, fate of the activated Tigit+ ILC2s remains elusive.

Results

To clearly identify Tigit+ ILC2s and follow the fate of Tigit+ ILC2s, we generated $Tigit^{Cre\text{-}ERT2}$ mice where IRES-Cre-ERT2 is inserted into 3' UTR of *Tigit* gene and crossed the $Tigit^{Cre\text{-}ERT2}$ mice to Rosa26-flox-stop-flox-tdTomato mice. To validate tdTomato expression in Tigit+ cells, we gave tamoxifen to the $Tigit^{Cre\text{-}ERT2}$: Rosa26-flox-stop-flox-tdTomato mice ($Tigit^{fm}$ mice) and confirmed that tdTomato expression correlates Tigit expression in Treg and NK cells both of which are known to express Tigit. The Lung ILC2s did not express tdTomato as steady state ILC2s do not express Tigit. Thus, our fate mapping system works well to label Tigit-expressing cells by tdTomato expression.

To induce tdTomato+ ILC2s in the lung, we intranasally administered papain and gave tamoxifen twice a week until day 21. One-to-two % of lung ILC2s expressed tdTomato since day 9. As the tdTomato+ ILC2s produced more IL-5 and IL-10 than tdTomato− ILC2s, they can be recognized as more activated ILC2s than tdTomato− ILC2s. Although number of lung ILC2s dramatically increased during repeated papain treatments, frequencies of tdTomato+

cells among the lung ILC2s were quite stable, suggesting that Tigit+ ILC2s do not have a tendency to accumulate at the site of chronic inflammation like exhausted-T cells. To address the question whether Tigit+ ILC2s live long in the convalescent phase of airway allergy, we examined tdTomato+ lung ILC2s a week or a month after cessation of papain treatment. Number of tdTomato+ ILC2s reduced by half a week after the last treatment and completely disappear another three weeks later. Thus, chronic allergy is required for the emergence of tdTomato+ ILC2s that never differentiate to memory-like ILC2s.

Given chronic allergy constantly gives rise to highly activated tdTomato+Tigit+ ILC2s that neither die nor leave the lung during inflammation, such tdTomato+ ILC2s would accumulate in the lung with chronic allergy. However, frequency of tdTomato+ lung ILC2s did not goes up as allergic inflammation deteriorated. To examine the possibility that tdTomato+ ILC2s migrate to lymph node or other organ through blood stream, we sought to identify tdTomato+ ILC2s in the lymph node and peripheral blood. However, tdTomato+ ILC2s did not exist there, suggesting that tdTomato+ ILC2s may not leave the lung. We then hypothesized that tdTomato+ ILC2s are destined to die due to overactivation. To explore whether tdTomato+ ILC2s tend to die, we sorted tdTomato− ILC2s and tdTomato+ ILC2s from the lung with chronic allergy and cultured the cells with IL-2/IL-7/IL-33 to keep activation status. More tdTomato+ ILC2s were dead than tdTomato− ILC2s. These data suggest that tdTomato+ ILC2s are in a high activation status just before cell death.

To determine physiological roles of activation-induced cell death of Tigit+ ILC2s during chronic allergy, we injected blocking antibody against Tigit to the Tigit^{fm} mice and induced chronic allergy as described above. Blockade of Tigit increased tdTomato+ ILC2s that were associated with increased eosinophil recruitment to the lung. Therefore, activation-induced cell death through Tigit+ ILC2s is an important regulatory mechanism during chronic airway allergy.

Discussion & Conclusion

Our new mouse system for fate-mapping of Tigit+ cells revealed that Tigit+ ILC2s represent a highly activated subpopulation of ILC2s destined to die during chronic allergy and in recovery period of allergy. Blockade of Tigit during chronic pulmonary allergy increased Tigit+ ILC2s in the lung. This is striking resemblance to exhausted Tigit+ CD8 T cells whose apoptosis is reduced by Tigit blockade. To clarify decisive factors of activation-induced cell death, we are currently investigating transcriptional and epigenetic changes in tdTomato+ ILC2s.

References

1. Ebihara T*. Dichotomous Regulation of Acquired Immunity by Innate Lymphoid Cells. Cells. 11;9(5):1193.2020.
2. Miyamoto C, Ebihara T*. Runx/Cbfβ complexes protect group 2 innate lymphoid cells from exhausted-like hyporesponsiveness during allergic airway inflammation. Nat Commun. 10:447, 2019.
3. Ebihara T* and Taniuchi I. Exhausted-like Group 2 Innate Lymphoid Cells in Chronic Allergic Inflammation. Trends Immunol. 40:1095-1104, 2019.

4. Ebihara T* et al. Trained innate lymphoid cells in allergic diseases. Allergology International. 70: 174-180. 2021.

一般の皆様へ

アレルギー炎症は増悪していく疾患傾向を持ちますが、その原因については未だ分かっていないことが多いです。私達は、免疫細胞の中でアレルギー炎症の記憶を持ち、アレルギー疾患の増悪に寄与する2型自然リンパ球（ILC2）の研究を行いました。ILC2 は炎症を経験した後、多様な細胞集団へと変化しますが、炎症の後も生き残り炎症の記憶を持つようになる細胞集団と死にゆく運命の細胞集団の区分は明らかになっていませんでした。私達は、Tigit という抑制性受容体を発現した ILC2 は活性化により常に死んでいく運命にあることを明らかにしました。

Development of urolithiasis therapy by immune response and repair mechanism

Takahiro Yasui
yasui@med.nagoya-cu.ac.jp
Nagoya City University Graduate School of Medical Sciences

Summary Abstract

Urolithiasis, a complex multifactorial disease, results from interactions between environmental and genetic factors. Recent literature has shown that oxidative stress and reactive oxygen species could be one such mechanistic pathway. We attempted to elucidate the mechanism of urethral stone formation by focusing on the in vivo immune response and repair mechanism. (1) Deregulated MTOR is responsible for autophagy defects exacerbating kidney stone development. (2) M1/M2-macrophage phenotypes regulate renal calcium oxalate crystal development. (3) Fatty acid-binding protein 4 downregulation drives calcification in the development of kidney stone disease
Key Words : Urolithiasis, macrophage, autophagy, transcriptomics

Introduction

Kidney stone disease has a high prevalence and recurrence rate, so that a number of patients would suffer from this illness. The recent studies with Randall's plaque, urinary components, as in vivo/vitro experiments, including gene manipulation, tried to unveil its pathogenesis; however, pieces of evidence were yet complicated to integrate to develop a novel therapy to cure this disease of its origin. One of the promising findings in renal and peripheral macrophages' involvement via the inflammatory process, which potentially leads to the therapeutic target.

Results

(1) Autophagy in renal tubular cells

As cellular damage in renal tubular cells (RTCs) is responsible for the disease, here, we focused on the role of macroautophagy/autophagy in RTCs. We found that autophagic activity was significantly decreased in mouse RTCs exposed to calcium oxalate (CaOx) monohydrate crystals and in the kidneys of GFP-conjugated MAP1LC3B (microtubule-associated protein 1 light chain 3 beta) transgenic mice with CaOx nephrocalcinosis induced by glyoxylate. This caused accumulation of damaged intracellular organelles, such as mitochondria and lysosomes, the normal functioning of which is mediated by functional autophagy. An impairment of autophagy was also observed in the mucosa with plaques of CaOx kidney stone formers. We determined that the decrease in autophagy was caused by an upregulation of MTOR (mechanistic target of rapamycin kinase), which consequently resulted in the suppression of the upstream autophagy regulator TFEB (transcription factor EB). Furthermore, we showed that an MTOR inhibitor could recover a decrease in autophagy and alleviate crystal-cell interactions and the formation of crystals associated

with increased inflammatory responses.

(2) Macrophage phenotypes for renal calcium oxalate crystal development

We investigated the role of M1/M2s in crystal development by using in vitro and in vivo approaches. The crystal phagocytic rate of bone marrow-derived M2Mφs was higher than that of bone marrow-derived Mφs and M1Mφs and increased on co-culture with renal tubular cells (RTCs). However, the amount of crystal attachment on RTCs reduced on co-culture with M2Mφs. In six hyperoxaluric C57BL/6J mice, M1Mφ transfusion and induction by LPS and IFN-γ facilitated renal crystal formation, whereas M2Mφ transfusion and induction by IL-4 and IL-13 suppressed renal crystal formation compared with the control.

These M2Mφ treatments reduced the expression of crystal-related genes, such as osteopontin and CD44, whereas M1Mφ treatment increased the expression of pro-inflammatory and adhesion-related genes such as IL-6, inducible NOS, TNF-α, C3, and VCAM-1.

(3) Fatty acid-binding protein 4 (FABP4) for calcification in the development of kidney stone disease

We aimed to utilize a transcriptomics approach to discover the missing link between these two epidemic diseases. We investigated gene expression profiling of nephrolithiasis patients by two RNA-sequencing approaches: comparison between renal papilla tissue with and without the presence of calcified Randall's plaques (RP), and comparison between the papilla, medulla, and cortex regions from within a single recurrent stone forming kidney. Results were overlaid between differentially expressed genes found in the patient cohort and in the severely lithogenic kidney to identify common genes. Overlay of these two RNA-sequencing datasets demonstrated there is impairment of lipid metabolism in renal papilla tissue containing RP linked to downregulation of FABP4. Immunohistochemistry of human kidney specimens and microarray analysis of renal tissue from a nephrolithiasis mouse model confirmed that FABP4 downregulation is associated with renal stone formation. In a FABP4 knockout mouse model, FABP4 deficiency resulted in the development of both renal and urinary crystals.

Discussion & Conclusion

(1) We conclude that autophagy compromised by MTOR deregulation is a fundamental feature in the pathology of kidney stone formation, and propose that chemical inhibition of MTOR could be a prospective strategy for disease suppression.

(2) The expression of M2Mφ-related genes was lower whereas that of M1Mφ-related genes was higher in papillary tissue of CaOx stone formers. Overall, our results suggest that renal crystal development is facilitated by M1Mφs, but suppressed by M2Mφs.

(3) Our study revealed that FABP4 plays an important, previously unrecognized role in kidney stone formation, providing a feasible mechanism to explain the link between nephrolithiasis and metabolic syndrome.

References

Taguchi K, Yasui T, et al. Kidney Int. 2020 May;97(5):1042-1056.

Okada A, Yasui T, et al. Active Phagocytosis and Diachronic Processing of Calcium Oxalate Monohydrate Crystals in an in vitro Macrophage Model. Kidney Blood Press Res. 2019;44(5):1014-1025.

Yasui T, et al. Pathophysiology-based treatment of urolithiasis. Int J Urol. 2017 Jan;24(1):32-38.

一般の皆様へ

尿路結石の再発率は 5 年で 50％と高いが、予防法は確立していない。尿路結石の形成機序は、結石内に 90 数％含まれる無機成分からのアプローチが主体であった。私たちは結石内にわずか数％しか含まれていない有機物質（マトリックス）が結石形成に重要な作用をしていると考え、細胞傷害を介し、マトリックスの発現を介して尿路結石が形成される分子機構を解明した。尿路結石モデルマウスでの腎結石が自然消失する」という現象を捉え、この現象に着目し、治療法開発にむけた尿細管上皮細胞・Ｍ φ・脂肪細胞らの免疫応答と細胞間ネットワークの機序解明を行った。

The model chicken of cardiac septum defect ; A new tool for analysis of structural heart disease

Saori Tani-Matsuhana
tmsaori@port.kobe-u.ac.jp
Kobe University

Summary Abstract

The cardiac neural crest cells arise in the caudal hindbrain and then migrate to the heart through the pharyngeal arches. These cells contribute to heart formation, including the outflow tract, and are unique to this neural crest population. MafB is a transcription factor expressed specifically in early migrating cardiac neural crest cells in addition to being expressed in rhombomeres (r) 5 and 6. We showed that MafB is a novel critical player in proper cardiac neural crest development, and propose that MafB is part of a gene regulatory subcircuit that is unique to the cardiac neural crest.

Key Words : Cardiac neural crest, Heart development, Cardiac defect, Gene regulatory mechanism

Introduction

The neural crest is an embryonic multipotent cell population characterized by migratory and differentiation abilities. They differentiate into peripheral neurons, pigment cells, craniofacial chondrocytes and connective tissue, and so on. Cardiac neural crest is a subpopulation of the neural crest and is positioned from the post-otic vesicle to the 3rd somite. They migrate through pharyngeal arches 3, 4 and 6 and contribute to the formation of the heart, including the septum of the aortic and pulmonary trunks, aortic arches and cardiac ganglions.

Results

To reveal the genome-wide profile in cardiac neural crest cells, we have used a FoxD3 neural crest enhancer to isolate a pure population of cardiac neural crest cells for transcriptome analysis. This has led to the identification of transcription factors, signaling receptors/ligands, and cell adhesion molecules upregulated in the early migrating cardiac neural crest. The transcription factor MafB, previously best known for its expression and function in rhombomeres 5 and 6, was isolated as the highest upregulated genes in the cardiac neural crest by the transcriptome analysis (ref.1).

1. Effects of MafB loss on other cardiac neural crest genes

To know the role of MafB in cardiac neural crest gene regulatory network, we examined the effects of MafB-loss of function on expression of other neural crest marker genes, *Sox10*, *Krox20*, *Ets1* as well as *MafB*

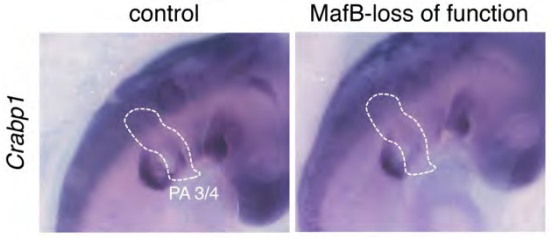

Fig. 1 *Crabp1* expression in MafB-loss of function embryo. PA3/4; Pharyngeal arches 3 and 4

itself. Expression of *Sox10* was reduced in the cardiac neural crest stream on the loss of function embryos, whereas cranial neural crest cells were unaffected. Expression of *Krox20*, *Ets1* and *MafB* itself was also reduced. We also analyzed the long-term effects of MafB-loss of function in later stage embryo. In migrating cardiac neural crest cells of pharyngeal arches (PA) 3 and 4, which is a known pathway of cardiac neural crest cell migration into the developing heart, MafB-loss of function embryo shows slightly reduced expression of *Crabp1* which is a later neural crest marker gene (Fig. 1).

2. MafB is a critical input for Sox10E2 enhancer activity in the cardiac neural crest

Sox10 is a neural crest marker gene expressed at all axial levels including the cardiac neural crest. The Sox10E2 enhancer is specifically expressed in the cranial plus post-otic neural crest, but absent from the trunk neural crest. We found that three previously unrecognized putative MafB binding sites, MafB (a), MafB (b) and MafB (c), within the Sox10E2 enhancer. To test the necessity of MafB sites to mediate reporter expression, we individually mutated each motif within the enhancer. Wild-type or mutant constructs driving GFP were electroporated onto chicken embryos together with wild-type Sox10E2 driving mCherry as a control reporter. Mutation of binding motifs MafB(b) and MafB(c) resulted in reduced GFP expression in cardiac neural crest cells. This result showed that MafB is a critical input for Sox10E2-driven *Sox10* expression in cardiac neural crest (ref. 1).

3. The transcriptional regulation mechanism to express MafB in cardiac neural crest cells

To know the transcriptional mechanism of cardiac neural crest specific expression in MafB gene, we have determined a cis-regulatory region controlling MafB expression by an in vivo reporter assay using chicken embryos. A reporter driven by this region can trace migrating cardiac neural crest cells and the activity is unique to cardiac neural crest cells among neural crest cell population. Taken this advantage of this reporter, we also succeeded to trace the migrating cardiac neural crest cells into the pharyngeal arches in later stages (Tani-Matsuhana and Inoue, *under review*).

Discussion & Conclusion

These results lead us to conclude that MafB is required for proper cardiac neural crest development and provided molecular insight into what makes the cardiac neural crest unique. The reporter gene driven by MafB cis-regulatory region will lead to a molecular technique tracing cell linage in the cardiac neural crest population of the heart. It can also be developed for cardiac neural crest-specific gene knockdown or overexpression experiments, which can be expected as a new tool for analysis of structural heart disease. Thus, the specificity of the MafB regulatory element in cardiac neural crest has potential for promoting our understanding of cardiac neural crest and heart development.

References

(1) Tani-Matsuhana, S., Vieceli, F. M., Gandhi, S., Inoue, K., Bronner, M. E.
(2018) Transcriptome profiling of the cardiac neural crest reveals a critical role for MafB. *Dev. Biol.* 444, S209-S218.

一般の皆様へ

心臓は生命維持に必須な器官です。心臓流出路は、初めは総動脈幹という一本の管ですが、次第に内部に隔壁ができ、大動脈と肺動脈の2本に分離します。この隔壁は心臓神経堤細胞によって形成されています。心臓神経堤細胞の欠損・発生異常は総動脈幹が分離しない総動脈幹遺残症（PTA）を引き起こします。心臓神経堤細胞の重要性は明らかであるにも関わらず、心臓神経堤細胞形成に関わる遺伝子制御機構についてはほとんどわかっていません。これまでの私の研究で、心臓神経堤細胞で特異的に発現するMafB遺伝子が心臓神経堤細胞の初期発生に必須であることを明らかにしました。ニワトリ胚内でMafBの機能を欠失させることで、心臓神経堤細胞由来の隔壁を失った総動脈幹遺残症（PTA）モデルニワトリ胚を作り出し、それを利用して心臓隔壁欠損を引き起こす分子機序の解明を目指しています。

Visualizing aging individuality

Yukinori Hirano
yukinori@ust.hk
Kyoto University

Summary Abstract

We aimed to understand the mechanism underlying aging variability as we define, aging individuality. To this end, we developed the visualizing tools of aging individuality, in which animals produces light when the aging individuality emerges.
Key Words : Aging, Individuality, Drosophila

Introduction

As our population rapidly ages, the promotion of healthy aging is of critical importance for modern society. Previous studies have identified conserved aging factors among different species, including Sirtuin family proteins (ref. 1), the mammalian target of rapamycin (mTOR) signaling (ref. 2), and the insulin/insulin-like growth factor 1 (IGF-1) signaling (ref. 3). However, age-related dysfunctions vary significantly among individuals. Therefore, in addition to searching for common factors related to aging, we must try to understand “aging individuality (the mutable variability in age-related dysfunctions)”.

Results

To investigate the gene expression profile of individual flies, we analyzed the heads and bodies separately from 36 aged males and 6 young males of Drosophila by RNA-seq analysis. We combined data analysis from well-known statistical analysis in RNA-seq (DESec2) to determine the significantly altered genes, and clustering analysis (WGCNA, ref. 4) which reveals the genes showing correlated expression pattern, and therefore indicates the specific pathway acting in the specific individuals. Though data analysis using our platform, we determined that aged flies display the multiple clusters of gene with altered expression only in the subset of individuals, which are different in male and females, and also in heads and bodies, suggesting that these genes could act as the genetic marker to define aging individuality. To visualize the aging individuality, representative genes from each cluster were selected, and transcriptional activators, GAL4, LexA, or QF were knocked into the C-terminus of each gene via CRISPR/Cas9 together with a T2A self-cleaving peptide, allowing the endogenous gene and activator to be synthesized separately from the same transcript. The transcriptional activators then induced expression of the bioluminescent proteins, Nanoluc, Eluc, and Akaluc, which emit light at the wavelengths of 460, 536, and 650 nm, respectively. Upon feeding a specific substrate for each bioluminescent protein on 96-well plates, the emitted light wan captured with band-pass filters in the luminometer. A maximum of three different reporters can be monitored in an individual at a time, enabling the visualization of the proportion (how many animals in a given population express the marker genes), the dynamics (when the marker genes are

expressed), and the complexity (how the marker gene expressions are overlapped) of aging individuality. To date, a total of 12 transgenic lines were constructed as the candidate genetic markers for aging individuality in male heads. The additional genes selected from male body, female head/body will be targeted similarly to below. Representative results of 4 lines with GAL4 insertion in rdgB (retinal function), CG14419 (unknown function), SPH93 (immune response), and PEPCK2 (gluconeogenesis) crossed with UAS-Eluc flies were shown (Fig. 1A-D). Consistent with the RNA-seq data, only a subset of the aged flies emitted light after substrate feeding (Fig. 1A-D, left panels). An EMCCD camera demonstrated the stereotyped localization of the signals: eyes in rdgB::GAL4 flies, mouth and genitalia in CG14419::GAL4 flies, and sparse, unspecified tissues in SPH93::GAL4 and PEPCK2::GAL4 flies (Fig. 1A-D, right panels). It is noteworthy that heterogenous light emission was observed in the stereotyped organs, indicating stochastic features; in rdgB::GAL4 flies, light was only emitted from one eye, but not from both eyes (Fig. 1A). In addition, the SPH93::GAL4 flies died 2-3 days after light emission, suggesting that this reporter is linked to life expectancy, while no such link was observed in other reporters. We are now trying to link the marker genes to the aging phenotypes, in addition to longevity, such as behavioral change (sleep, locomotor, sensation, or feeding), and metabolic change. We will further try to understand mechanism underlying the aging individuality by forward genetic screening in fly.

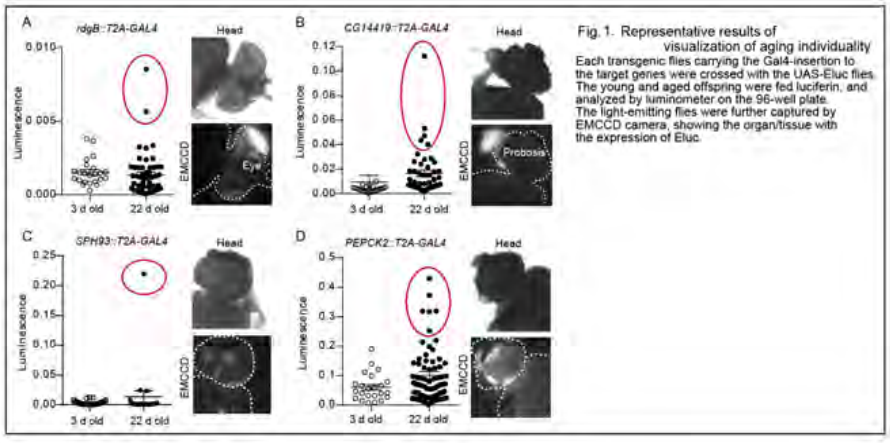

Fig. 1. Representative results of visualization of aging individuality
Each transgenic flies carrying the Gal4-insertion to the target genes were crossed with the UAS-Eluc flies. The young and aged offspring were fed luciferin, and analyzed by luminometer on the 96-well plate. The light-emitting flies were further captured by EMCCD camera, showing the organ/tissue with the expression of Eluc.

Discussion & Conclusion

Although aging is ubiquitous in all animals, the related dysfunctions differ between individuals; conditions in humans range from cancers, cardiovascular diseases, cognitive disorders, and diabetes. The central question here is “why age-related dysfunctions vary among individuals”. We now obtained a tool to access the aging individuality. After we conduct a forward genetic screen in Drosophila to identify the genes or pathways that regulate aging individuality, hopefully we could determine the entry point to tackle the age-related multiple dysfunctions. The long-term goal of this study is to elucidate the mechanisms underlying aging individuality, which could contribute to the development of personalized therapies for age-related dysfunction.

References

1, Kaeberlein, M., McVey, M. & Guarente, L. The SIR2/3/4 complex and SIR2 alone promote longevity in Saccharomyces cerevisiae by two different mechanisms. Genes & development 13, 2570-2580, doi:10.1101/gad.13.19.2570 (1999).
2, Kaeberlein, M. et al. Regulation of yeast replicative life span by TOR and Sch9 in response to nutrients. Science 310, 1193-1196, doi:10.1126/science.1115535 (2005).
3, Kenyon, C. The plasticity of aging: insights from long-lived mutants. Cell 120, 449-460, doi:10.1016/j.cell.2005.02.002 (2005).
4, Zhang, J. et al. Weighted Gene Co-expression Network Analysis for RNA-Sequencing Data of the Varicose Veins Transcriptome. Frontiers in physiology 10, 278, doi:10.3389/fphys.2019.00278 (2019).

一般の皆様へ

老化は各器官、例えば神経系や心血管系、消化器系、運動器系といった様々な器官の機能障害を引き起こし、高齢者の社会的活動を著しく制限する。老化に伴う機能低下は、各個体で訪れる時期は様々で、また均一にすべての器官で機能低下を示すわけではない。従って老化に伴う器官機能不全に立ち向かうためには、特定の器官で機能低下を示した個体を識別した上で、解析し、さらには機能低下を改善させる方法論を見出していかなければならない。そこで私は、個体間の老化プロセスの違い「老化個性」に焦点を当て、それを可視化する方法論の確立が必要不可欠であると考え、老化個性を可視化する本研究を行った。

In vivo imaging the brain defines new mechanisms of leukocytes migration cascade in Central Nervous System Lupus

Yoshishige Miyabe
y-miyabe@nms.ac.jp
Department of Cell Biology, Institute for Advanced Medical Sciences, Nippon Medical School

Summary Abstract

How chemoattractants (CAs) control leukocytes entry into central nervous system (CNS) is largely unknown. We recently established the technique of in vivo imaging the brain to define new mechanism of leukocyte migratory behavior in CNS lupus.
Key Words : chemoattractant, leukocytes migration, central nervous system lupus

Introduction

Chemoattractant-induced arrest of circulating leukocytes and their subsequent diapedesis is a fundamental component of inflammation[1]. Thus, the control of leukocyte entry into the tissue represents a major point at which new therapeutics could be developed to attenuate inflammation[1]. Central nervous system (CNS) lupus is clinically involved in approximately 40% of all systemic lupus erythematosus patients. How leukocytes infiltrate into CNS in the pathogenesis of CNS lupus is not well understood. Recently, we have developed the technique of in vivo imaging the brain to elucidate the mechanism how leukocytes entry into the CNS in the pathogenesis of CNS lupus.

Results

Recent advances in imaging technology have provided unprecedented views into immune cell function in live animals, providing entirely new paradigms for immune cell function. In fact, the applicant has developed techniques to apply intravital imaging technology to study the arthritic joint[2]. Our new joint imaging technique has discovered new unexpected biology concerning the specific functions of chemoattractants (CAs) in regulating leukocyte entry in joints *in vivo*. For example, we have found that classical complement C5a receptor C5aR1 plays a unique role in capturing neutrophils on the endothelium in the inflamed joints[3]. In addition, we have demonstrated that atypical C5a receptor C5aR2 on endothelium transports C5a to initiate neutrophil adhesion and inflammation in the inflamed joints[4].

The aim of our study is that we will apply the technique of in vivo imaging the brain to take our understanding of CNS lupus to an entirely new level by allowing the real time visualization of the events that lead to encephalitis in live mice.

It has reported that CAs, such as chemokines, lipid mediators and complement components in central nervous fluids (CFs) derived from CNS lupus patients are increasing than those of healthy donors, suggesting that CAs might play important roles of leukocytes recruitment into CNS in the pathogenesis of CNS lupus. However, the mechanism how CAs in CFs promote leukocytes entry into CNS in the pathogenesis of CNS lupus remain

unclear.

Thus, we hypothesized that CAs were transported into CFs from blood and might control leukocytes recruitment into CNS in the pathogenesis of CNS lupus. Our project consists of (1) study if CAs can entry into CFs from blood, (2) establish in vivo brain imaging and (3) define the mechanism how leukocytes can entry into CNS in an animal model of CNS lupus, and has been conducted since 2020, with a 3 year plan.

In 2020, we have determined whether CAs in blood could entry into CFs. We intravenously (i.v.) injected with several dose of CAs or sterile PBS as control, into wild-type (WT) mouse and isolated CFs from WT mice at several time course. The concentration of CAs in CFs was measured by ELISA. We found that the concentration of CAs in CFs derived from WT mice injected with CAs i.v. was increased than those of WT mice injected PBS, and a dose dependent manner. Also, we observed some subsets of leukocyte infiltration into brain when we intravenously injected with CAs into WT mouse.

To develop the technique of in vivo brain imaging, mice were anesthetized and positioned on a stereotactic surgical stage, and the skull immobilized. Hair in the frontal and parietal regions of the skull was cleaned with an electrical hair clippers and chemical depilatory agent. Skin was excised from top of the skull, and the underlying periosteum scraped off. Using a high-speed air-turbine drill with a burr tip size of 0.8mm in diameter, a groove was made to form a circle of approximately 4mm in the parietal bone of the skull. This area was made thinner by cautious and continuous drilling of the groove until the bone flap became loose. Using a blunt microblade, the bone flap was separated from dura mater underneath, leaving the dura intact. After removal of the bone flap, the dura mater was continuously kept moist with PBS. The window was then sealed by adhering a cover glass to the bone using a tissue glue. After the cranial window surgery, in vivo brain imaging was performed under a confocal microscopy. We could observe leukocytes migratory behavior in brain.

Discussion & Conclusion

Our recent work has demonstrated that CAs were generated within the tissue, and then transported by atypical CA receptors into vessel lumen. Transported CAs bind with CA receptors on circulating leukocytes and induce to migration into the tissue in inflammation[2,3]. In contrast, the mechanism how CAs control leukocytes entry into CNS in CNS lupus is largely unknown.

Our preliminary data has demonstrated that CAs in blood might entry into CFs in WT mice and then promote leukocytes entry into CNS. However, the mechanism how CAs are transported into CNS from blood remains unclear. Also, if transported CAs could directly promote circulating leukocytes entry into CNS is unknown. We will apply the technique of in vivo imaging the brain to clarify the mechanism of CAs-mediated leukocytes migration in an animal model of CNS lupus.

References

1. Miyabe Y, Lian J, Miyabe C, Luster AD. 2019. Chemokines in Rheumatic Diseases and Therapeutic Implications. *Nature Reviews Rheumatology* 15(12), 731-746.
2. Miyabe Y, Kim ND, Miyabe C, Luster AD. 2016. Studying Chemokine Control of

Neutrophil Migration In Vivo in a Murine Model of Inflammatory Arthritis. *Methods in Enzymology* 570: 207-31.
3. Miyabe Y, Miyabe C, Mani V, Mempel TR, Luster AD. 2019. Atypical complement receptor C5aR2 transports C5a to initiate neutrophil adhesion and inflammation. *Science Immunology* 4, eaav5951.
4. Miyabe Y, Miyabe C, Murooka TT, Kim YE, Newton GA, Kim ND, Haribabu B, Luscinskas FW, Mempel TR, Luster AD. 2017. Complement C5a Receptor is the Key Initiator of Neutrophil Adhesion Igniting Immune Complex-induced Arthritis. *Science Immunology* 2, eaaj2195.

一般の皆様へ

近年、サイトカイン阻害を目的とした生物学的製剤が続々と開発され、効果的に活性化免疫細胞を抑制可能となり、自己免疫疾患の予後は劇的に改善しました。一方で、これらは全身性に免疫細胞の“活性化”を阻害する為、重篤な感染症や二次発癌などの副作用が問題となっています。生命現象の根底にある細胞の“動き”は炎症病態の根底にあり、その機序を解明する事で細胞の“動き”を臓器特異的に制御可能な次世代免疫療法の開発につながると期待されます。

Molecular Pathology of Moyamoya Disease

Daisuke Morito
morito@med.showa-u.ac.jp
Showa University School of Medicine

Summary Abstract

Mysterin, also known as RNF213 or ALO17, is a large cellular protein that contains locomotive ATPase modules and ubiquitin ligase domain(s). Mutations found in the ubiquitin ligase domain elevate the risk of cerebrovascular moyamoya disease to a varying degree. We demonstrated its unexpected role and pathogenic effects of the moyamoya mutations.
Key Words : moyamoya disease, mysterin, RNF213, ubiquitin, AAA+ ATPase

Introduction

Moyamoya disease is a unique cerebrovascular disorder characterized by bilateral stenosis/occlusion of the terminal region of internal carotid arteries and following brain infarction and hemorrhage. I performed the molecular cloning of its causal gene and named it mysterin (also known as RNF213 or ALO17) as a final touch of genetic analysis of moyamoya disease (#Liu, #Morito et al., PLOS ONE, 2011; patent 5854423). I have demonstrated the ATPase and ubiquitin ligase activities of mysterin protein and its physiological function in cells (i.e., metabolic regulation of lipid droplets; Sci Rep, 2014, 2015, 2019; J Cell Biol, 2019). Mutations found in the ubiquitin ligase domain of mysterin elevate the risk of moyamoya disease to a varying degree, while molecular mechanism underlying moyamoya disease remained elusive.

Results

Precise imaging analysis for the first time revealed that mysterin protein rapidly shuttles between the cytosol and the lipid droplets (LDs) that are the organelles specialized for cellular lipid storage and metabolism, suggesting the physiological contribution of mysterin to the lipid metabolism (Figure). Localization of mysterin to the LDs resulted in specific elimination of several LD surface proteins including ATGL, the primary lipase that regulates the stability of the LDs, and led to immobilization (stabilization) of the LDs. Both ATPase activity and ubiquitin ligase activity of mysterin are indispensable for this process (i.e., LD localization and immobilization). Ubiquitin ligase activity of mysterin is partly spoiled by the patient mutations in the ubiquitin ligase domain, resulting in the lack of LD localization of mysterin. Instead, the mutant mysterin protein forms aggregate-like structure in cells, suggesting the previously-unexpected link between the LD metabolism and moyamoya disease.

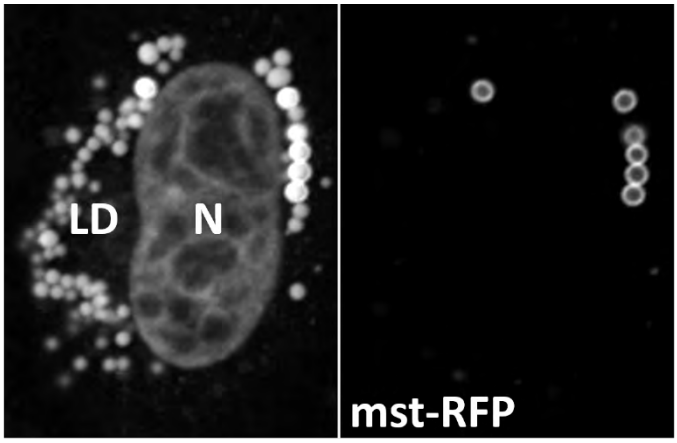

Figure. The left panel shows an entire view of a single cell (HeLa), in which nucleus (N) and lipid droplets (LD) are stained. The right panel shows the same cell, but only the signal of mysterin-RFP is shown. Thus, mysterin protein surrounds cellular lipid droplets and affect their stability thru regulation of the major lipase ATGL.

Recent structural analysis demonstrated that mysterin's ATPase domain forms a dynein-like ATPase core and may have a motor-like (locomotive) activity (Clausen and colleagues, eLife, 2020). Given the lack of LD localization of ATPase mutant mysterin, the putative locomotive ATPase activity possibly underlies the dynamic shuttling of mysterin between the cytosol and the LDs.

In addition, the study suggested that mysterin protein contains two independent ubiquitin ligase domains. We examined each involvement in mysterin's intracellular behavior and found that the two domains have distinct functions, one of which is associated with mysterin's intracellular localization.

Furthermore, a study recently reported showed a surprising function of mysterin (Otten, Randow and colleagues, Nature, 2021). It was observed that mysterin ubiquitylates non-proteinous substrate LPS decollating the surface of Salmonella that invades the cells. Given the LD localization and ubiquitylation (unpublished observation) by mysterin, mysterin could be a ubiquitin ligase which has an affinity to cellular/exogenous membranes and triggers ubiquitin-related pathways on the membrane (e.g., autophagic defense against Salmonella).

We are now evaluating the mechanism by which mysterin recognizes specific membranes and mechanistic involvement of dynein-like ATPase and potential two ubiquitin ligase activities. Also, we are evaluating the potential cytotoxic effect of the aggregation of mutant mysterin.

Discussion & Conclusion

Mysterin is the 21st largest protein within those encoded in the human genome (Uniprot), which has a unique combination of enzymatic activities (ATPase and ubiquitin ligase). It is specifically targeted to the LDs and the invading Salmonella and ubiquitylates their membrane surfaces, which further leads to downstream events (e.g., autophagy). Many of mutations associated with moyamoya disease have been found in mysterin's ubiquitin ligase domain and led to the aggregate-like pattern of mysterin in cells. One of the currently most important question is what is the exact role of each potential ubiquitin ligase activity of mysterin. We are promoting functional analyses on mysterin, focusing on several points including this question.

References

1. Sugihara M, Morito D (corresponding), Shiori Ainuki, Yoshinobu Hirano, Kazutoyo Ogino, Akira Kitamura, Hiromi Hirata, Kazuhiro Nagata. AAA+ ATPase/ubiquitin ligase mysterin stabilizes cytoplasmic lipid droplets. ***J Cell Biol.*** 2019 Mar 4; 218(3):949-960.
2. Kotani Y, Morito D (corresponding), Kenshiro Sakata, Shiori Ainuki, Munechika Sugihara, Tomohisa Hatta, Shun-ichiro Iemura, Seiji Takashima, Tohru Natsume, Kazuhiro Nagata. Alternative exon skipping biases substrate preference of the deubiquitylase USP15 for mysterin/RNF213, the moyamoya disease susceptibility factor. ***Sci Rep***. 2017 Mar 9;7:44293
3. Morito D (co-corresponding) and Nagata K. Molecular Biology of Mysterin/RNF213. ***Moyamoya Disease Explored Through RNF213***, Book Chapter, Springer, pp45-57 (2017)
4. Morito D (co-corresponding) and Nagata K. Physiological Role of Mysterin/RNF213 in Zebrafish. ***Moyamoya Disease Explored Through RNF213***, Book Chapter, Springer, pp59-67 (2017)
5. Kotani Y, Morito D (co-corresponding), Satoru Yamazaki, Kazutoyo Ogino, Koichi Kawakami, Seiji Takashima, Hiromi Hirata, Kazuhiro Nagata. Neuromuscular regulation in zebrafish by a large AAA+ ATPase/ubiquitin ligase, mysterin/RNF213. ***Sci Rep.*** 2015 Nov 4;5:16161
6. Morito D, Kouki Nishikawa, Jun Hoseki, Akira Kitamura, Yuri Kotani, Kazumi Kiso, Masataka Kinjo, Yoshinori Fujiyoshi, Kazuhiro Nagata. Moyamoya disease-associated protein mysterin/RNF213 is a novel AAA+ ATPase, which dynamically changes its oligomeric state. ***Sci Rep.*** 2014 Mar 24;4:4442
7. Liu W, Morito D (co-first) , Seiji Takashima, Yohei Mineharu, Hatasu Kobayashi, Toshiaki Hitomi, Hirokuni Hashikata, Norio Matsuura, Satoru Yamazaki, Atsushi Toyoda, Kenichiro Kikuta, Yasuchi Takagi, Kouji H. Harada, Asao Fujiyama, Roman Herzig, Boris Krischek, Liping Zou, Jeong Eun Kim, Masafumi Kitakaze, Susumu Miyamoto, Kazuhiro Nagata, Nobuo Hashimoto, Akio Koizumi Identification of RNF213 as a susceptibility gene for moyamoya disease and its possible role in vascular development. ***PLoS One.*** 2011;6(7):e22542.

一般の皆様へ

もやもや病は東アジア地域の子どもに多い脳血管疾患です。脳の真下のあたりの動脈が狭くなり、血が通りにくくなります。その結果、脳への血液供給が不足し、脳梗塞などが起こります。なぜ動脈が狭くなるのか、なぜこの箇所で起こるのかなど、ほとんど謎のままです。私たちはもやもや病の原因遺伝子と考えられる新たな遺伝子ミステリンを物質として取り出すことに成功しました（分子クローニング、2011）。以来、解析を進め、この遺伝子から合成されてくるタンパク質ミステリンの分子としてのはたらきや、体の中での機能、またもやもや病患者さんから見つかった遺伝子変異により機能がどのように変化するかを順番に明らかにしてきました。まだ研究の途上ですが、もやもや病発病メカニズムのヒントをつかみつつあります。本財団や公的組織をふくむ各方面からの支援を受けながら、近い将来の病態解明を目指して研究を続けています。

Role of actin cytoskeletal fluctuation in retinal organoid formation

Satoru Okuda
satokuda@staff.kanazawa-u.ac.jp
Kanazawa University

Summary Abstract

Epithelial cell extrusion is observed in organoid formation. Various molecular factors have been reported as key drivers of epithelial extrusion; however, little is known about how these factors are linked to the mechanical process. We developed a simple mathematical model that explains cell extrusions under a wide range of physiological and pathophysiological conditions. The model shows that cells can be extruded from homogeneous sheets, owing to the inherent mechanical instability of the 3D foam geometry of the epithelial monolayer.

Key Words : Cell extrusion, cytoskeletal contractility, organoid

Introduction

In cell extrusion, a cell embedded in an epithelial monolayer loses its apical or basal surface and is subsequently squeezed out of the monolayer by neighboring cells. Cell extrusions occur during apoptosis, epithelial-mesenchymal transition, or precancerous cell invasion. They play important roles in embryogenesis, homeostasis, carcinogenesis, and many other biological processes. Although many of the molecular factors involved in cell extrusion are known, little is known about the mechanical basis of cell extrusion.

Results

We used a three-dimensional (3D) vertex model (Ref. 1) to investigate the mechanical stability of cells arranged in a monolayer with 3D foam geometry. We created a geometric model of a cell sheet in which the cells are represented as polyhedrons with average volume within a planar sheet with homogeneous thickness. Here, we parameterized the thickness by introducing cell density into the sheet.

Cell extrusions occasionally occur even without the active generation of force by the extruding cells, suggesting that mechanical instability inherent in the 3D geometry of the epithelial monolayer might be sufficient to drive cell extrusion. As a result, the energy landscape led to mechanical instability and subsequent extrusion. For example, the decrease in ka destabilized the dual-sided state and stabilized the apical extrusion state.

We found that when the cells composing the monolayer have homogeneous mechanical properties, cells are extruded from the monolayer when the symmetry of the 3D geometry is broken because of an increase in cell density or a decrease in the number of topological neighbors around single cells. Those results suggest that mechanical instability inherent in the 3D foam geometry of epithelial monolayers is sufficient to drive epithelial cell extrusion.

In the situation in which cells in the monolayer actively generate contractile or adhesive forces under the control of intrinsic genetic programs, the forces act to break the symmetry

of the monolayer, leading to cell extrusion that is directed to the apical or basal side of the monolayer by the balance of contractile and adhesive forces on the apical and basal sides.

Discussion & Conclusion

We presented a theoretical model that describes the mechanical stability of cellular monolayers. The model shows that the cellular monolayer has inherent mechanical instability that is sufficient to cause cell extrusion without any additional provoking factors, even when the cells have homogenous mechanical properties. Analytical calculations show that the instability depends on the cell density, topology, and mechanical properties within the monolayer. The active generation of forces by an extruding cell can provoke extrusion and direct the extrusion to the apical or basal side of the monolayer, suggesting that cells utilize the mechanical instability of the epithelial geometry to regulate extrusion.

References

1. Okuda, S., Inoue, Y., & Adachi, T. (2015). Three-dimensional vertex model for simulating multicellular morphogenesis. *Biophysics and physicobiology*, *12*, 13-20.

一般の皆様へ

上皮組織では、多数の細胞が密に並んだシート状の組織であり、シート内の各細胞は、脳の初期発生等の過程に置いて多層化したり脱離したりします。この細胞脱離の仕組みの理解は、胚発生・組織再生・がん疾患などの幅広い現象の解明にとって重要な課題です。本研究では、上皮組織のシート構造を簡単化して捉え、力学エネルギーに基づいた理論的な解析を行うことにより、上皮組織に内在する力学的な不安定性が細胞脱離を引き起こす仕組みを明らかにしました。

Elucidating the system to generate dormancy that confer chemotherapy-resistance to cancer cells

Keisuke Nimura
nimura@gts.med.osaka-u.ac.jp
Division of Gene Therapy Science, Graduate School of Medicine, Osaka University

Summary Abstract

Most ovarian cancers respond to initial chemotherapy, but some cancer cells that have developed resistance to treatment remain and can cause recurrence. In order to overcome this problem, the underlying causes of cancer cell resistance must be identified and targeted for treatment. One of the major mechanisms of resistance to chemotherapy is the entry of cancer cells into a quiescent state. However, the system by which the quiescent state of cancer cells is formed and maintained is largely unknown.In this study, we will identify quiescent cancer cells, which are resistant to chemotherapy, by single cell sequencing and other methods, and clarify the entire tumor microenvironment including these cells. Based on these results, we aim to develop cancer therapeutics targeting quiescent cancer cells.
Key Words : ovarian cancer, dormant cancer cell

Introduction

Cancer cells that have acquired resistance to treatment exist in cancers that recur after anticancer drug treatment, but the full picture of the mechanism is unknown. Previous in vitro studies using cancer cell lines have shown that some cancer cells remain by entering a quiescent phase and becoming tolerant to anticancer drugs, and then repopulate by acquiring resistance. On the other hand, the applicants have clarified the dynamic chromatin structure conversion mechanism during the transition from quiescent to proliferative phase using B cells as a model. In the quiescent phase, naïve B cells have a highly aggregated chromatin structure, but upon receiving an activation signal, they quickly convert to a loose chromatin structure by transcription factor Myc and histone acetylation to enable repopulation. This suggests that a dynamic chromatin structure conversion mechanism is required for the repopulation of quiescent cells in cancer, but the molecular mechanism by which quiescent cancer cells convert to a chromatin structure that allows repopulation has not yet been clarified.

Results

We analyzed single-cell gene expression of 10,000 cells from three cases, two cases of primary serous adenocarcinoma and one case of recurrent serous adenocarcinoma, respectively. 10,116 and 8,968 single-cell gene expression data were obtained from the library of primary serous adenocarcinoma using cellranger. We obtained single cell gene expression data for 10,116 cells and 8,968 cells from the library of first-episode serous adenocarcinoma. We obtained single-cell gene expression data for 10,296 cells from the library of recurrent serous adenocarcinoma, with an average of 61.7k reads per cell. We were

able to detect the expression of 2500 genes per cell. The obtained data was analyzed by t-SNE and visualization was performed. As a result, we were able to identify EPCAM- and PAX8-positive epithelial cancer cells, CD4- and CD8-positive T cells, macrophages, and dendritic cells. The immune cells showed relatively similar gene expression patterns among the cases, whereas the epithelial cancer cells showed slightly different gene expression patterns among the cases. In addition, 8% of the cells were found to be EPCAM-negative, oncogene MYC-positive, and mesenchymal marker THY1-positive mesenchymal carcinoma cells. Furthermore, these mesenchymal carcinoma cells were negative for MKI67, suggesting that they are in a quiescent state compared to epithelial carcinoma cells.

High-grade serous adenocarcinoma is the most frequent form of ovarian cancer, and although it responds well to initial chemotherapy, it recurs in most cases. We performed flow cytometric analysis of high-grade serous adenocarcinoma tissues from more than 10 cases, including both first-episode and recurrent cases, using three antibodies: CD45, a marker of blood cell lineage; EpCAM, a marker of epithelial lineage; and THY1, a marker of mesenchymal lineage. The results showed that high-grade serous adenocarcinomas contain about 10% cells that express extremely high levels of THY1. Similar analysis of recurrent high-grade serous adenocarcinoma tissues showed that the number of cells expressing THY1 was increased in the tumor. Furthermore, gene expression analysis of seven cell types separated by CD45, EpCAM, and THY1 expression showed that THY1-expressing cells had higher expression of ABCG2, which is involved in drug efflux, and NOTCH3, which is involved in cancer progression, while preliminary results showed that THY1-expressing cells had significantly lower expression of the cell proliferation marker MKI67. The preliminary results showed that the expression of the cell proliferation marker MKI67 was markedly low while the expression of ABCG2, which is responsible for cancer efflux, and NOTCH3, which is involved in cancer progression, were high. Next, we searched for transcription factors that are specifically expressed in THY1-expressing cells and identified several mesenchymal-related transcription factors. Next, we performed SNP analysis using genes that were commonly highly expressed in the seven isolated cells in cases where normal tissue could be recovered. Clustering analysis revealed that THY1-positive cells, unlike normal tissues, had a SNP pattern similar to that of tumor cells. These results strongly suggest that THY1 high-expressing cells are not just a population of mesenchymal cells.

The mouse ovarian cancer cell line ID8 forms peritoneal dissemination nests and produces ascites when administered into the peritoneal cavity of mice. To verify the presence of slow-growing mesenchymal carcinoma cells in the seeded nests formed by ID8, we generated a cell line capable of detecting slow-growing cells. We expressed the BFP gene fused with histone H2B at the tetracycline promoter, which can transiently express the gene in a doxycycline-inducible manner. This construct was knocked into the ROSA locus to avoid the effects of expression of other genes. In addition, this ID8 retains the luciferase gene, so that the IVIS system can measure tumor growth in the abdominal cavity over time without killing the mice. Now, by adding doxycycline to these ID8-tet-H2B-BFP cells, we were able to construct cells expressing H2B-BFP. First, under culture conditions, H2B-BFP is transiently expressed; since H2B-BFP is incorporated into chromatin, it does not decrease without division. By collecting cells that retain H2B-BFP after long-term culture, it is possible to recover slow-growing cells.

Discussion & Conclusion

In this study, single cell analysis of ovarian cancer clinical specimens and gene expression analysis of cell populations isolated and collected by flow cytometry suggested the presence of ~10% mesenchymal carcinoma cells in ovarian cancer. These mesenchymal carcinoma cells expressed the mesenchymal marker THY1 and the oncogene MYC, but not the epithelial marker EPCAM or the fibroblast marker FSP1. Furthermore, although preliminary, THY1-positive cells were found in peritoneal disseminated nests collected after chemotherapy, suggesting that some of these cells may persist after chemotherapy and lead to recurrence. To prove that these mesenchymal carcinoma cells are truly cancer cells, we also transplanted an ovarian cancer cell line into mice and collected THY1-expressing cells from the tumor. After confirming that this cell population shows the same gene expression pattern as the clinical samples, we will implant them into mice to prove their tumorigenic potential. Through these experiments, we will prove that THY1-expressing cells are mesenchymal carcinoma cells and that they are likely to persist after chemotherapy. If we can prove the existence of these THY1-expressing cells, it will provide a basis for the development of new therapies targeting this cell population.

一般の皆様へ

がん治療上の問題点の 1 つとして、がん細胞が抗がん剤の抵抗性を獲得することがあげられます。抗がん剤の多くは細胞増殖が盛んな細胞に対して効果を示します。がんの中には細胞増殖が極めて遅いがん細胞が存在すると考えられており、このような細胞増殖の遅いがん細胞には抗がん剤は効きにくいと考えられます。ところが、このようながん細胞がどのような性質を持つのかあまりはっきりしていません。私達は、細胞増殖の遅いがん細胞の性質を明らかにして、この細胞を除去する治療法の開発を進めています。

Mechanism and targeting therapy for TGF pathway-dependent diffuse-type gastric cancer

Yoku Hayakawa
hayakawayoku@gmail.com
The University of Tokyo Hospital

Key Words : Gastric cancer, TGF pathway, mouse model, LRG1, CD38

Introduction

Gastric cancer is a disease with a high morbidity and mortality rate. Signet ring cell type gastric cancer, so-called scirrhous gastric cancer, has a particularly poor prognosis among gastric cancers. In this cancer, signet ring cell carcinoma invades the stomach wall diffusely, causing early metastasis to the whole body including peritoneal dissemination, and are resistant to many cancer therapies. Since signet ring cell carcinoma is hereditary in families with mutations in the CDH1 gene, the importance of the CDH1 gene has been suggested. In addition, genomic analysis revealed frequent abnormalities in the TGF / SMAD pathway in this subtype. We attempted to establish a mouse model that mimics scirrhous gastric cancer by combining a gastric epithelial-specific labeled mouse (TFF1-Cre) with Cre-dependent genetically modified mice. As a result, we established a mouse model of scirrhous gastric cancer that causes early mucosal infiltration and leads to cancer death by combining three gene mutations, CDH1, TGFBR2, and p53. Using these TFF1-PTC mice, we pursued a new treatment method for scirrhous gastric cancer.

Results

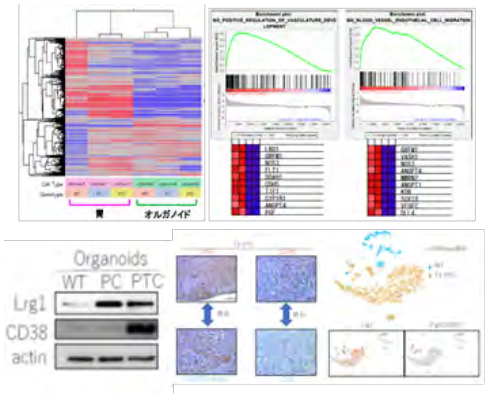

We performed RNAseq analyses using TFF1-PTC stomach and gastric organoid samples. Compared to healthy stomach, TFF1-PTC stomach is enriched with genes associated with angiogenesis and fibrosis. Among these genes, we found that both TFF1-PTC stomach and gastric organoid express markedly higher level of CD38 and LRG1, compared to normal samples. CD38 is known to bind to CD31, an endothelial cell surface marker, and regulate immune cell migration. LRG1 is known to bind to CD105 (also known as endoglin), and regulate angiogenesis and fibrosis. In vitro experiments suggest that LRG1 and CD38 upregulation is caused specifically by simultaneous knockout of CDH1 and Tgfbr2, and also modulated by BMP-dependent signals. By performing scRNAseq, we revealed that CD105 is expressed in a subset of endothelial cells.

We examined the effects by CD38 and CD105 inhibition by using our TFF1-PTC mouse model. TFF1-PTC mice were treated with specific antibodies that target CD38 or CD105 for

2 weeks, and gastric tumor sections were pathologically compared. As a result, both anti-CD38 and anti-CD105 antibodies significantly decreased tumor invasion in the stomach, with reduction of fibroblasts and endothelial cells in tumor stroma. Thus, these data suggest that LRG1 and CD38 are critical factors that regulate robust angiogenesis and fibrosis in this type of gastric cancer, and can be a therapeutic target by blocking tumor-stromal interaction.

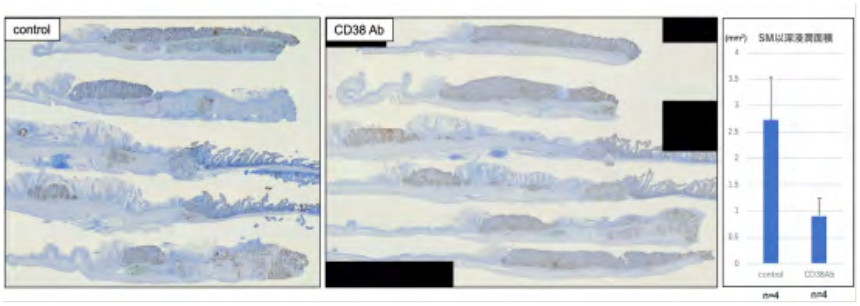

Discussion & Conclusion

Among all cancers, scirrhous gastric cancer is the most deadly cancer. Furthermore, it is difficult to identify high-risk groups for this type of gastric cancer, given that this cancer occurs even in young people who are not infected with H. pylori. Thus, our discovery that CD38 and LRG1 may be a promising treatment target for scirrhous gastric cancer would greatly contribute to improving prognosis of patients with advanced gastric cancer. In addition, since a similar mechanism may exist in other cancer cases with same mutations, this might contribute to establish precision medicine for cancers with mutations in CDH1 and TGF pathways.

一般の皆様へ

本研究では、予後不良の癌であるスキルス胃癌の新規治療標的を、独自のマウスモデルを用いて同定した。樹立したスキルス胃癌マウスサンプルの網羅的遺伝子発現解析によって、この癌で特徴的に発現上昇する遺伝子として LRG1 と CD38 を同定した。これらの分子は腫瘍内の血管新生や線維化に重要であり、特異的抗体によるマウスモデルの治療によって、スキルス胃癌の進展を抑制することが可能であった。LRG1・CD38 標的治療は、腫瘍間質相互作用を阻害することでスキルス胃癌の治療に有用であると考えられる。

Mechanisms involved in regulation of osteoclast formation by glucan recognition via immune receptors

Wataru Ariyoshi
arikichi@kyu-dent.ac.jp
Division of Infections and Molecular Biology, Kyushu Dental University

Summary Abstract

Our previous studies reported that β-glucans suppress osteoclast formation by suppressing NFATc1, an essential transcriptional factor for osteoclastogenesis. In this study, we focused on the molecular mechanisms by which β-glucans suppress NFATc1 expression mediated by interaction with dectin-1. β-glucans reduced RANKL-induced Blimp1 expression and upregulated Irf-8 expression, suggesting that suppression of the RANKL-stimulated Blimp1 expression leading to the upregulation of transcriptional repressors might be involved in the inhibitory effect of β-glucans on NFATc1 expression. Our findings indicate that further research on β-glucans may be useful in the treatment of osteoclast-related diseases, such as osteoporosis.

Key Words : β-glucan, dectin-1, osteoclast, blimp-1

Introduction

Various signaling cascades mediated by immunoreceptors have been found to regulate osteoclast differentiation, suggesting that immune cells interact with osteoclasts through several signaling factors [1]. Dectin-1 is a type II membrane receptor which recognizes β-glucans. We have demonstrated the obvious inhibitory effect of curdlan, laminarin, lichenan, glucan from baker's yeast, and β-1,3-glucan from *Euglena gracilis* on osteoclast differentiation. However, glucan from black yeast and β-D-glucan from barley showed a lesser inhibitory effect on osteoclast differentiation compared with other β-glucans.

To explore these discrepancies, we performed structural analyses of β-glucans.

Furthermore, we investigated the effects of β-glucans on the expression of negative regulators of osteoclastogenesis.

Results

It is possible that diverse effect of β-glucans on osteoclast differentiation reflect differences of purity and three-dimensional structure (e.g., β-(1,6)-linked side chains) of each of the β-glucans (Table 1, [2]).

β-glucan	Source	Structure
Curdlan	*Alcaligenes faecalis* var. *myxogenes*	Linear chain of β-D-(1-3)-glucopyranosyl units
Laminarin	*Laminaria* sp.	Linear chain of β-D-(1-3)-glucopyranosyl units with some 6-O-branching in the main chain and some β-(1,6)-intrachain links
Lichenan	*Cetraria islandica*	Linear chains of β-D-glucopyranosyl units linked via (1,3) and (1,4) linkage
Glucan from baker's yeast	*Saccharomyces cerevisiae*	Linear chain of β-D-(1-3)-glucopyranosyl units
β-1,3-glucan from *Euglena gracilis*	*Euglena gracilis*	Linear chain of β-D-(1-3)-glucopyranosyl units
Glucan from black yeast	*Aureobasidium pullulans*	Backbone of β-D-(1-3)-glucopyranosyl units with one β-D-(1-6)-branching unit every three residues
β-D-glucan from barley	*Hordeum vulgare* L	Linear chains of β-D-glucopyranosyl units linked via (1,3) and (1,4) linkage

Source and structure of β-glucans [Ref 2]

To prepare the dectin-1 retrovirus vector, cDNA-encoded mouse dectin-1 was cloned into the pFB-Neo plasmid. GP2-293 packaging cells were transfected by a plasmid mixture containing dectin-1/pFB-Neo and pVSV-G with Lipofectamine LTX. The culture supernatant of GP2-293 cells was harvested as a retrovirus fluid for dectin-1 transfection. RAW264.7 cells were cultured with the virus vector in the presence of 8 μg/ml Polybrene for 48 h. Cells expressing dectin-1 (d-RAW) were maintained in α-MEM containing 10% FBS, penicillin G (100 units/ml), streptomycin (100 μg/ml) and G418 disulfate aqueous solution (50 mg/ml). For the negative control of d-RAW cells, a control virus vector without dectin-1 cDNA was used for infection (c-RAW).

c-RAW cells and d-RAW cells were cultured with 40 ng/ml of osteoclast differentiation factor (receptor activator of nuclear factor-kappa B ligand; RANKL) for 7 days. On Day 7, cells were subjected to TRAP analysis. Remarkably, β-glucan (25 μg/ml) inhibited the osteoclast differentiation of d-RAW cells more effectively than c-RAW cells (Figure 1). These data suggested that β-glucan directly binds to dectin-1 expressed on the surface of osteoclast progenitors and suppresses their differentiation into osteoclasts.

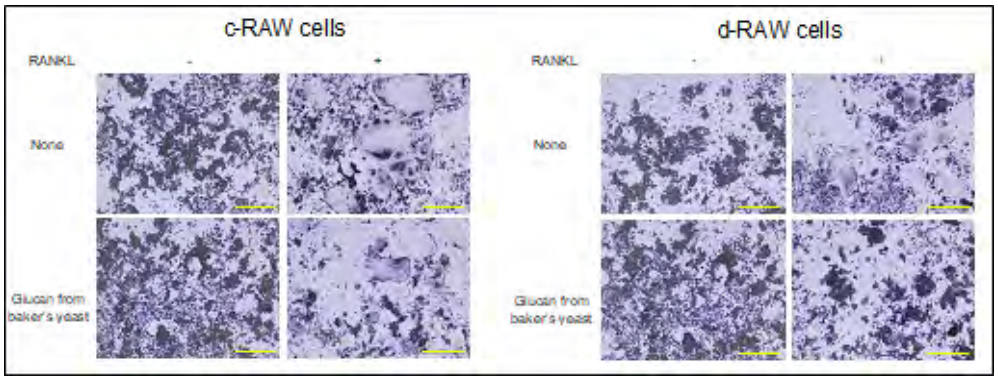

Figure 1 Effect of β-glucan on osteoclast differentiation [Ref 3]

Previous studies have shown that nuclear factor of activated T cell c1 (NFATc1) is strongly induced by RANK-RANKL signaling and plays an important role as a key transcriptional regulator in osteoclast terminal differentiation [4]. Given that NFATc1 has been suggested to be a target of the essential transcription factor of osteoclast differentiation, we asked the effect of β-glucans on the induction of NFATc1 expression. We found that although RANKL

upregulated NFATc1 protein level in d-RAW cells, β-glucan also suppressed this induction (Figure 2).

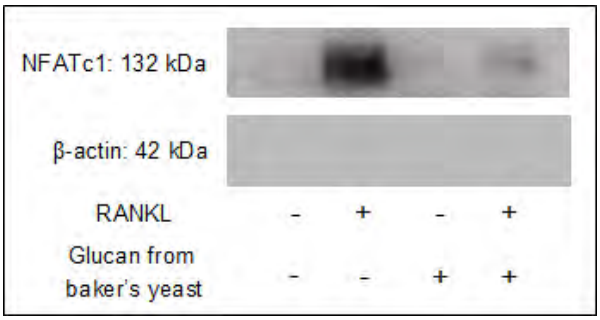

Figure 2 Effect of β-glucan on NFATc1 expression [Ref 3]

Recently, various molecules that control osteoclast differentiation have been identified. Several transcription repressors that suppress osteoclast differentiation, such as v-maf musculoaponeurotic fibrosarcoma oncogene homolog B (MafB), interferon regulatory factor-8 (Irf-8), and B cell lymphoma 6 (Bcl6) are rapidly downregulated by RANKL stimulation [5-7]. Blimp-1 binds to the promoters and suppresses the transcription of these factors [8]. These previous studies have suggested that the RANK-RANKL interaction enhances transcription factors that promote osteoclast differentiation, while inhibits the activity of transcription repressors for osteoclastogenesis. Thus, we investigated the effects of β-glucans on these negative regulators of osteoclastogenesis.

d-RAW cells were incubated with RANKL and β-glucan (25 μg/ml) for the indicated times. The mRNA level of Blimp1, MafB, Irf-8, and Bcl6 were assessed using real-time RT-qPCR. Protein level of Blimp1 in whole-cell lysates were detected by western blot analyses. β-actin served as loading control.

Glucan from baker's yeast significantly downregulated Blimp1 and showed a slight increase in the expression of Irf-8 gene. The RANKL-induced upregulation of Blimp1 protein was also suppressed by glucan from baker's yeast (Figure 3).

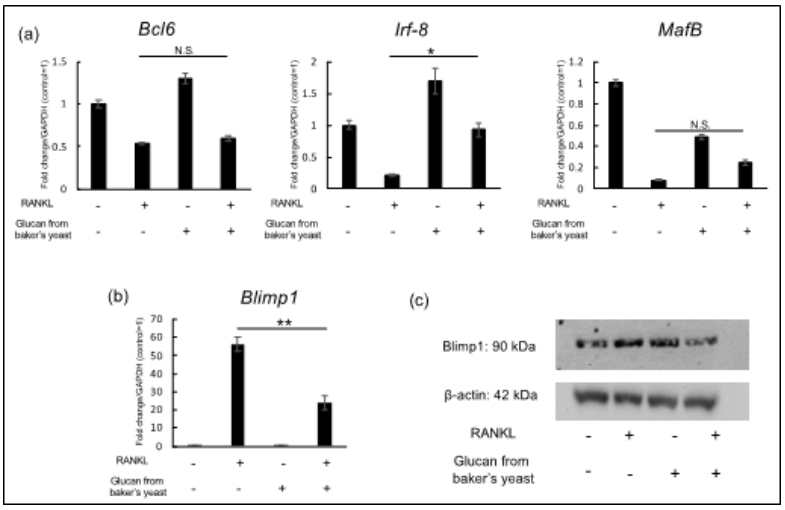

Effect of β-glucan on Blimp1-mediated negative regulators of osteoclastogenesis [Ref 3]

Discussion & Conclusion

As for the structure of β-glucans, it is known that a certain amount of molecular weight is required for the biological activity of β-glucans. A recent study reported that a split-luciferase complementation assay is useful strategy to characterize the side chain structure of β-glucans [9]. Structural analyses of β-glucans are also currently under investigation in our laboratory.

Next, we focused on the inhibitory factors of osteoclast differentiation as the candidates involved in the downregulation of NFATc1 by the interaction of β-glucans and dectin-1. β-glucans significantly reduced RANKL-induced Blimp1 expression and upregulated Irf-8 expression. Although additional research is needed to elucidate the molecular mechanisms by which β-glucans regulate Blimp1 expression, our data suggest that the suppression of the RANKL-stimulated Blimp1 expression leading to the upregulation of transcriptional repressors might be involved in the inhibitory effect of β-glucans on NFATc1 expression.

We demonstrated that β-glucans attenuate RANKL-induced osteoclast differentiation by downregulating NFATc1 activation. Our findings indicate that further research on β-glucans may be useful in the treatment of osteoclast-related diseases, such as osteoporosis.

References

1. Shinohara M, Takayanagi H (2007) Novel osteoclast signaling mechanisms. Curr Osteoporos Rep, 5, 67–72.
2. Ariyoshi W, Hara S, Koga A, Nagai-Yoshioka Y, Yamasaki R (2021) Biological Effects of β-Glucans on Osteoclastogenesis. Molecules, 26, 1982.
3. Hara S, Nagai-Yoshioka Y, Yamasaki R, Adachi Y, Fujita Y, Watanabe K, Maki K, Nishihara T, Ariyoshi W (2021) Dectin-1-mediated suppression of RANKL-induced osteoclastogenesis by glucan from baker's yeast. J Cell Physiol, 236, 5098-5107.
4. Takayanagi H, Kim S, Koga T, Nishina H, Isshiki M, Yoshida H, Saiura A, Isobe M, Yokochi T, Inoue J, Wagner EF, Mak TW, Kodama T, Taniguchi T (2002) Induction and activation of the transcription factor NFATc1 (NFAT2) integrate RANKL signaling in terminal differentiation of osteoclasts. Dev Cell, 3, 889-901.
5. Kim K, Kim J, Lee J, Jin HM, Kook H, Kim KK, Lee SY, Kim N. (2007) MafB negatively regulates RANKL-mediated osteoclast differentiation. Blood, 109, 3253–3259.
6. Miyauchi Y, Ninomiya K, Miyamoto H, Sakamoto A, Iwasaki R, Hoshi H, Miyamoto K, Hao W, Yoshida S, Morioka H, Chiba K, Kato S, Tokuhisa T, Saitou M, Toyama Y, Suda T, Miyamoto T (2010) The Blimp1-Bcl6 axis is critical to regulate osteoclast differentiation and bone homeostasis. J Exp Med, 751-762.
7. Zhao B, Takami M, Yamada A, Wang X, Koga T, Hu X, Tamura T, Ozato K, Choi Y, Ivashkiv LB, Takayanagi H, Kamilio R (2009) Interferon regulatory factor-8 regulates bone metabolism by suppressing osteoclastgenesis. Nat Med, 15, 1066-1071.
8. Nishikawa K, Nakashima T, Hayashi M, Fukunaga T, Kato S, Kodama T, Takahashi S, Calame K, Takayanagi H, Rao A (2010) Blimp 1-mediated repression of negative regulators is required for osteoclast differentiation. Proc Natl Acad of Sci U S A, 107, 3117–3122.
9. Yamanaka D, Kurita S, Hanayama Y, Adachi Y (2021) Split Enzyme-Based Biosensors for Structural Characterization of Soluble and Insoluble β-Glucans. Int J Mol Sci, 22, 1576.

一般の皆様へ

真菌や細菌、海藻などが含有する糖鎖であるβ -glucan は、免疫系細胞が持つ受容体である dectin-1 に認識されることで、種々の生物学的機能を発揮します。私達はβ -glucan が、破骨細胞前駆細胞上の dectin-1 に結合し、破骨細胞への分化や骨吸収活性を低下させることを証明しました。そこで本申請では、β -glucan の破骨細胞の分化抑制メカニズムに着目し、破骨細胞分化に重要な分子に対する負の調節機能を発揮することを見出しました。β -glucan の創薬への応用が、骨粗鬆症や歯周病などに対して、破骨細胞の骨吸収活性の低下を介した効果的な治療法の提案へと繋がると考えており、今後も研究を続けて参ります。

Weighted gene co-expression network analysis in Drosophila

Michiko Sekiya
mmsk@ncgg.go.jp
National Center for Geriatrics and Gerontology

Summary Abstract

The fruit fly *Drosophila melanogaster* has been used as an efficient genetic model in basic biology research. Recently, various human pathological conditions including neurodegenerative diseases have been modeled in *Drosophila*. These fly models are widely used to investigate disease mechanism and for drug discovery. In this study, we aimed to unravel the similarities and differences between human and *Drosophila* at a gene regulatory network level using weighted gene co-expression network analysis.
Key Words : Weighted gene co-expression network, *Drosophila*

Introduction

The fruit fly *Drosophila melanogaster* has been used to model various human pathological conditions including neurodegenerative diseases. These *Drosophila* models are widely used to investigate disease mechanisms and to perform drug screen. Recently, an integrative network analysis that use multi-omics data sets are used to identify the disease mechanisms and novel therapeutic targets (Wang M. Li, A., Sekiya, M. *et al.* ***Neuron***, 2021). To further utilize and integrate *Drosophila* models into a drug discovery pipeline, it is important to understand the similarities and differences between human and *Drosophila* at a gene regulatory network level.

Results

To construct the weighted gene co-expression networks in *Drosophila*, we extracted the RNA from the heads of flies and performed the RNA sequencing (RNA-seq). The expression data was obtained by the mapping of the sequences.

Drosophila

Wild type Canton-S line was used in this study. Flies were maintained in standard cornmeal media at 25°C, 40–50% humidity with 12 hr light/dark cycle. More than 2000 flies were collected for and flash-frozen in liquid nitrogen at the age of 7 days.

RNA extraction

Eighteen group were prepared with more than 100 flies as one group. Heads of flies were mechanically isolated, and total RNA was extracted using TRIzol Reagent (Thermo Fisher Scientific) according to the manufacturer's protocol with an additional centrifugation step (16,000 x g for 10 min) to remove cuticle membranes prior to the addition of chloroform. The quality of RNAs were evaluated by Bioanalyzer (Agilent Technologies) and the RNAs with RNA integrity number (RIN) more than 8 were used for construction of RNA library. We prepared 18 RNAs and the RIN ranged 8.2~9.1.

Library preparation

Preparation of samples for RNA-seq analysis was performed using the TruSeq

Stranded mRNA Library Prep kit (Illumina). Briefly, polyA containing mRNAs were isolated, fragmented and used for cDNA synthesis. Synthesized double strand cDNAs were ligated with appropriate adaptors for sequencing and amplified. The size and concentration of the RNA-seq libraries were measured by Bioanalyzer. All 16 samples met the quality required for sequence analysis.

RNA sequence and data analysis

Paired-end sequencing reads (150bp) were generated on a NovaSeq 6000 platform. Average read number was 68 million reads/sample and the average percentage of bases with a quality Score greater than 30 was 90.2%. The raw sequencing reads were aligned to fly genome BDGP6 using HISAT2 aligner (v2.1.0) and gene-level expression were quantified by StringTie (v2.1.2) based on Ensembl BDGP6.22.98 annotation model.

Visualization of weighted gene co-expression network

Using iDEP (integrated Differential Expression and Pathway) analysis application, weighted gene co-expression networks in *Drosophila* were visualized (Figure 1).

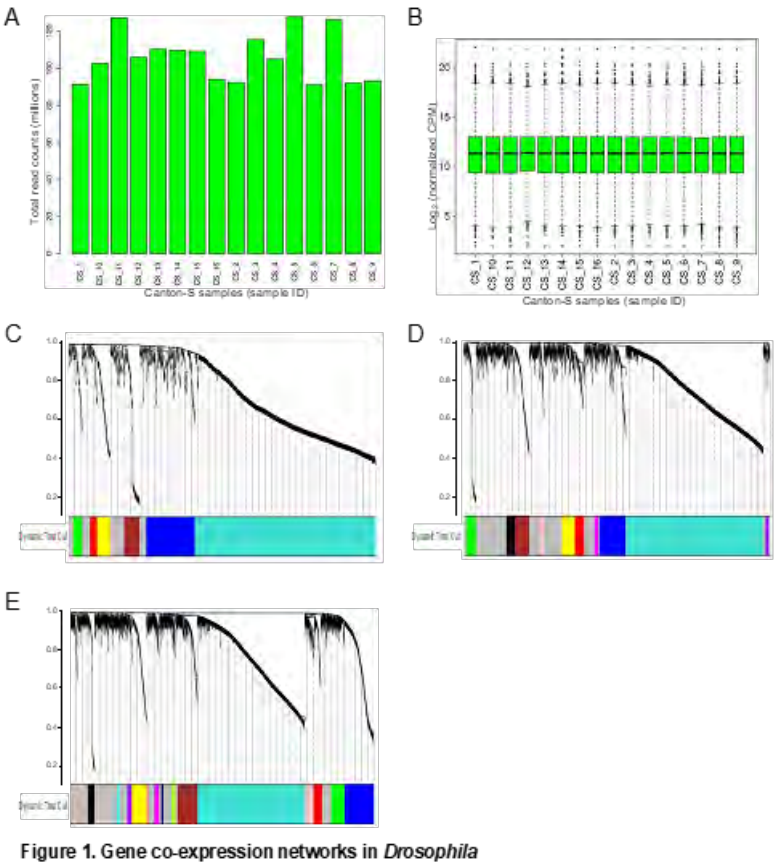

Figure 1. Gene co-expression networks in *Drosophila*
A. Total read counts in each sample. **B**. Distributions of normalized data. **C-E**. Co-expression network in *Drosophila*. **C**. Most variable 1000 genes make 6 modules (Soft threshold: 5, Minimal module size: 20 gens). **D**. Most variable 2000 genes make 10 modules (Soft threshold: 6, Minimal module size: 20 gens). **E**. Most variable 3000 genes make 15 modules (Soft threshold: 6, Minimal module size: 20 gens).

We found that a gene network can be constructed by 16 sets of transcriptome data from *Drosophila*. Depending on the setting, the number and size of networks required to build a gene network were changed significantly. As the next step, we will perform the network analysis using the WGCNA package (R package), which is capable of extracting gene members in the network and detailed information. After that analysis, we will compare the genes from human gene co-expression networks and conduct verification experiments using *Drosophila*.

Discussion & Conclusion

In this study, we obtained gene expression data of the 32870 gene from the head of wild-type *Drosophila* by RNA sequencing. Based on the variations of gene expressions, we are currently constructing co-expression networks. If necessary, we will integrateadditional RNA sequencing data to build a more reliable network. In the future, we will compare these Drosophila networks with the gene networks constructed from human gene expression data. Such information will be helpful to appropriately integrate genetic or pharmacologic screening data from *Drosophila* into drug discovery in human diseases. We expect that comparing gene regulatory networks are important to further understand the similarities and differences between *Drosophila* and humans and to best utilize fly models of human diseases. Disease models have different phenotypes for each model organism, which may also be explained by the differences in the genetic network of each organism.

References

Wang M. Li, A., Sekiya, M. *et al.* ***Neuron***., 2021, 109(2):257-272.

一般の皆様へ

キイロショウジョウバエは有用な遺伝学モデルとして使用されていますが、最近では神経変性疾患をはじめとした様々なヒト病態モデルが開発され、疾患研究、創薬分野においても多用されています。一方、生体内（特に脳内）での変化を包括的に捉え、疾患の発症機序解明、治療薬標的の同定へとつなげる１つのアプローチとして、遺伝子ネットワーク解析が有用であることが分かってきました。疾患研究において、さまざまなモデル動物と遺伝子ネットワーク解析を用いることで、疾患・創薬研究は飛躍的に進むことが予想されます。遺伝子ネットワークレベルでのショウジョウバエとヒトとの類似性と違いを解析し理解することで、疾患研究におけるショウジョウバエの有用性も高まると考えられます。

Elucidation of the promotion mechanism in plant shoot regeneration by environmental stimuli.

Sachihiro Matsunaga
sachi@edu.k.u-tokyo.ac.jp
Department of Integrated Biosciences, Graduate School of Frontier Sciences
The University of Tokyo

Summary Abstract

The environmental stimuli influence plant regeneration, but the molecular mechanism has not been elucidated. Our in vitro shoot regeneration via dedifferentiation of roots demonstrates that shoot regeneration occurs a few weeks later after the callus formation from roots. Using this system, we elucidated the mechanism of shoot regeneration by the gamma-ray irradiation as an environmental stimulation. We successfully developed the method to promote shoot regeneration by irradiation and identified the stress genes involved in shoot regeneration.
Key Words : shoot regeneration, gamma-ray, environmental stimuli, stress response

Introduction

Our de novo shoot regeneration is based on callus formation from roots (1, 2). Callus is a pluripotent cell mass derived from an explant placed in an auxin-rich callus inducing medium (CIM). Subsequently, de novo shoots are regenerated from callus cultured on cytokinin-rich shoot inducing medium (SIM). It is known that cell fate changes during this regeneration processes. It is unknown whether the accumulation of DNA damage impacts on shoot regeneration.

Results

We found that γ-ray irradiation before CIM transfer enhanced shoot regeneration. First, we irradiated *A. thaliana* with gamma-ray at several irradiation doses. We successfully determined an irradiation dose of gamma-ray, which most efficiently enhanced shoot regeneration. Second, we investigated whether the period before irradiation impacts shoot regeneration efficiency. The gamma-ray irradiation enhanced shoot regeneration irrespective of the developmental stage of seedlings. Third, we investigated whether the period after irradiation affects shoot regeneration efficiency. Callus at a particular time for incubation after irradiation enhanced shoot regeneration. Fourth, we investigated whether the CIM period affects shoot regeneration efficiency. Callus for a particular time of incubation also enhanced shoot regeneration.

Based on the above condition, we investigated whether DNA repair impacts shoot regeneration efficiency. In *A. thaliana*, two kinases, Ataxia Telangiectasia and Rad3 Related Protein (ATR) and Ataxia Telangiectasia Mutated (ATM), are involved in DNA damage response. However, *atr* and *atm* mutants irradiated with gamma-ray exhibited enhancement of shoot regeneration compared with the control. Thus, the DNA repair pathway involved in

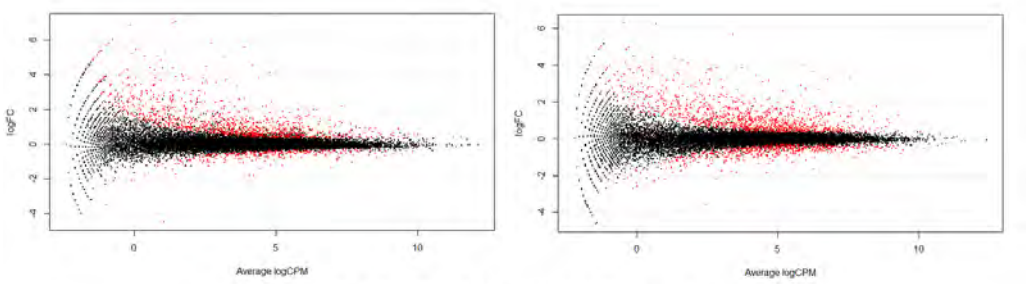

(red dots : FDR<0.01), (FC : fold change), (CPM : counts per million)

ATM and ATR did not regulate the enhancement of shoot regeneration by gamma-ray.

Thus, to find the novel regulators for the enhancement of shoot regeneration, we performed the transcriptome analysis by RNA-seq at the onset of callus induction gamma-ray irradiation 6 days prior to callus induction alters the gene expression pattern at both callus periods, contributing to the enhancement of the shoot regenerative competency.

We performed Gene Ontology (GO) enrichment analysis among up-regulated genes in the CIM 0 and 6 days. GO analysis demonstrated that at the 6 days after irradiation, the expression of genes associated with stress response was upregulated. We identified the stress response genes, which are probably responsible for the enhancement of shoot regeneration.

We also performed ChIP-seq analyses of H3K4me2. We got consistent data with the above RNA-seq data. Our integrated studies revealed the molecular and 1 day before shoot induction. In CIM 0days and CIM 6days, 409 and 415 genes, were up-regulated, and 512 and 777 genes were down-regulated as shown in graphs below. The result indicated that the mechanism by regulators of the stress response.

Furthermore, we examined the enhancement in shoot regeneration by other DNA damage stress except for the irradiation. We tried to add heavy metal, including excess copper, to the medium. We found a mutant responsible for shoot formation under the excess copper (3). We also developed a novel live-imaging technique to analyze the shoot regeneration via the environmental stimuli (4). Based on the research, we will do our best to publish the primary data about the relationship between shoot regeneration and gamma irradiation as an academic paper in the future.

Discussion & Conclusion

We revealed that several stress response genes regulated the enhancement in shoot regeneration by environmental stimuli. We used gamma-ray irradiation as environmental stimuli, which induce DNA damage. Our data showed that the initiation kinases of DNA repair, ATR and ATM were not involved in the enhancement of shoot regeneration, suggesting that the enhancement is not related to DNA repair pathway. Our seq-analyses demonstrated that some stress response genes regulate the mechanism. The molecular genetic analyses of these genes will contribute to developing new breeding techniques for enhancement in shoot regeneration or shoot formation in plants.

References

1. Ishihara, H.[#], Sugimoto, K.[#]*, Tarr, P. T, Temman, H., Kadokura, S., Inui, Y., Sakamoto, T., Sasaki, T., Aida, M., Suzuki, T., Inagaki, S., Morohashi, K., Seki, M., Kakutani, T., Meyerowitz, E. M., and Matsunaga, S.* (2019) Primed histone demethylation regulates shoot regenerative competency. *Nature Commun.*, 10, 1786. [#]These authors equally contributed to this work.
2. Sugimoto, K., Temman, H., Kadokura, S., and Matsunaga, S.* (2019) To regenerate or not to regenerate: factors that drive plant regeneration. *Curr. Opin. Plant. Biol.*, 47, 138-150.
3. Sakamoto, Y., Sato, M., Sato, Y., Harada, A., Suzuki, T., Goto, C., Tamura, K., Toyooka, K., Kimura, H., Ohkawa, Y., Hara-Nishimura, I., Takagi, S. and Matsunaga, S.* (2020) Subnuclear gene positioning through lamina association affects copper tolerance. *Nature Commun.*, 11, 5914.
4. Shibuta, M. K., Sakamoto, T., Yamaoka, T., Yoshikawa, M., Kasamatsu, S., Yagi, N., Fujimoto, S., Suzuki, T., Uchino, S., Sato, Y., Kimura, H. and Matsunaga, S.* (2021) A live imaging system to analyze spatiotemporal dynamics of RNA polymerase II modification in *Arabidopsis thaliana*. *Commun. Biol.*, 4, 580.

一般の皆様へ

植物が環境刺激を受けることで器官再生が促進するメカニズムを明らかにすることができた。ヒトや動物とは異なり脳や神経系を持たない植物が、外部環境の変動を捉えて、器官再生にどのように結びつけているのかを分子的メカニズムの一端がわかった。今後、このメカニズムを利用して、植物の再生促進法の開発が可能になることが期待される。

Analyses of pain regulation mechanisms by IL-27

Hiroki Yoshida
yoshidah@cc.saga-u.ac.jp
Saga University Faculty of Medicine

Summary Abstract

IL-27 is an anti-inflammatory cytokine. Recently we reported that IL-27 has a pain regulatory role. To address IL-27-producing cells and/or cells responsible for IL-27-mediated pain regulation, we generated IL-27-reporter mice. By taking advantage of this reporter mouse, we tried to identify IL-27-producing cells in the pain sense transmission. Unfortunately, we were unable to detect IL-27-producing cells in the skin, neuron fibers, and brain. However, by electrophysiological study, three types of neuronal fibers were shown to be possibly responsible for pain regulation.
Key Words : IL-27, pain, neuralgia

Introduction

Interleukin 27 (IL-27) is a member of IL-12 cytokine family and is composed of p28 subunit and EBI-3 subunit. IL-27 has immunosuppressive effects on various immune cells although it was originally reported as a Th1-inducing cytokine. Lack of IL-27 signaling (p28-deficient mice and IL-27 receptor (WSX-1)-deficient mice), surprisingly demonstrated lower threshold to various pain and neuralgia symptom while administration of IL-27 in p28-deficient mice restored the susceptibility to normal levels. These data indicate that IL-27 has a novel function to regulate pain sensitivity. Precise mechanisms by which IL-27 regulates pain is unknown.

Results

IL-27 is reportedly produced by macrophages and dendritic cells stimulated by microbial products, such as LPS. However, both p28-deficient and WSX-1-deficient mice showed spontaneous neuralgia and lower threshold to pain without any additional stimulation or priming to pain. This indicates that IL-27 is constitutively produced and exerts its pain-regulation effects. To address the question where and in which type of cells IL-27 is produced in the pathway of pain sense transmission, we have developed an IL-27-reporter mouse in which Venus (a fluorescent protein) is produced under p28 promoter regulation. The reporter mice work well in that macrophages/dendritic cells from LPS-administrated mice emit sufficient fluorescent signal by flow cytometric detection. We assume that either keratinocytes and/or Langerhans cells in the skin, neurons to sense various types of pain, or brain cells including glia cells, are the producer of IL-27 in terms of pain regulation. However, we have been unable to detect p28-Venus signal in any of above-mentioned cells by fluorescence microscopic examination. These results indicate that constitutive production of IL-27 p28 is very weak for detection by this method. Interestingly, although dendritic cells isolated from LPS-administrated mice expressed p28/Venus ex vivo, dendritic cells from

untreated mice failed to respond to in vitro LPS stimulation by p28/Venus production. This suggests that IL-27 production by dendritic cells and/or cells involved in pain regulation may require additional stimulation.

Besides the detection of p28-Venus signal, we performed a functional assay where p28-deficient or WSX-1-deficient neurons were isolated and tested for (hyper-) sensitivity to stimulation. In our previous report, live mice were tested for their sensitivity against mechanical stimulation, heat/cold stimulation, and chemical stimulations. In the current study, hindlimb skin-saphenous nerve preparations were isolated ex vivo and used for electrophysiological analysis of nociceptors. C-fibers from WSX-1-deficient and p28-deficient mice showed hyper discharge rate over wild-type neurons against mechanical stimulation with lower threshold for excitation. Repeated experiments for confirmation and for statistical analysis, however, is required. In the isolated nerve specimen, we were unable to detect p28 nor WSX-1 gene expression by RT-PCR method.

We have not examined the direct pain-regulatory effects of IL-27 in the brain in the current study. Lack of IL-27 signaling does not affect brain development or behavior in the mice. IL-27 is known to be abundantly expressed in the brain (and in the central nervous system) of mice. Recently, IL-27 is reported to be expressed by astrocytes and microglia cells in inflammatory settings. The precise role of IL-27 in the brain has yet to be clarified, although some reports showed that IL-27 is pro-inflammatory rather than anti-inflammatory in this context. We have confirmed the expression of IL-27 in astrocytes and microglia. The pain regulatory role of IL-27 in these cells is completely unknown.

To address the above-mentioned, unsolved questions of IL-27-producing cells in the pain sensation, we started conditional p28 knockout mice in which cell (such as neurons, Langerhans cells, and astrocyte)-specific gene destruction is possible. With this strain of mice, further clarification of responsible cells and responsible mechanisms of IL-27-mediated pain regulation will be possible.

Discussion & Conclusion

We have successfully generated IL-27 (p28)-Venus reporter mice, which is one of the aims of this study. Unfortunately, we were unable to detect IL-27 production in the assumed cells assumed to be responsible in pain regulation in unstimulated mice. This suggests that the constitutive expression of IL-27 is too low to be detected by this method and/or IL-27 expression required additional stimulation in this pathway. Electrophysiological study indicates neurons (C fibers) may be responsible, but further examination is necessary.

For the further analyses, we started generating p28 conditional mice. By taking advantage of this strain of mice, identification of responsible cells and mechanisms in IL-27-mediated pain regulation will be possible.

References

1. Sukhbaatar, O., D. Kimura, M. Miyakoda, S. Nakamae, K. Kimura, H. Hara, H. Yoshida, S. I. Inoue, and K. Yui. 2020. Activation and IL-10 production of specific CD4(+) T cells are regulated by IL-27 during chronic infection with Plasmodium chabaudi. Parasitol Int 74: 101994.
2. Ishikawa, A., Y. Miyake, K. Kobayashi, Y. Murata, S. Iizasa, E. Iizasa, S. Yamasaki, N.

Hirakawa, H. Hara, H. Yoshida, and T. Yasaka. 2019. Essential roles of C-type lectin Mincle in induction of neuropathic pain in mice. Sci Rep 9: 872.
3. Kanai, K., A. M. Park, A. Watanabe, T. Arikawa, T. Yasui, H. Yoshida, I. Tsunoda, and O. Yoshie. 2018. Murine gamma-Herpesvirus 68 Induces Severe Lung Inflammation in IL-27-Deficient Mice with Liver Dysfunction Preventable by Oral Neomycin. J Immunol 200: 2703-2713.
4. Sasaguri, T., T. Taguchi, Y. Murata, K. Kobayashi, S. Iizasa, E. Iizasa, M. Tsuda, N. Hirakawa, H. Hara, H. Yoshida, and T. Yasaka. 2018. Interleukin-27 controls basal pain threshold in physiological and pathological conditions. Sci Rep 8: 11022.

一般の皆様へ

インターロイキン 27（IL-27）は、免疫抑制作用を持つサイトカインとして、自己免疫疾患や感染時の過剰な炎症（サイトカインストームなど）に対する治療応用に関する研究が進んでいます。今回、IL-27 による全く新しい痛み知覚制御作用を発見し、現在その詳細を解析しています。これは、モルヒネや消炎鎮痛剤とは異なる作用によるものであり、新しい疼痛の治療法の開発につながることが期待されます。

Molecular and neural mechanism associated with social behavior

Teiichi Furuichi
tfuruichi@rs.tus.ac.jp
Tokyo University of Science

Summary Abstract

Autism spectrum disorder (ASD) affects approximately 1 in 40 children and is highly inheritable. As there is no cure for ASD, understanding its pathophysiology is an important health issue. In this study, we performed a comprehensive brain transcriptome and behavioral analyses of BTBRTF/ArtRbrc (BTBR/R) mice. Our data identified potentially important genes, non-coding RNAs, and RNA interactions which are probably critical to brain development and/or function. Collectively, we showed that BTBR/R have mild but significant deficits in social behavior and is an excellent animal model that can contribute to the understanding of the genetic underpinnings of autism susceptibility.
Key Words : autism spectrum disorder; ASD; transcriptome; social behavior; mouse model

Introduction

Autism spectrum disorder (ASD) is a complex neurodevelopmental disorder characterized by social and communication deficits, and stereotyped repetitive behaviors with restricted interests. ASD is highly heritable and is also affected by environmental factors. Gene transcriptional profiling in ASD has been performed by utilizing post-mortem brain samples. The restricted availability of brain tissue from humans with ASD represents a significant challenge. From this point of view, animal models are valuable for analyzing the molecular and pathological mechanisms of ASD at the gene and protein expression level. In this study, we performed a comprehensive brain transcriptome analysis in the cerebral cortex and striatum, in which altered cortico-striatal connectivity has been suggested to be present in patients with ASD, between BTBR/R mice and C57BL/6J (B6) mice with high sociality. Our results revealed the differential transcription profiles in microarray expression levels as well as cellular-regional levels in the cerebral cortex and striatum of BTBR/R mice and B6 mice, and suggested that BTBR/R mice have a slight autistic-like tendency in terms of social novelty recognition and stereotypic behavior.

Results

To compare the transcriptome features in the cerebral cortex and striatum between BTBR/R and B6 mice, we performed DNA microarray analysis. The data indicated that BTBR/R mice exhibited the differential expression of 1,280 transcripts (974 downregulated, 306 upregulated) in the cerebral cortex and striatum compared to B6 mice (Fig. 1A). Using the bioinformatics databases, we classified types of the differentially expressed genes (DEGs) identified, as shown in Fig. 1B. Downregulated and upregulated transcript groups consisted of 524 and 184 protein-coding transcripts, 387 and 111 non-coding transcripts,

33 and 6 pseudogenes, and 30 and 5 other transcripts, respectively. Using RNA–RNA interaction network analysis tool, we further suggested the differential regulation of transcription and translation in the cerebral cortex and striatum between two strains via RNA–RNA interactions. To gain an insight into the biological significance in altered gene expression between BTBR/R and B6 mice, we performed the functional gene classification of DEGs by the gene ontology (GO) enrichment, the KEGG pathway and weighted correlation WGCNA analyses. Overall, our comprehensive bioinformatics analyses of gene expression highlighted functional alterations in the cerebral cortex and striatum of BTBR/R mice. We next explored whether BTBR/R mice DEGs were the known ASD candidate genes by utilizing the autism gene database AutDB, and identified 53 genes (40 downregulated and 13 upregulated) out of 1,280 DEGs to be ASD candidate genes. We comprehensively analyzed the spatial cellular expression of DEGs in the BTBR/R and B6 mice brains in a qualitative manner using the *in situ* hybridization (ISH) method (Fig. 2A, B). Finally, we analyzed ASD-related social behavior of BTBR/R and showed that, compared to B6 mice, BTBR/R mice have a mild impairment in social recognition (Fig. 3A-C) as well as increased stereotypic behavior (Fig. 3D).

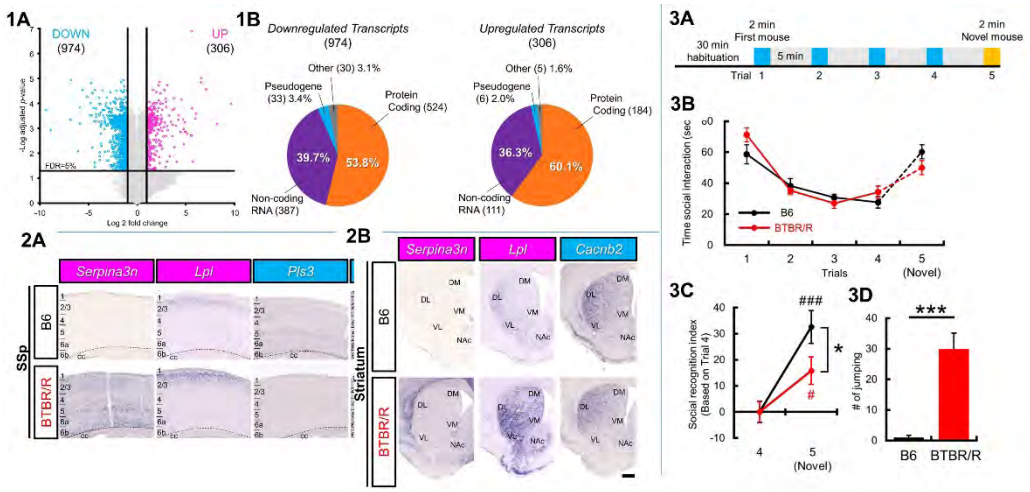

Discussion & Conclusion

In conclusion, we characterized the transcriptomic features of the cerebral cortex and striatum of BTBR/R mice in comparison with B6 mice, using microarray and ISH analyses together with comprehensive bioinformatics approaches. We identified DEGs (upregulated and downregulated) and co-expression as well as interaction RNA networks in BTBR/R mice brains. In addition, the BTBR/R mice data were comprehensively compared to those reported in the previous studies of subjects with ASD as well as ASD animal models, including another BTBR subline *T+ Iptr3*^{tf}/J (BTBR/J) mice. Our results allow us to propose potentially important genes and ncRNAs that may be associated with brain function and behaviors characteristic to BTBR/R mice that are indicative of an autistic-like phenotype. Taken together, the results of our study suggest the genetic aspects of BTBR/R mice brain function, which is informative to the understanding of the genetics of the observed behavioral defects. To contribute further to the understanding of ASD genetics and biology, further studies regarding detailed cellular expression patterns as well as functional aspects

of the DEGs in BTBR/R mice brain are required, considering the differences and/or similarities with socially impaired BTBR/J mice and highly social B6 mice.

*Remarks: We also studied mouse models for oxytocin release and associated social behavior as well as brain-derived neurotrophic factor (BDNF) release.

References

Mizuno S, Hirota JN, Ishii C, Iwasaki H, Sano Y, and Furuichi T. Comprehensive Profiling of Gene Expression in the Cerebral Cortex and Striatum of BTBRTF/ArtRbrc Mice Compared to C57BL/6J Mice. *Front Cell Neurosci.* 2020, 14:595607. doi: 10.3389/fncel.2020.595607.

Kojima M, Ishii C, Sano Y, Mizui T, and Furuichi T. Journey of brain-derived neurotrophic factor: from intracellular trafficking to secretion. *Cell Tissue Res.* 2020, 382(1):125-134. doi: 10.1007/s00441-020-03274-x.

一般の皆様へ

自閉スペクトラム症（ASD）は、社会的コミュニケーションの欠損と常同行動・興味の限局を特徴とし世界各国で高い有病率を示します。原因が不明で完治療法がないため、病因究明や治療法の確立が課題となっています。遺伝要因が強い多因子疾患と考えられていますが、ヒト脳での遺伝子解析には限界があります。本研究では、高社会性を示すB6マウスと比較して、BTBR/Rマウスの社会性が低下していること、両マウスの脳内の遺伝子発現（トランスクリプトーム）の比較解析とバイオインフォマティクス解析によりASDの遺伝因に示唆的な情報を示すことができました。今後、BTBR/RマウスがASD関連の研究開発に寄与する有用な動物モデルとなると期待されます。

Development of H_2S-Activatable Near-Infrared-dye Probes: Bioimaging and Therapy

Yusuke Ishigaki
yishigaki@sci.hokudai.ac.jp
Hokkaido University

Summary Abstract

Zigzag bisquinodimethanes (BQDs) with eight aryl groups were designed as redox-switchable molecules that undergo four-electron oxidation to produce doubly twisted tetracationic pentacenes. In contrast to one-stage four-electron oxidation of BQDs, stepwise two-electron reduction of tetracationic pentacenes occurs to give the original BQDs via dicationic anthracenes. Since both tetracations and dications exhibit near-infrared (NIR) absorptions (-1400 nm) based on an intramolecular charge-transfer interaction, changes in not only their structures but also their UV-Vis-NIR spectra can be controlled by redox stimuli. Such NIR absorbing cationic dyes are potential candidates for H_2S-activatable probes, which will be clarified in due course.

Key Words : Near-Infrared Absorption, Organic Redox Systems, Cationic Dyes

Introduction

Recently, much attention has been focused on developing electrochromic material (EM), by which the electric potential as an input is transduced into the color change as an output. With regard to the use in biological systems, NIR absorption properties are of great importance for bioimaging and phototherapy.[1–3] However, only limited numbers of such NIR EM have been reported so far. In this study, we designed and synthesized novel NIR EM, which can be applicable for H_2S-activatable probes.

Results

In this study, we proposed a new approach for preparing extended [*n*]acenes by electrochemical oxidation, and demonstrated unprecedented hysteretic three-state redox interconversion among neutral bisquinodimethanes (BQDs), tetracationic pentacenes, and dicationic anthracenes, in which both cations exhibit significantly red-shifted absorptions in the near-infrared (NIR) region based on an intramolecular charge-transfer (CT) interaction.

The target BQs were prepared from 5,7,12,14-pentacenetetrone over 4 steps, where stepwise introduction of aryl groups was conducted by Suzuki-Miyaura cross-coupling reaction following dibromoolefination. According to X-ray analyses, these BQDs with three non-fused benzene rings adopt a zigzag conformation. By treatment with four equivalents of $(4\text{-}BrC_6H_4)_3N^{+\bullet}SbCl_6^-$ (Magic Blue), tetracationic $(SbCl_6^-)_4$ salts were obtained quantitatively. X-ray analyses revealed that the tetracations have a fully conjugated planar pentacene core, which is almost orthogonal to the diarylmethylium moieties. The original BQDs were completely recovered when tetracations were treated with an excess amount of Zn powder,

which demonstrates that reversible redox interconversion between neutral donors and tetracations can proceed.

To investigate the redox properties in detail, we conducted cyclic voltammetry in CH_2Cl_2. For methoxyphenyl derivative, the voltammogram showed a one-wave four-electron oxidation peak at +1.12 V (vs. SCE). The one-stage four-electron process for oxidation was verified by using ferrocene as an external standard and confirmed by differential pulse voltammetry. As a result of the change in structures, return peaks, where two-stage two-electron reduction occurs via intermediate dication, appeared in the far cathodic region (E^{red}/V: +0.55 for tetracation and +0.27 for dication). Such a cathodic peak shift is a characteristic feature of dynamic redox (*dyrex*) systems,[4,5] in which the steady-state concentration of intermediate radical species is negligible. Similar redox behavior was observed for *tert*-butylphenyl derivative (E^{ox}/V: +1.26 for neutral donor; E^{red}/V: +0.89 for tetracation and +0.76 for dication).

To obtain further information regarding the structure of the intermediary dications as expected by the voltammetric analyses of BQDs, we performed a titration experiment on the chemical reduction of tetracations, which was monitored by UV-Vis-NIR spectroscopy. Upon the addition of aliquots of Bu_4NI (TBAI) in CH_2Cl_2, the UV-Vis-NIR spectrum of tetracation with *tert*-butylphenyl groups changed to that of neutral species via the intermediate dication in a stepwise fashion, where several isosbestic points were observed in both stages. Especially in the first stage, the absorption maxima at 498 and 1094 nm for tetracation in the visible and NIR region shifted to 509 and 1005 nm for dication (Figure 1). Similar results were obtained by using methoxyphenyl derivative with decamethylferrocene. The NIR absorption of dications suggested that localized dication with an anthracene skeleton fused with an anthraquinodimethane (AQD) unit stabilized by intramolecular CT interaction would be likely, and this idea is supported by the fact that the DFT method gave no energy-minimized structure for the quinoidal form.

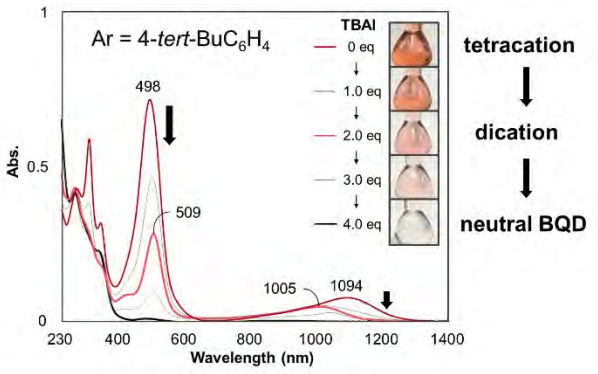

Figure 1. Change in UV-Vis-NIR spectrum of tetracationic $(SbCl_6^-)_4$ salt (6.00 μM) upon the addition of several aliquots of TBAI in CH_2Cl_2.

After many trials, dications could be isolated in pure form. Upon two-electron reduction of tetracationic $(SbCl_6^-)_4$ salts in CH_3CN with two equivalents of reducing reagent, dicationic $(SbCl_6^-)_2$ salts were isolated quantitatively. These structures of dications are

bis(diarylmethylium)-substituted anthracene fused with an AQD unit, as characterized by ^{1}H NMR spectra and finally determined by single-crystal X-ray analyses. Additionally, when dications were treated with two equivalents of Magic Blue and with an excess amount of Zn powder, tetracations and original BQDs were isolated quantitatively for both reactions. Therefore, unprecedented hysteretic three-state redox interconversion among tetracationic pentacenes, dicationic anthracenes, and neutral BQDs, as shown by cyclic voltammetry, was demonstrated on a preparative scale (Scheme 1).[6]

Scheme 1

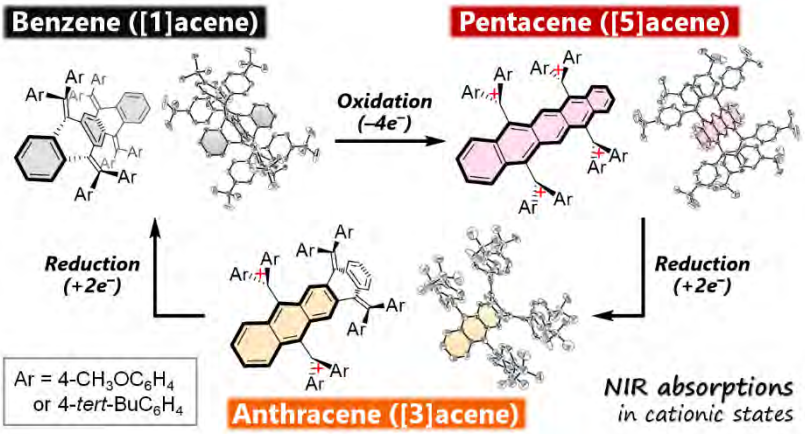

Discussion & Conclusion

In conclusion, we designed and synthesized zigzag-structured BQD derivatives with non-fused benzene rings, which undergo one-stage four-electron oxidation to produce tetracationic pentacene derivatives with a doubly twisted conformation. When tetracationic pentacenes were reduced, two-stage two-electron reduction occurs via dicationic anthracenes to the original BQDs. Such hysteretic three-state redox interconversion among them demonstrates perfect control of the number of fused benzene rings ([1] -> [5] -> [3] -> [1]) in the [*n*]acene structure by redox conversion. It is noteworthy that cationic species can be isolated even for pure hydrocarbons. Furthermore, since these cations exhibit significantly red-shifted NIR absorptions (-1400 nm) based on intramolecular CT interaction, changes in structure as well as UV-Vis-NIR absorptions can be controlled by redox switching. These results provide a new tactic for creating [*n*]acene-based redox switches with fully controlled multiple-electron transfer, and for dynamically interconverting their structures and properties in a unimolecular fashion. Such NIR absorbing cationic dyes are potential candidates for H_2S-activatable probes, which will be clarified in due course.

References

[1] L. Wu, Y. Sun, K. Sugimoto, Z. Luo, Y. Ishigaki, K. Pu, T. Suzuki, H. Chen, D. Ye, *J. Am. Chem. Soc.* **2018**, *140*, 16340–16352.

[2] L. Wu, Y. Ishigaki, Y. Hu, K. Sugimoto, W. Zeng, T. Harimoto, Y. Sun, J. He, T. Suzuki, X. Jiang, et al., *Nat. Commun.* **2020**, *11*, 446.

[3] Y. Ishigaki, T. Harimoto, K. Sugimoto, L. Wu, W. Zeng, D. Ye, T. Suzuki, *Chem. – An Asian J.* **2020**, *15*, 1147–1155.

[4] T. Suzuki, Y. Ishigaki, M. Takata, J. Nishida, T. Fukushima, *Heterocycles* **2021**, *102*, 419–450.
[5] Y. Ishigaki, Y. Uchimura, T. Shimajiri, T. Suzuki, *Bull. Chem. Soc. Jpn.* **2021**, *94*, 1385–1393.
[6] Y. Ishigaki, T. Harimoto, K. Sugawara, T. Suzuki, *J. Am. Chem. Soc.* **2021**, *143*, 3306–3311.

一般の皆様へ

電気化学的な刺激によって色調が変化するエレクトロクロミック材料（EM）は様々な応用の観点で注目を集めています。目に見える波長（約 400–780nm）よりもエネルギーの弱い近赤外光（約 780–2500nm）を吸収する EM は、バイオイメージングなどへ応用できますが、重金属が入っていない有機分子で作ることは容易でないため、報告例が限られていました。そこで本研究では、近赤外光を吸収する新たな有機 EM を設計・合成しました。電気化学的な刺激によって生じる近赤外色素では、1400nm に及ぶ光を吸収するため、バイオイメージングと医療への応用が期待されます。

Identification of molecular mechanism underlying drug resistance by tumor-stroma derived exosome

Takatsugu Ishimoto
taka1516@kumamoto-u.ac.jp
The International Research Center for Medical Sciences (IRCMS), Kumamoto University

Summary Abstract

This study elucidates a novel molecular mechanism through which Annexin A6 in CAF-EV activates FAK-YAP by stabilizing b1 integrin at the cell surface of gastric cancer cells and subsequently induces drug resistance.

Key Words : tumor microenvironment, cancer-associated fibroblasts (CAFs), gastric cancer

Introduction

Cancer-associated fibroblasts (CAF) are found among stromal cells in solid tumors and play a central role in cancer progression, and the molecular mechanisms of CAFs have been extensively investigated. Extracellular vesicles (EV) from CAFs are composed of diverse payloads. Although CAFs impact the aggressive characteristics of gastric cancer cells, the contribution of CAF-EV to gastric cancer progression has not been elucidated.

Results

To quantify the amount of Cancer associated fibroblasts (CAFs) in gastric cancer (GC) tissues, resected tissues from 335 GC patients were subjected do immunohistochemical staining using an antibody specific for alpha-smooth muscle actin. CAF-high GC patients exhibited significantly shorter overall survival. Moreover, stage IV GC patients with CAF-high tumors who received chemotherapy had remarkably shorter overall survival. Based on these results, we first hypothesized that CAFs in the tumor stroma are involved in mediating the drug resistance of GC cells.

At first, we cultured GC cells with CAF-conditioned medium (CM) in extracellular matrix (ECM) exhibited characteristic network formation and remarkable drug resistance. Next, we conducted RNA sequencing to identify unique molecular patterns in GC cells in the ECM after CAF-CM treatment. Based on the results from these analyses, we presumed that CAF derived extracellular vesicles (EVs) might be involved in network formation

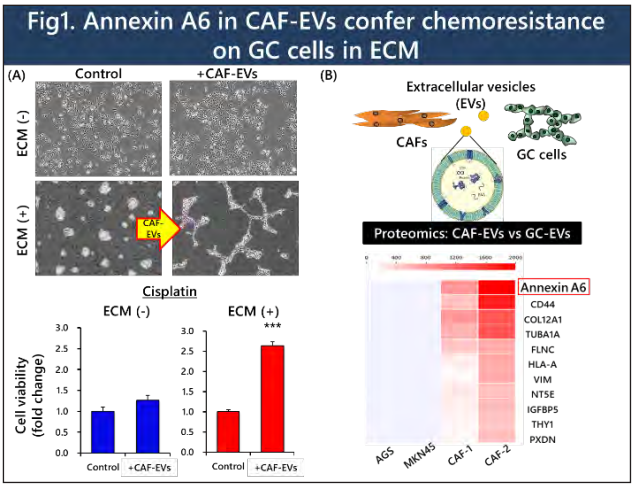

and drug resistance. Thus, we extracted CAF-EVs by ultracentrifugation, and showed that EVs contained in CAF-CM play a central role in network formation and drug resistance in GC cells.

We conducted a comprehensive proteomic analysis using GC-EVs or CAF-EVs and focused on annexinA6 most specifically expressed in CAF-EVs. AnnexinA6-depleted CAF-EVs diminished both the network formation and drug resistance of GC cells in the ECM (Figure 1).

According to the results from the network analysis of the RNA sequencing data, we focused on β1 integrin and showed that the CAF-EV-induced increase in cell surface β1 integrin expression in GC cells is critical for network formation and drug resistance in the ECM.

Annexin A6 and β1 integrin have been found to be important in GC cell network formation in the ECM; thus, we predicted that annexin A6 and β1 integrin interact with one another. We conducted such as protein stability assay, flow cytometry and immunofluorescence analyses and revealed that β1 integrin expression at the surface of GC cells in the ECM is enhanced by annexin A6 in CAF-EVs.

Because signaling pathways downstream of integrin are regulated by protein-protein interactions, we further performed a comprehensive proteomic analysis of GC cells treated with and without CAF-CM as well as RNA sequencing. Differentially expressed genes related to focal adhesion and the PI3K-AKT and Hippo signaling pathways were identified in GC cells treated with CAF-CM according to a pathway analysis of the comprehensive transcriptomics and proteomics data. Further functional analyses indicate that integrin-FAK signaling and subsequent YAP activation play a critical role in network formation in the ECM and drug resistance of GC cells treated with CAF-EVs.

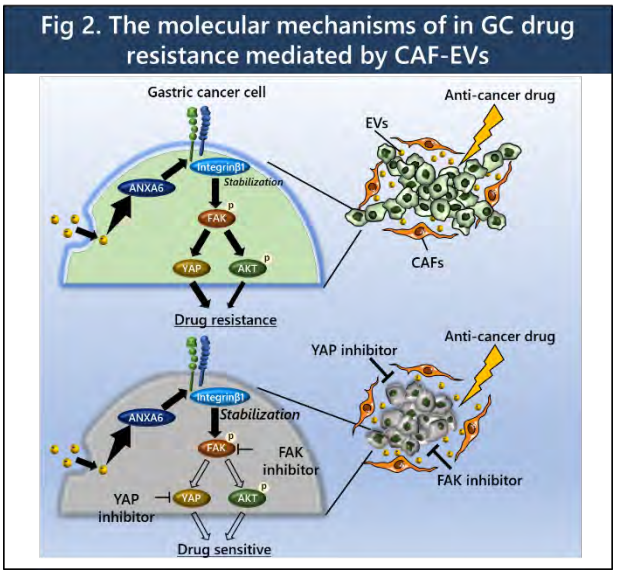

Fig 2. The molecular mechanisms of in GC drug resistance mediated by CAF-EVs

To verify the significance of CAF-EVs in GC drug resistance in an in vivo model, GC cells were injected into the peritoneal cavities of nude mice. This model elucidated that annexinA6 in CAF-EVs play a role in the drug resistance of GC cells in vivo as well as in vitro. We then examined whether FAK and YAP inhibitors could attenuate the cisplatin resistance of GC cells mediated by CAF-EVs. The antitumor effect of cisplatin was recovered by additional treatment with the FAK and YAP inhibitors (Figure 2).

Discussion & Conclusion

Annexin A6 in EVs derived from CAFs stabilizes b1 integrin at the plasma membrane of gastric cancer cells in the ECM. Subsequently, phosphorylated FAK leads to AKT activation

and YAP accumulation, which results in the network formation of gastric cancer cells in the ECM and their substantial drug resistance. Moreover, blockade by an FAK or a YAP inhibitor but not an AKT inhibitor effectively inhibited the drug resistance of gastric cancer cells. The findings of this study provide evidence demonstrating that FAKYAP signaling activated by Annexin A6 in CAF-EVs from the tumor stroma is a novel target for combination therapy with currently available anticancer drugs.

References

1, Bu L, Baba H, Yoshida N, Miyake K, Yasuda T, Uchihara T, Tan P, **Ishimoto T***. Biological heterogeneity and versatility of cancer-associated fibroblasts in the tumor microenvironment. ***Oncogene.*** 38(25):4887-4901. 2019

2, Bu L, Baba H, Yasuda T, Uchihara T, **Ishimoto T***. Functional diversity of cancer-associated fibroblasts in modulating drug resistance. ***Cancer Sci.*** 111(10):3468-3477. 2020

3, Uchihara T, Miyake K, Yonemura A, Komohara Y, Itoyama R, Koiwa M, Yasuda T, Arima K, Harada K, Eto K, Hayashi H, Iwatsuki M, Iwagami S, Baba Y, Yoshida N, Yashiro M, Masuda M, Ajani J, Tan P, Baba H, **Ishimoto T***. Extracellular Vesicles from Cancer-Associated Fibroblasts Containing Annexin A6 Induces FAK-YAP Activation by Stabilizing β1 Integrin, Enhancing Drug Resistance. ***Cancer Res.*** 15;80(16):3222-3235. 2020

一般の皆様へ

胃がんに対して抗がん剤治療が効きにくくなる「治療抵抗性」に関わる因子として、CAFs が分泌する細胞外小胞（EVs）中のアネキシン A6 が胃がん細胞に取り込まれることで、抗がん剤の効果が低下することが分かりました。アネキシン A6 タンパク質や EVs を分泌する CAFs をターゲットにした新たな癌治療法の可能性を見出しました。

Stabilization mechanism of amyloid aggregates revealed by protein engineering techniques

Koki Makabe
makabe@yz.yamagata-u.ac.jp
Yamagata university

Summary Abstract

Amyloid is a proteinous aggregate which involves several neurodegenerative diseases such as Alzheimer's. Thus, the basic understanding of amyloid biophysical properties is important for understanding such diseases. Although important, insoluble and heterogeneous nature of amyloid humpers its characterization. Here, we report the structural analysis of amyloid edge using a model protein system.
Key Words : Amyloid, beta-sheet, model protein, protein engineering

Introduction

Amyloid is a proteinous aggregate which involves several neurodegenerative diseases such as Alzheimer's. Thus, the basic understanding of amyloid biophysical properties is important for understanding such diseases. Although important, insoluble and heterogeneous nature of amyloid humpers its characterization. To overcome this limitation, we have developed a protein model system to capture the amyloid core structure into a globular protein, termed peptide self-assembly mimic (PSAM). Here, we evaluated the structural property of the elongation edge of beta-sheet which mimics the edge of amyloid.

Results

To mimic the elongation edge of amyloid, we constructed a PSAM variant whose C-terminal beta-sheet edge was exposed to the solvent. To do this, the C-terminal domain of the original PSAM was deleted by gene engineering method. By deleting the C-terminal domain, the C-terminal beta-strand of the central single layer beta-sheet was no longer caped by the C-terminal domain. We termed this variant as PSAM-edge. PSAM-edge was expressed in E.coli and purified by His tag affinity chromatography.

We confirmed that PSAM-edge is monomeric in a solution buffer by size exclusion chromatography (SEC). Because beta-sheet edge of PSAM-edge is exposed to solvent, it is surprising that PSAM-edge does not form any aggregate.

Stability of the PSAM-edge was evaluated by urea-induced chemical denaturation method by monitoring the CD values. The resulting titration denaturation curve of PSAM-edge showed clear sigmoidal transition with a single transition. We fitted this denaturation curve with a two-state unfolding model and the experimental data well fitted with the two-state model suggesting that the beta-sheet region co-operatively unfolded with the N-terminal domain.

SEC and chemical denaturation experiments clearly demonstrate that PSAM-edge behaves as a general globular protein. It means the elusive beta-sheet edge properties can

be observed by using this PSAM variants. Thus, we next tried to determine the molecular structure of PSAM-edge by x-ray crystal structure analysis. We successfully obtained single crystals for x-ray diffraction experiments. One of the crystals diffracts to the resolution of 2.2 angstrom. The phase of the diffraction data was determined by molecular replacement method using a wildtype OspA structure without the C-terminal domain, which was the original scaffold for PSAM construction. There were four molecules in the asymmetric unit and these four molecules were almost identical with a root mean square deviation (RMSD) values below 1.3 angstrom. Thus, we analyzed the one of the four structures (denoted as molA) for further analysis. The electron density map of PSAM-edge is clear to the final beta-strand. Only the C-terminal four residues are disordered. This observation indicated that even the absence of the C-terminal capping domain, the central beta-sheet is stably formed except for the terminal four residues. We initially expected that terminal few beta-strand must be disordered because of the flexible nature of the terminal structure. The crystal structure unexpectedly demonstrated that the initial our expectation was wrong. Thus, in actual amyloid, the elongation edge of the fibril must be stable to attach and incorporate the next molecule. At the same time, if the terminal structure is stable, it is also a danger of intermolecular aggregation. From the PSAM-edge structure, the flexible nature of the terminal four residues may play a key role to prevent the aggregation. Fluctuating terminal portion may exclude the attaching molecule and preventing the association.

To observe the dynamic movement of PSAM-edge, we performed the MD simulation. The MD simulation period was 50 ns and we evaluated the molecular fluctuation of PSAM-edge. In MD trajectory, we found that the central beta-sheet is stably formed same as the crystal structure. During the simulation, only the terminal four residues fluctuated which is also same with the crystal structure observation where these residues are disordered. The striking consistency between the crystal structure and MD simulation suggests the exposed beta-sheet stability is general.

Discussion & Conclusion

We successfully modeled beta-sheet edge by deleting the capping C-terminal domain from original PSAM. In general, natural proteins prevent the exposure of the beta-sheet edge because of its high tendency for the aggregation. In this viewpoint, it is interesting to see the structure of the exposed beta-sheet edge of PSAM-edge. Although PSAM-edge exposes the beta-sheet edge, it is highly soluble and monodisperse. The aggregation resistant property of PSAM-edge could be attributable to the fluctuation of the C-terminal residues observed in the crystal structures and MD simulation. The fluctuation should prevent edge-to-edge interaction. In the future study, it is interesting to compare the edge property of actual amyloids and PSAM edge. In addition to that, the knowledge about the edge property of PSAM-edge will expand the designability of beta-sheet rich protein in protein design field.

References

1. Shiga S. and Makabe K.
Structural analysis of the β-sheet edge of peptide self-assembly using a model protein.
Proteins, in press, 2021 doi: 10.1002/prot.26063.

一般の皆様へ

この研究ではアルツハイマー病などの病変部位で見つかる、蛋白質凝集体の性質を明らかにするために、病変蛋白質そのものではなくて、別の扱いやすい蛋白質に凝集体の構造を移植して評価を行いました。特に、βシートと呼ばれる蛋白質の分子構造が集まって、病気の凝集体になるところをモデル系によって、詳細な構造で評価しました。詳細な構造から、そのようなβシートは単独でも安定に構造ができていることがわかりました。これは病気を引き起こす凝集が非常に安定なことと関連があるかもしれません。

Identification of the lipid species which regulate epidermis differentiation in Arabidopsis.

Mitsutomo Abe
mabe@bio.c.u-tokyo.ac.jp
Department of Life Sciences, Graduate School of Arts and Sciences,
The University of Tokyo

Summary Abstract

The differentiation of distinct cell types in appropriate patterns is a fundamental process in the development of multicellular organisms. The protodermal cell is an ideal system for studying position– and lineage–dependent cell differentiation in plants. In this study, I found that very-long-chain fatty acid-containing ceramides which are predominantly synthesized in the outermost cells, bind to a lipid-binding domain of ATML1 and stabilize the ATML1 protein only in the outermost cells.

Key Words : *Arabidopsis thaliana,* epidermis, protoderm, ATML1, VLCFA-ceramide

Introduction

Sessile lifestyle imposes a bewildering array of biotic and abiotic stresses on vascular land plants. To defend against a hostile environment on land, plants have a specialized defensive cell layer called the epidermis at the interface between the plant body and the external environment. In *Arabidopsis*, ATML1 plays an essential role in protoderm differentiation and effectively orchestrate a variety of protoderm-specific events (Abe et al., 2001, 2003). However, little is known about the molecular basis of the positional signal that confines the expression of this key regulator to the outermost cell layer.

Results

Forming the crucial interface between the plant and the outside world, the outermost cell layer derives from a meristem called the protoderm. While protoderm differentiation is known to be driven by the homeodomain-containing transcription factor ARABIDOPSIS THALIANA MERISTEM LAYER 1 (ATML1), the positional signals that restrict protodermal differentiation to the outermost position are still poorly understood. I and my colleagues first found that *ATML1* expressed in the outermost cells of the lateral root primordia and is required for lateral root formation. Interestingly, when ATML1-EGFP is expressed ubiquitously, it is only retained in the nuclei of outermost layer of lateral root but not in those of the inner cells. These results indicate the existence of an unidentified signal that relays the information of cell position and is required to maintain ATML1 expression.

ATML1 protein is characterized by a steroidogenic acute regulatory protein (StAR)-related lipid-transfer (START) domain. In order to identify the amino acid residue crucial for the lipid binding, I compared the amino acid sequence of the START domains of ATML1 with the known ligand contact site of mammalian START domains. Based on the sequence alignments, Tryptophan 471 (W471) residue of ATML1 protein exhibits strong similarity with

the ligand contact site of mammalian START domains. Thus, we focused on W471 as a putative lipid contact site in ATML1.

To analyze the function of W471 in the position-dependent modulation of ATML1, I introduced a W471L point mutation into ATML1 based on the previous study by using site-directed mutagenesis methods and generated transgenic Arabidopsis ubiquitously expressing ATML1^{W471L}-EGFP. Interestingly, when I induced ATML1^{W471L}-EGFP in all cells of root tissue, EGFP fluorescence was not observed even in the nuclei of the outermost cells. These observations indicate that W471 is crucial for the stability of ATML1 protein in the outermost cells.

In order to screen for potential lipid species that interact with the ATML1 START domain, I next performed *in vitro* protein–lipid binding assays and found that the recombinant GST-tagged START domain of ATML1 binds to very-long-chain fatty acid (VLCFA)-containing ceramides (VLCFA-Cers), ceramide-1-phosphates, phosphatidic acids, phosphatidylserines, and several phosphatidylinositol phosphates. Interestingly, further evaluation of the effect of the W471L mutation revealed that the W471L mutation specifically attenuates the interaction between GST-START and VLCFA-Cers. Thus, VLCFA-Cers emerge as a candidate lipid mediating the positional information and affecting ATML1 function.

To determine whether the post-translational regulation of ATML1 is affected by VLCFA-Cers, I treated transgenic Arabidopsis seedlings, expressing ATML1^{WT}–EGFP, with an inhibitor of VLCFA biosynthesis (cafenstrole). The cafenstrole treatment resulted in disappearance of the fluorescence of ATML1^{WT}-EGFP in outermost cells, confirming that the stability of ATML1 protein is indeed affected by VLCFA-Cers. We also analyzed the expression pattern of PASTICCINO2 (PAS2), encoding an essential enzyme for VLCFA biosynthesis. In *gPAS2-EGFP* containing Arabidopsis, the fluorescence of PAS2–EGFP was restricted to the outermost cells. Collectively, these findings indicate that VLCFA-Cers in the outermost cells play a essential role in the position-dependent stability of ATML1 protein.

Discussion & Conclusion

Here, I have provided an initial characterization of VLCFA-Cers-mediated positional signaling in *Arabidopsis*. I also found that stabilization of the ATML1 protein is dependent on the interaction with VLCFA-Cers and that the interaction between ATML1 and VLCFA-Cers is crucial for the function of ATML1 in the outermost cells. Therefore, VLCFA-Cers are considered as an essential component of cell position-dependent signaling in *Arabidopsis*. The START domain is also conserved in another class of homeodomain proteins, which are key transcription factors in vascular development and leaf polarity. Given that the association between the START domain and the homeodomain is confined to the plant kingdom, such a plant-specific lipid-protein complex that mediates positional signaling might represent an inevitable evolutionary strategy for sessile plants.

References

Abe, M., Takahashi, T. and Komeda, Y. (2001). Identification of a cis-regulatory element for L1 layer-specific gene expression, which is targeted by an L1-specific homeodomain protein. Plant J. 26, 487-494.

Abe, M., Katsumata, H., Komeda, Y. and Takahashi, T. (2003). Regulation of shoot epidermal cell differentiation by a pair of homeodomain proteins in *Arabidopsis*. Development 130, 635-643.

Nagata, K., Ishikawa, T., Kawai-Yamada, M., Takahashi, T. and Abe, M. (2021). Ceramides mediate positional memory in *Arabidopsis thaliana* protoderm differentiation. *Development* 1**48,** dev194969.

一般の皆様へ

陸上植物は、乾燥をはじめとする環境ストレスや病害を引き起こす有害な生物に囲まれて生きています。そこで、植物は特殊化した細胞（表皮細胞）を外部環境との境界に発達させ、自らを保護しているのです。本研究によって、外部環境との境界、すなわち「位置」を認識し、正しい場所に表皮細胞を分化させる際に、特殊な脂質が重要なはたらきをしていることがわかりました。今後、地球環境の劇的な変化が予想されることから、過酷な環境でも丈夫に生育可能な植物の作出につながると期待しています。

Publication - the 33rd (FY2019) Grant Recipients

Title of the research project	Evolution of membrane morphogenesis in Asgard archaea
Recipient (Institution)	Yosuke Senju（Research Institute for Interdisciplinary Science (RIIS),Okayama University）
Journal article / other material	Springer Science+Business Media, LLC, part of Springer Nature 2021 doi.org/10.1007/978-1-0716-1142-5_14
Title of the paper	Liposome Co-sedimentation and Co-flotation Assays to Study Lipid–Protein Interactions

Title of the research project	Functional mechanisms and dynamics of oxytocin in autism spectrum disorder
Recipient (Institution)	Teruhiro Okuyama（The University of Tokyo,Institute for Quantitative Biosciences (IQB),Associate professor）
Journal article / other material	bioRxiv June 25, 2021 doi.org/10.1101/2021.06.25.449869
Title of the paper	Disrupted social memory ensembles in the ventral hippocampus underlie social amnesia in autism-associated Shank3 mutant mice
Journal article / other material	Current Opinion in Neurobiolog, June 2021 doi.org/10.1016/j.conb.2020.12.008
Title of the paper	Distinct functions of ventral CA1 and dorsal CA2 in social memory
Journal article / other material	Development, Growth & Differentiation, December 2020 doi: 10.1111/dgd.12697
Title of the paper	Diverse sensory cues for individual recognition

Title of the research project	Cell senescence effects on transcriptional regulation and differentiation in beige preadipocytes
Recipient (Institution)	Kenji Ikeda（Department of Molecular Endocrinology and Metabolism,Tokyo Medical and Dental University）
Journal article / other material	Front Endocrinol (Lausanne). 2020 Jul 28; 11: 498 doi: 10.3389/fendo.2020.00498
Title of the paper	UCP1 Dependent and Independent thermogenesis in Brown and Beige Adipocytes

Title of the research project	Molecular mechanism underlying development of memory-like Group 2 innate lymphoid cells
Recipient (Institution)	Takashi Ebihara（Department of Medical Biology,Akita University Graduate School of Medicine）

Journal article / other material	Cells 2020, 9, 1193; doi:10.3390/cells9051193
Title of the paper	Dichotomous Regulation of Acquired Immunity by Innate Lymphoid Cells
Journal article / other material	Allergology International 70 (2) 2021, 174-180 doi.org/10.1016/j.alit.2020.11.007
Title of the paper	Trained innate lymphoid cells in allergic diseases

Title of the research project	In vivo Imaging of Brain in CNS Lupus Defines Unique Roles for Chemoattractants
Recipient (Institution)	Yoshishige Miyabe（Institute for Advanced Medical Sciences,Nippon Medical School）
Journal article / other material	JMA J. 2020;3(3): doi: 10.31662/jmaj.2020-0019
Title of the paper	Targeting the Chemokine System in Rheumatoid Arthritis and Vasculitis

Title of the research project	Mechanisms involved in regulation of osteoclast formation by glucan recognition via immune receptors
Recipient (Institution)	Wataru Ariyoshi（Division of Infections and Molecular Biology,Kyushu Dental University）
Journal article / other material	Molecules 2021, 26, 1982 doi.org/10.3390/molecules26071982
Title of the paper	Biological Effects of β-Glucans on Osteoclastogenesis

Title of the research project	Elucidation of the promotion mechanism in plant shoot regeneration by environmental stimuli
Recipient (Institution)	Sachihiro Matsunaga（Matsunaga Laboratory, Department of Applied Biological Science, Faculty of Science and Technology,Tokyo University of Science）
Journal article / other material	NATURE COMMUNICATIONS (2020) 11:5914 doi.org/10.1038/s41467-020-19621-z
Title of the paper	Subnuclear gene positioning through lamina　association affects copper tolerance
Journal article / other material	Communications biology 14, May 2021 doi.org/10.1038/s42003-021-02106-0
Title of the paper	A live imaging system to analyze spatiotemporal　dynamics of RNA polymerase II modification in Arabidopsis thaliana

Title of the research project	Molecular and neural mechanism associated with social behavior
Recipient (Institution)	Teiichi Furuichi（Department of Biological Science, Faculty of Science and Technology,Tokyo University of science）
Journal article / other material	Front. Cell. Neurosci. 2020, 14: 595607. doi: 10.3389/fncel.2020.595607.
Title of the paper	Comprehensive Profiling of Gene Expression in the Cerebral Cortex and Striatum of BTBRTF/ArtRbrc Mice Compared to C57BL/6J Mice.
Journal article / other material	Cell Tissue Res. 2020, 382(1):125-134. doi: 10.1007/s00441-020-03274-x.
Title of the paper	Journey of brain-derived neurotrophic factor: from intracellular trafficking to secretion
Journal article / other material	The Journal of Neuroscience, May 19, 2021 doi.org/10.1523/JNEUROSCI.3240-20.2021
Title of the paper	CAPS2 Deficiency Impairs the Release of the Social Peptide Oxytocin, as Well as Oxytocin-Associated Social Behavior

Title of the research project	Identification of molecular mechanism underlying drug resistance by tumor-stroma derived exosome
Recipient (Institution)	Takatsugu Ishimoto（Division of Translational Research and Advanced Treatment Against Gastrointestinal Cancer,Kumamoto University Hospital）
Journal article / other material	Cancer Res. 2020; 80(16): 3222-3235 doi: 10.1158/0008-5472.CAN-19-3803
Title of the paper	Extracellular Vesicles from Cancer-Associated Fibroblasts Containing Annexin A6 Induces FAK-YAP Activation by Stabilizing b1 Integrin, Enhancing Drug Resistance

Title of the research project	The ultrastabilization mechanism of amyloid revealed by a protein engineering technique
Recipient (Institution)	Koki Makabe（School of science and engineering, Makabe lab.,Yamagata university）
Journal article / other material	2021 Wiley Periodicals LLC, 8 February 2021 doi: 10.1002/prot.26063
Title of the paper	Structural analysis of the β-sheet edge of peptide self-assembly using a model protein

Title of the research project	Identification of the lipid species which regulate epidermis differentiation in Arabidopsis
Recipient (Institution)	Mitsutomo Abe（Graduate School of Arts and Sciences,The University of Tokyo）
Journal article / other material	The Company of Biologists, Development (2021) 148, dev194969. doi:10.1242ldev.194969
Title of the paper	Ceramides mediate positional signals in Arabidopsis thaliana protoderm differentiation

＜論文掲載＞第 33 回（2019 年度）受賞者

助成タイトル	アスガルド古細菌に探る細胞形態の制御機構の分子進化
受賞者	千住 洋介（岡山大学異分野基礎科学研究所）
論文掲載誌・書誌事項	Springer Science+Business Media, LLC, part of Springer Nature 2021 doi.org/10.1007/978-1-0716-1142-5_14
論文タイトル	Liposome Co-sedimentation and Co-flotation Assays to Study Lipid–Protein Interactions

助成タイトル	自閉症スペクトラムにおける、オキシトシン作用機序の解明
受賞者	奥山 輝大（東京大学定量生命科学研究所）
論文掲載誌・書誌事項	bioRxiv June 25, 2021 doi.org/10.1101/2021.06.25.449869
論文タイトル	Disrupted social memory ensembles in the ventral hippocampus underlie social amnesia in autism-associated Shank3 mutant mice
論文掲載誌・書誌事項	Current Opinion in Neurobiolog, June 2021 doi.org/10.1016/j.conb.2020.12.008
論文タイトル	Distinct functions of ventral CA1 and dorsal CA2 in social memory
論文掲載誌・書誌事項	Development, Growth & Differentiation, December 2020 doi: 10.1111/dgd.12697
論文タイトル	Diverse sensory cues for individual recognition

助成タイトル	肥満に伴う細胞老化がベージュ脂肪前駆細胞の転写調節及び分化に及ぼす影響
受賞者	池田 賢司（東京医科歯科大学大学院医歯学総合研究科分子内分泌代謝学分野）
論文掲載誌・書誌事項	Front Endocrinol (Lausanne). 2020 Jul 28; 11: 498 doi: 10.3389/fendo.2020.00498
論文タイトル	UCP1 Dependent and Independent thermogenesis in Brown and Beige Adipocytes

助成タイトル	メモリー様 2 型自然リンパ球の分化制御機構の解析
受賞者	海老原 敬（秋田大学大学院医学系研究科微生物学講座）
論文掲載誌・書誌事項	Cells 2020, 9, 1193; doi:10.3390/cells9051193
論文タイトル	Dichotomous Regulation of Acquired Immunity by Innate Lymphoid Cells

論文掲載誌・書誌事項	Allergology International 70 (2) 2021, 174-180 doi.org/10.1016/j.alit.2020.11.007
論文タイトル	Trained innate lymphoid cells in allergic diseases

助成タイトル	脳内インビボイメージングシステムによる Central Nervous System Lupus 病態解明への挑戦
受賞者	宮部 斉重（日本医科大学先端医学研究所細胞生物学部門）
論文掲載誌・書誌事項	JMA J. 2020;3(3): doi: 10.31662/jmaj.2020-0019
論文タイトル	Targeting the Chemokine System in Rheumatoid Arthritis and Vasculitis

助成タイトル	免疫受容体による糖鎖認識を介した破骨細胞分化修飾能の分子基盤
受賞者	有吉 渉（九州歯科大学感染分子生物学分野）
論文タイトル	Molecules 2021, 26, 1982 doi.org/10.3390/molecules26071982
論文掲載誌・書誌事項	Biological Effects of β-Glucans on Osteoclastogenesis

助成タイトル	環境刺激による植物のシュート再生促進メカニズムの解明
受賞者	松永 幸大（東京理科大学理工学部応用生物科学科松永研究室）
論文掲載誌・書誌事項	NATURE COMMUNICATIONS (2020) 11:5914 doi.org/10.1038/s41467-020-19621-z
論文タイトル	Subnuclear gene positioning through lamina association affects copper tolerance
論文掲載誌・書誌事項	Communications biology 14, May 2021 doi.org/10.1038/s42003-021-02106-0
論文タイトル	A live imaging system to analyze spatiotemporal dynamics of RNA polymerase II modification in Arabidopsis thaliana

助成タイトル	社会性行動に関連する分子・神経機構の解明
受賞者	古市 貞一（東京理科大学理工学部応用生物科学科）
論文掲載誌・書誌事項	Front. Cell. Neurosci. 2020, 14: 595607. doi: 10.3389/fncel.2020.595607.
論文タイトル	Comprehensive Profiling of Gene Expression in the Cerebral Cortex and Striatum of BTBRTF/ArtRbrc Mice Compared to C57BL/6J Mice.

論文掲載誌・書誌事項	Cell Tissue Res. 2020, 382(1):125-134. doi: 10.1007/s00441-020-03274-x.
論文タイトル	Journey of brain-derived neurotrophic factor: from intracellular trafficking to secretion
論文掲載誌・書誌事項	The Journal of Neuroscience, May 19, 2021 doi.org/10.1523/JNEUROSCI.3240-20.2021
論文タイトル	CAPS2 Deficiency Impairs the Release of the Social Peptide Oxytocin, as Well as Oxytocin-Associated Social Behavior

助成タイトル	腫瘍間質由来エクソソームによる胃がん治療抵抗性機構の解明
受賞者	石本 崇胤（熊本大学病院消化器癌先端治療開発学）
論文掲載誌・書誌事項	Cancer Res. 2020; 80(16): 3222-3235 doi: 10.1158/0008-5472.CAN-19-3803
論文タイトル	Extracellular Vesicles from Cancer-Associated Fibroblasts Containing Annexin A6 Induces FAK-YAP Activation by Stabilizing b1 Integrin, Enhancing Drug Resistance

助成タイトル	蛋白質工学によって解明するアミロイド凝集の異常安定化
受賞者	真壁 幸樹（山形大学大学院理工学研究科）
論文掲載誌・書誌事項	2021 Wiley Periodicals LLC, 8 February 2021 doi: 10.1002/prot.26063
論文タイトル	Structural analysis of the β-sheet edge of peptide self-assembly using a model protein

助成タイトル	シロイヌナズナの表皮細胞分化を制御する脂質種の同定
受賞者	阿部 光知（東京大学大学院総合文化研究科）
論文掲載誌・書誌事項	The Company of Biologists, Development (2021) 148, dev194969. doi:10.1242ldev.194969
論文タイトル	Ceramides mediate positional signals in Arabidopsis thaliana protoderm differentiation

Ⅲ.

Reports from the Recipients of Grants for International Meetings

Report on Research Meeting

Sept. 30, 2021

1. Name of Research Meeting / Conference
   The International Centenarian Consortium: ICC 2021

2. Representative
   Yasumichi Arai, Professor, Faculty of Nursing and Medical Care, Keio University/
   Center for Supercentenarian Medical Research, Keio University School of Medicine

   35, Shinnaomachi, Shinjuku-ku, Tokyo, Japan
   P.O. 160-8582
   Tel: +81 3 5269 2468
   e-mail: yasumich@keio.jp

3. Opening period and Place
   Web site conference: June 22, 2021 ~ July 3, 2021
   On line session: June 22, 2021 ~ July 3, 2021

4. Number of participants / Number of participating countries and areas
   Number of participants: 82
   Number of participating countries and areas: 12
   (Japan, Korea, Switzerland, USA, Spain, Australia, Netherland, UK, Portugal, Italia, Sweden, Hong Kong.)

5. Total cost
   740,371Yen

6. Main use of subsidy
   Outsourcing fee for web site and on-line session.

7. Result and Impression

   The International Centenarian Consortium (ICC) meeting was originally scheduled in June 2020; however, it was postponed for one year due to the COVID-19 pandemic. In this year, ICC2021 was held online from June 22 to July 3, 2021, by the Center for Supercentenarian Medical Research at the Keio University School of Medicine and the Osaka University Graduate School of Human Sciences.

   In this website conference, about 20 researchers presented their centenarian research as on-demand presentation with voice.

   During this period, the ICC2021 Live Conference was also held on June 29 from 9:00 p.m. to 12:00 a.m. Japan Standard Time, with approximately 80 researchers in the fields of longevity and centenarians participating from around the world. The number of participants in ICC2021 was quite larger than usual, as the number of participants in previous years' ICCs has been around 30-50. At first, Prof. Nobuyoshi Hirose (Keio Univ.) and Prof. Peter Martin (Iowa State University), the leader of the ICC, gave opening

remarks, including the history of the ICC and the history of the online conference due to the corona pandemic.

Next was the Biomedical Session chaired by Professor Yasumichi Arai (Keio University), in which the three prominent researchers gave lectures. Next was the Psychosocial Session chaired by Prof. Yasuyuki Gondo (Osaka University), which featured lectures by the three prominent researchers. The next session, chaired by Prof. Yasumichi Arai (Keio Univ.), was the Presentation Award session, which was attended by newcomers Prof. Kwangsung Park (Chonnam National University, South Korea) and student award winners Dr. Giulia Accardi (University of Palermo, Italy) Dr. Giulia Accardi (University of Palermo, Italy), Dr. Niccolo Tesi (Amsterdam UMC, The Netherlands), and Dr. Rotem Arieli (Iowa State University, United (University of Palermo, Italy), and Dr. Rotem Arieli (Iowa State University, United States) gave 10-minute presentations, which were followed by a Q&A session.

In the last session, Prof. Ingmar Skoog (University of Gothenburg, Sweden) announced the next ICC meeting, which will be held on May 25-28 in Marstrand, near Gothenburg, Sweden. The meeting ended with closing remarks by Prof. Yasuyuki Gondo.

Although it was only three hours long, it was a dense three hours with six keynote speakers, four award sessions, and many questions and answers. While online conferences are a great tool for simultaneous participation and discussion from many regions, including Europe, the Americas, Oceania, and Asia, I also felt the desire of many people to have face-to-face meetings after the COVID19 pandemic.

8. Additional description
ICC2021 conference site is assessable with this link;

https://activenet-tv.jp/icc2021/

We have acknowledged The NOVARTIS Foundation (Japan) for the Promotion of Science on the website.

ICC2021 WEB conference is supported by Keio Global Research Institute (KGRI), Osaka University Graduate School of Human Sciences Center for collaborative future creation project aging and death study Lab (CCFC), and The NOVARTIS Foundation (Japan) for the Promotion of Science.

Report on Research Meeting

1. Name of Research Meeting / Conference
   3rd Mini-symposium on the blood-brain barrier: from basic to clinical research

2. Representative
   President: Kentaro Hayashi (Shimane University)
   Vice President Yoichi Morofuji (National Nagasaki Medical Center)
   Advisers: Masami Niwa (PharmaCo-Cell Company Ltd.)
   Yasufumi Kataoka (Fukuoka University)
   Takayuki Matsuo (Nagasaki University)
   William A. Banks (University of Washington)
   Maria A. Deli (Biological Research Centre)

3. Opening period and Place
   International lounge, Faculty of Medicine, Shimane University, Izumo, Shimane, Japan
   March 26th (Fri) & 27th (Sat), 2021

4. Number of participants / Number of participating countries and areas
   Total number of participants: 109
   Web 50, Shimane University 22, Nagasaki Satellite 25, Fukuoka Satellite 11
   Number of participating countries and areas: Japan, USA, Hungary, Slovakia, Korea, China, Bangladesh

5. Total cost
   JPY 1,400,000

6. Main use of subsidy
   Printing cost and travel expenses for inviting presenters

7. Result and Impression

   Mini-symposium on the blood-brain barrier: from basic to clinical research is a conference designed for both scientists and physicians with common interests with blood-brain barrier and drug development for central nervous system. It was founded by three research groups: Nagasaki University (Japan), Biological Research Centre (Hungary), and University of Washington (USA) in 2019. Facing the COVID-19 pandemic and its various effects, cities around the world had to take actions towards the safety and health of their habitants. Responding to the pandemic, we made a decision that our symposium should be held on a reduced scale and apply web conference style. 3rd Mini-symposium on the blood-brain barrier: from basic to clinical research was successfully held at International lounge, Faculty of Medicine, Shimane University, Izumo, Shimane, Japan from March 26th to 27th, 2021 (Conference Chair: Professor Kentaro Hayashi, Shimane University, Japan). In total 108 participants from 7 countries joined this event on site or on line.

   The symposium covered a wide range of topics in blood-brain barrier, from

fundamental researches, such as in vitro modeling, HIV infection, tryptophan kynurenine pathway, to translational researches including SARS-CoV-2, stroke, and epilepsy. All participants were satisfied with a friendly conference and enjoyed fruitful discussion in all presentations.

8. Additional description
We are grateful to the NOVARTIS Foundation (Japan) for its generous financial support.

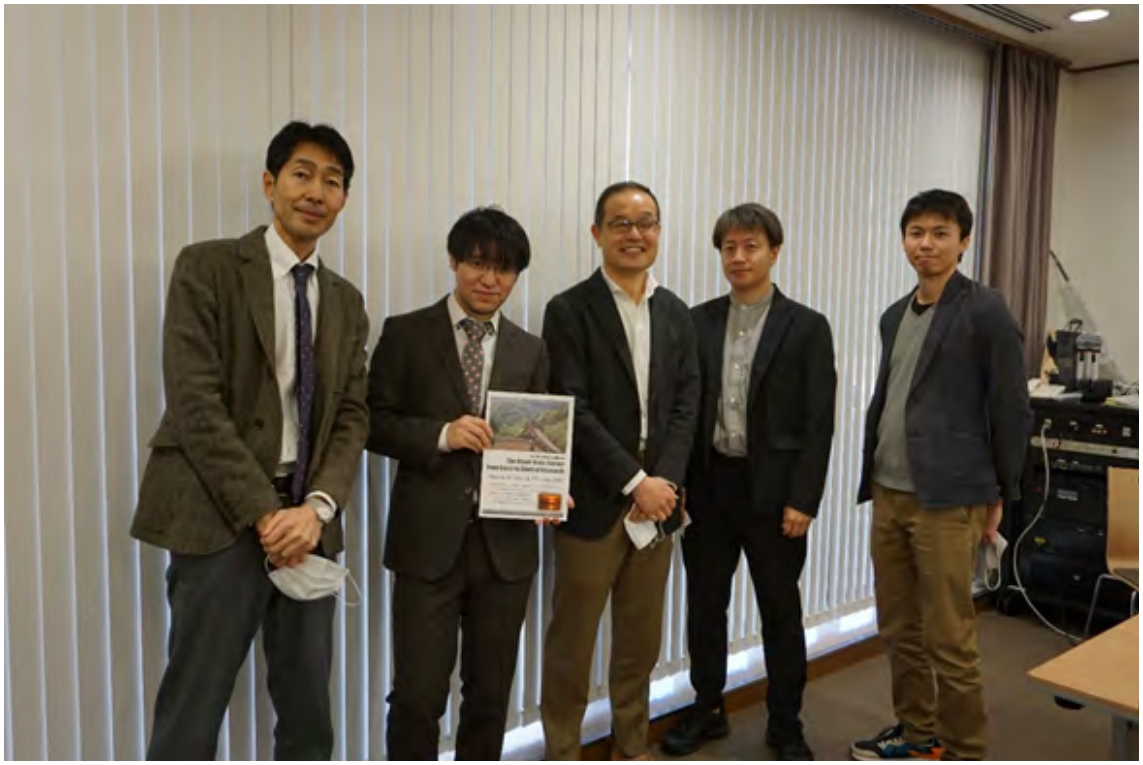

34th Grant Report (FY2020)

The foundation has been conducting public interest activities such as research grant, meeting grant and international exchange programs since its establishment on Sep. 4, 1987 in Japan under authorization of the Ministry of Education, Science, Sports and Culture, followed by a transition to a public interest incorporated foundation on Apr. 1, 2012. The grants conducted in FY 2020 are as follows.

34th Novartis Research Grant:	39 Researchers (JPY 1 mil.),	Subtotal JPY 39.0mil.
Research Meeting Grant:	7 Meetings (JPY 0.4 mil.),	Subtotal JPY 3.6mil.
		Total JPY 42.6mil.

34th Novartis Research Grant (FY2020)

The Grant is to aim supporting creative research in Japan in the field of Bio, life science and relevant chemistry.

#	Name	Institution	Title	Research Project
1	Koji Tokoyoda	Department of Immunology, Tottori University	Professor	Roles of memory helper T cells in vivo
2	Akihide Yoshimi	Cancer RNA Research Unit, National Cancer Center Research Institute	Section Head	Targeting Spliceosomal Mutant Leukemias by a Novel ASO Therapy
3	Minako Ito	Division of Allergy and Immunology, Medical Institute of Bioregulation, Kyushu University	Associate Professor	Significance of acquired immune cells during embryonic and developmental stages in brain formation
4	Chiaki Maruyama	Developmental Neuroscience Project, Tokyo Metropolitan Institute of Medical Scienece	Project leader	Functional analysis of subplate layer in neocortical formation of the developing mouse cortex
5	Daisuke Kurotaki	International Research Center for Medical Science, Kumamoto University	Specially Appointed Associate Professor	Molecular basis for early dendritic cell lineage specification during pathogen infection
6	Naoki Takahashi	Department of Nephrology, University of Fukui	Associate professor	Elucidation of the mechanisms of new tubulointerstitial nephritis with IgM-positive plasma cells and comprehensive analysis of IgM-type autoantibodies in the serum
7	Ken Ohmori	Department of Chemistry, School of Science, Tokyo Institute of Technology	Associate Professor	Synthesis and development of flavan-derived polyphenol with protective effect against amyloid-beta-induced toxicity
8	Yuki Yoshida	Faculty of Advanced Science and Technology, Kumamoto University	Project Assistant Professor	Molecular genetic analysis of plant sub-stomatal chamber development
9	Jun Ishihara	School of pharmaceutical sciences, Pharmaceutical organic chemistry department, Nagasaki University	Professor	Highly Efficient Synthesis of Rare Macrolides, Directing Drug Discovery

#	Name	Institution	Title	Research Project
10	Kazuaki Ishihara	Graduate School of Engineering, Nagoya University	Professor	Catalytic Enantioselective α-Halogenation of Acylpyrazoles Directed towards Synthesis of Chiral Drugs
11	Midori Arai	Chemical Biology Lab., Department of Bioscience & Informatics Faculty of Science and Technology, Keio University	Professor	Invasive evolution of pathogenic bacteria and cryptic gene activation
12	Fuun Kawano	Graduate school of Arts and Sciences, Laboratory of Prof. Moritoshi Sato, The University of Tokyo	Assistant Professor	Development and evolution of an optogenetic gene expression system with red-light.
13	Keiichiro Ishiguro	Institute of Molecular Embryology and Genetics, Kumamoto University	Associate Professor	Research on infertility
14	Jafar SHARIF	Developmental Genetics Laboratory, Center for Integrative Medical Sciences (IMS), RIKEN	Senior Research Scientist	Multidimensional regulation of DNA replication by a genome-epigenome-transcriptome (GET) network during cellular senescence
15	Kanae Ando	Graduate school of science, Department of Biological Sciences, Tokyo Metropolitan University	Associate professor	A chemical genetics approach to identify direct substrates of Alzheimer's disease-associated kinase MARK4 in neurons
16	Kazunori Kanemaru	School of Medicine, Division of Cellular and Molecular Pharmacology, Nihon University	Associate Professor	Establishment of in vivo Ca2+ imaging method for analysis of insulin dynamics
17	Ko Matsui	Graduate School of Life Sciences, Super-network Brain Physiology, Tohoku University	Professor	Glial control of behavioral disorders induced by social distancing
18	William Addison	Division of Molecular Signaling and Biochemistry, Kyushu Dental University	Assistant Professor	Genome wide analysis of DNA methylation and transcription dynamics in ICF syndrome
19	Kenichi Noma	Institute for Genetic Medicine, Hokkaido University	Professor	Elucidating the 3D genome structure and its related protein composition in human senescent cells
20	Kosei Takeuchi	Department of Medical Biology, Aichi Medical University	Professor	Elucidation of the hyper-adaptation mechanism by reconstruction of synapse-formations and AI motion capture systems - Challenging for the hyper-amelioration from spinal cord injury-
21	Shinobu Takizawa	The Institute of Scientific and Industrial Research, Osaka University	Associate Professor	Exploration of pharmaceutical resources based on rapid synthesis and machine learning analysis of optically active compounds
22	Nobutaka Fujieda	Graduate School of Life and Environmental Sciences, Biophysical Chemistry, Osaka Prefecture University	Associate Professor	Development of Protein Ligand Library for Stereodivergent Synthesis
23	Yuki Takamatsu	Department of Virology I, National Institute of Infectious Diseases	Senior Researcher	Revealing the intra-cellular dynamics of SARS-CoV2.

#	Name	Institution	Title	Research Project
24	Takao Iwawaki	Division of Cell Medicine, Medical Research Institute, Kanazawa Medical University	Professor	Molecular and cell biological approach to understanding the mechanisms of fatigue by studying the cellular stress response and the inflammatory response
25	Hisayuki Amano	Department of Biochemistry, Kindai University, Faculty of Medicine	Assistant Professor	Sirt1-NAD+ pathway represses fibrosis in inflammatory bowel disease and colitis-associated colorectal cancer
26	Ken Takai	Breast Oncology, Saitama Cancer Center	Chief physician	Targeting the host factors essential for breast cancer metastasis in PDX mouse models
27	Katsutomo Okamura	RNA molecular medicine, Nara Institute of Science and Technology	Professor	Identification of RNA-binding proteins that regulate miRNA processing by integrated computational and biochemical analysis
28	Hideaki Fujiwara	Department of Hematology and Oncology, Okayama University Hospital	Assistant Professor	Development of novel GVHD mechanism and therapy targeting metabolic disturbance of intestinal epithelial cells that leads to dysbiosis.
29	Shinya Kimura	Development of pharmaceutical chemistry, Meiji Pharmaceutical University	Assistant Professor	Development of supramolecular hydrogel that enable drug delivery into central nervous system
30	Aya Tanatani	Faculty of Core Research, Natural Science Division, Ochanomizu University	Professor	Development of potent non-secosteroidal vitamin D derivatives based on the structure of bile acid
32	Takeshi Yamamoto	Blood Purification Center, Osaka University Hospital	Clinical Fellow	Unraveling the pathophysiology of AKI to CKD transition by integrating single cell RNA sequencing and lipidomic analyses
33	Mashito Sakai	Department of Biochemistry and Molecular Biology, Nippon Medical School	Professor	Deciphering hepatic feeding-state-dependent metabolic gene regulation coordinated by intercellular crosstalk
34	Takuya Imamura	Biomedical Program, Graduate School of Integrated Sciences for Life, Hiroshima University	Professor	Systems approaches towards the non-coding RNA-based production of humanized mice
35	Tomoe Nishitani	Department of Pharmacology, Wakayama Medical University	Professor	Novel mechanism of energy metabolism by Ca2+ regulatory proteins
36	Yoshito Yamashiro	Life Science Center for Survival Dynamics, TARA, University of Tsukuba	Assistant Professor	The Role of fibulin-4 in endothelial functions and application for clinical study
37	Ritsuko Suyama	Graduate School of Frontier Biosciences, Osaka university	Specially Appointed Assistant Professor	Identification of the molecular mechanisms in the microbes enhanced oogenesis
38	Hiroshi Kurosaka	Department of Orthodontics and Dentofacial Orthopedics, Osaka University Graduate School of Dentistry	Associate Professor	Investigating novel treatment strategies for Pseudohypoparathyroidism
39	Hiroshi Inoue	Metabolism and Nutrition Research Unit, Institute for Frontier Science Initiative, Kanazawa University	Professor	Investigation of hepatic metabolic homeostasis and its deterioration by physiological and bioinformatic analyses of vagus nerve-mediated organ-crosstalk

FY2020 Research Meeting Grant

(JPY 400 thousand x 9 = 3.6 million)

#	Meeting	Place / Date	Institution / Title	Name
1	2021 Asia Pacific Drosophila Neuroscience Conference	Saitama / 2023.3	Laboratory for Neurodiversity, RIKEN Center for Brain Science	Adrian W Moore
2	The International Centenarian Consortium	Tokyo / 2021.6.22–7.03	Center for Supercentenarian Medical Research, Keio University School of Medicine	Yasumichi Arai
3	International Symposium on the Biosynthesis of Natural Products	2022	Graduate School of Pharmaceutical Sciences, The University of Tokyo	Ikuro Abe
4	Minisymposium on the blood-brain barrier: from basic to clinical research	Nagasaki / 2021.3.26-27	Department of Neurosurgery, Nagasaki University	Yoichi Morofuji
5	The 39th Sapporo International Cancer Symposium	Sapporo / 2021.7.5-7	Division of Carcinogenesis, Japanese Foundation for Cancer Research	Takuro Nakamura
6	The 2nd International Symposium on Hybrid Catalysis	Aichi / 2022.7	Institute of Transformative Bio-Molecules, Nagoya University	Takashi Ooi
7	13th AFMC International Medicinal Chemistry Symposium (AIMECS 2021)	Tokyo/ 2021.11.29-12.2	Laboratory of Synthetic Organic Chemistry, Graduate School of Pharmaceutical Sciences, The University of Tokyo	Motomu Kanai
8	64th Annual Meeting of Japanese Neurochemistry Society	Nara / 2021.9.29-10.1	Department of Anatomy and Neuroscience, Nara Medical University	Akio Wanaka
9	39th JES Summer on Endocrinology & Metabolism	Chiba / 2021.7.8-10	Department of Molecular Diagnosis, Graduate School of Medicine, Chiba University	Tomoaki Tanaka

第34期（2020年度）助成事業報告

当財団は、文部大臣の認可を得て1987年9月4日に設立されて以来、研究助成を中心とした公益事業を行って来ました。2012年4月1日には、制度改革に伴い、公益財団法人へ移行しております。2020年度は、下記の総額4,260万円の助成事業を実施しました。

第34回ノバルティス研究奨励金	39件（1件100万円）	3,900万円
研究集会助成	9件（1件 40万円）	360万円
		総額 4,260万円

第34回ノバルティス研究奨励金（2020年度）

この事業は、生物・生命科学および関連する化学の領域において、我が国で行われる創造的な研究の助成を目的としています。

（受付順、敬称略、所属職位は申請時、贈呈額：1件 100万円）

No.	氏　名	所　属	職位	研究課題
1	常世田好司	鳥取大学 医学部　免疫学分野	教授	生体内における記憶ヘルパーT細胞の役割
2	吉見　昭秀	国立研究開発法人国立がん研究センター 研究所 がん RNA 研究ユニット	独立ユニット長	スプライシング変異白血病に対する新規 ASO 治療法の開発
3	伊藤美菜子	九州大学 生体防御医学研究所 アレルギー防御学分野	准教授	脳形成における胎生期・発達期の獲得免疫細胞の意義
4	丸山　千秋	公益財団法人 東京都医学総合研究所 脳神経回路形成プロジェクト	プロジェクトリーダー	胎生期マウス大脳新皮質形成におけるサブプレート層の機能解明
5	黒滝　大翼	熊本大学 国際先端医学研究機構	特任准教授	感染防御における樹状細胞系譜早期運命決定の機序解明
6	髙橋　直生	福井大学 医学系部門 腎臓病態内科学分野	診療准教授	IgM 陽性形質細胞を伴う新腎炎のメカニズムの解明と血中に存在する IgM 型自己抗体の網羅的解析
7	大森　　建	東京工業大学 理学院化学系	准教授	アミロイドβ凝集抑制作用を有するフラバンポリフェノール類の合成と機能開拓
8	吉田　祐樹	熊本大学 大学院先端科学研究部	特任助教	植物の気孔腔形成メカニズムの分子遺伝学的解析
9	石原　　淳	長崎大学 薬学部 薬品製造化学研究室	教授	高効率的合成に基づく稀少多環性マクロリド天然物の創薬展開
10	石原　一彰	名古屋大学 工学研究科 有機・高分子化学専攻 触媒有機合成学研究室	教授	光学活性医薬品合成を指向したアシルピラゾールの触媒的不斉α－ハロゲン化反応の開発
11	荒井　　緑	慶應義塾大学 理工学部生命情報学科 ケミカルバイオロジー研究室	教授	病原微生物の浸潤進化に学ぶ休眠遺伝子活性化法の開発
12	河野　風雲	東京大学 大学院総合文化研究科 佐藤守俊研究室	助教	赤色光作動性の遺伝子発現光操作技術の開発と改良研究
13	石黒啓一郎	熊本大学 発生医学研究所	准教授	不妊不育に関わる原因遺伝子の解明
14	シャリフ ジャファル	理化学研究所　生命医科学研究センター（IMS） 免疫器官形成研究チーム	専任研究員	ゲノム・エピゲノム・トランスクリプトーム（GET）による DNA 複製の多層的な制御及び細胞老化におけるその生物学的な機能

No.	氏　名	所　属	職位	研究課題
15	安藤香奈絵	東京都立大学 大学院理学研究科 神経分子機能研究室	准教授	アルツハイマー病発症機構解明に向けた神経細胞内 MARK4 基質の網羅的な同定
16	金丸　和典	日本大学 医学部細胞分子薬理学部門	准教授 （研究所）	新規生体内 β 細胞 Ca2+ イメージング法による生体内インスリン動態解析
17	松井　広	東北大学大学院 生命科学研究科 超回路脳機能分野	教授	社会的隔離による行動障害と脳内グリア機能の連関の解明
18	アディソン ウィリアム	九州歯科大学 分子情報生化学	助教	ICF 症候群の間葉系幹細胞モデルにおける DNA メチル化と転写制御のゲノムワイド解析
19	野間　健一	北海道大学 遺伝子病制御研究所	教授	ヒト老化細胞に形成される 3D ゲノム構造とその形成に関わるタンパク質組成の解明
20	武内　恒成	愛知医科大学 医学部生物学	教授	AI モーションキャプチャーによる中枢神経損傷後生理機能回復－シナプスコネクターと再生阻害因子制御を利用した脊髄損傷後超回復モデル－
21	滝澤　忍	大阪大学 産業科学研究所	准教授	光学活性化合物の迅速合成と機械学習を基盤とする医薬資源の探索
22	藤枝　伸宇	大阪府立大学 大学院生命環境科学研究科 生物物理化学研究室	准教授	立体分岐型合成を実現するタンパク質配位子ライブラリーの開発
23	高松　由基	国立感染症研究所 ウイルス第一部	主任 研究官	新型コロナウイルスの細胞内動態の解明
24	岩脇　隆夫	金沢医科大学 総合医学研究所 細胞医学研究分野	教授	細胞ストレス応答と炎症反応の解析から迫る「疲労メカニズム」の分子細胞生物学的な解明
25	天野　恭志	近畿大学医学部 生化学教室	助教	Sirt1–NAD+ 経路による炎症性腸疾患とその関連大腸がんの抑制機構の解明
26	高井　健	埼玉県立がんセンター 乳腺腫瘍内科	医長	PDX モデルにおける乳癌転移に必須な宿主因子の解析と標的治療の探索
27	岡村　勝友	奈良先端科学技術大学院大学 RNA 分子医科学研究室	教授	miRNA 生合成制御に関わる RNA 結合蛋白質の網羅的同定のための数理学生化学解析的アプローチの開発
28	藤原　英晃	岡山大学病院 血液・腫瘍内科	助教	Dysbiosis に基づく腸管上皮細胞代謝異常を標的とする新規 GVHD 機序の解明と治療応用
29	木村　真也	明治薬科大学 薬化学研究室	助教	中枢への薬物輸送を可能にする超分子ヒドロゲルの開発
30	棚谷　綾	お茶の水女子大学 基幹研究院自然科学系	教授	胆汁酸をリードとした高活性な非セコステロイド型ビタミン D 誘導体の創製
31	鈴木　匠	茨城大学 発生生物学研究室	助教	神経幹細胞が多種多様な神経を作り分ける分子機構の解明
32	山本　毅士	大阪大学医学部附属病院 血液浄化部	医員	シングルセル解析とリピドーム解析を用いた、急性腎障害が慢性腎臓病へ移行する機序の解明
33	酒井真志人	日本医科大学 大学院医学研究科 分子遺伝医学分野	教授	肝臓における摂食依存性の遺伝子発現の細胞間相互作用を介した制御機構の解明
34	今村　拓也	広島大学 大学院統合生命科学研究科 生命医科学プログラム	教授	ヒト形質賦与マウス作製に向けたノンコーディング RNA 情報活用システムズアプローチ
35	西谷　友重	和歌山県立医科大学 薬理学講座	教授	Ca2+ シグナル制御因子を介した新規エネルギー代謝調節機構の解明
36	山城　義人	筑波大学 生存ダイナミクス研究センター	助教	細胞外マトリクスを介した血管機能を制御する新しい分子メカニズムの解析とマウスモデルを用いた治療効果の検証

No.	氏　名	所　属	職位	研究課題
37	須山　律子	大阪大学 大学院生命機能研究科 生殖生物学研究室	特任 助教	マイクロバイオームが亢進する生殖機能とその分子機構の解明
38	黒坂　寛	大阪大学大学院歯学研究科 顎顔面口腔矯正学教室	講師	胎生時期に着目した偽性副甲状腺機能低下症の新規治療方法の開発
39	井上　啓	金沢大学 新学術創成研究機構栄養・代謝研究ユニット	教授	神経性臓器連関のメカニズムから読み解く肝代謝恒常性とその破綻の解明

2020年度研究集会助成

この事業は、生物・生命科学および関連する化学の領域において、我が国で開催される国際色豊かな研究集会の助成を目的としています。2020年度は9件の助成を行いました。

（受付順、敬称略、所属・職位は申請時、贈呈額：1件40万円）

No.	氏　名	所　属	職位	開催地／開催日	研究集会名
1	ムーア エイドリアン	理化学研究所 脳神経科学研究センター 神経細胞多様性研究チーム	チームリーダー	埼玉県／2023.3	2021 Asia Pacific Drosophila Neuroscience Conference
2	新井　康通	慶應義塾大学 医学部百寿総合研究センター	専任講師	東京／2021.6.22-7.3	国際百寿者研究会
3	阿部　郁朗	東京大学大学院 薬学系研究科	教　授	2022	天然物生合成国際シンポジウム
4	諸藤　陽一	長崎大学 脳神経外科	助　教	長崎／2021.3.26-27	血液脳関門シンポジウム ―基礎から臨床まで―
5	中村　卓郎	公益財団法人 がん研究会 がん研究所発 がん研究部	副所長	札幌／2021.7.5-7	第39回札幌国際がんシンポジウム
6	大井　貴史	名古屋大学 トランスフォーマティブ生命分子研究所	教　授	愛知／2022.7	第2回ハイブリッド触媒に関する国際会議
7	金井　　求	東京大学 大学院薬学系研究科 有機合成化学教室	教　授	東京／2021.11.29-12.2	第13回 アジア医薬化学連合 国際メディシナルケミストリーシンポジウム
8	和中　明生	奈良県立医科大学 解剖学第二講座	教　授	奈良／2021.9.29-10.1	第64回日本神経化学会大会
9	田中　知明	千葉大学大学院 医学研究院 分子病態解析学	教　授	千葉／2021.7.8-10	第39回 内分泌代謝学サマーセミナー

Promotion Results according to the PROGRAM

(Unit : 10k yen)

Year	Research Grants		Meeting Grants		Japan-Europe Research Exchange		Oversea Reseach Trip	
	# of people	Amount	# of people	Amount	# of people	Amount	# of people	Amount
1987	18	1,800	8	400	0	0	0	0
1988	39	3,900	8	400	7	1,740	0	0
1989	42	4,200	8	400	9	2,260	0	0
1990	51	7,650	10	500	8	2,440	0	0
1991	55	11,000	11	550	9	2,710	9	250
1992	50	10,000	10	500	10	3,315	8	265
1993	50	10,000	10	500	11	3,511	9	300
1994	50	10,000	10	500	8	2,530	6	155
1995	50	6,500	10	500	7	2,020	6	170
1996	45	5,850	10	500	6	1,600	4	120
1997	41	4,920	10	500	6	1,610	2	55
1998	41	4,920	10	500	4	1,070	8	160
1999	41	4,920	10	500	4	710	8	160
2000	41	4,100	8	400	3	660	0	0
2001	41	4,100	7	350	2	440	0	0
2002	40	4,000	8	400	0	0	0	0
2003	40	4,000	4	200	0	0	0	0
2004	45	4,500	5	200	0	0	0	0
2005	45	4,500	5	200	0	0	0	0
2006	46	4,600	6	240	0	0	0	0
2007	50	5,000	6	240	0	0	0	0
2008	45	4,500	7	280	0	0	0	0
2009	30	3,000	6	240	0	0	0	0
2010	38	3,800	5	200	0	0	0	0
2011	41	4,100	6	240	0	0	0	0
2012	40	4,000	6	240	0	0	0	0
2013	42	4,200	5	200	0	0	0	0
2014	42	4,200	6	240	0	0	0	0
2015	35	3,500	6	240	0	0	0	0
2016	35	3,500	5	200	0	0	0	0
2017	41	4,100	5	200	0	0	0	0
2018	37	3,700	5	200	0	0	0	0
2019	37	3,700	5	200	0	0	0	0
2020	39	3,900	9	360	0	0	0	0
Total	1,347	163,060	236	10,760	94	26,616	60	1,635

Promotion Results according to the PROGRAM

(Unit : 10k yen)

Year	Travel Expense to Japan		Special Grant		Total # of people	Total Amount
	# of people	Amount	# of people	Amount		
1987	0	0	0	0	26	2,200
1988	0	0	0	0	54	6,040
1989	0	0	0	0	59	6,860
1990	0	0	0	0	69	10,590
1991	0	0	0	0	84	14,510
1992	0	0	0	0	78	14,080
1993	0	0	0	0	80	14,311
1994	0	0	2	110	76	13,295
1995	0	0	1	50	74	9,240
1996	0	0	0	0	65	8,070
1997	0	0	1	30	60	7,115
1998	0	0	0	0	63	6,650
1999	0	0	4	130	67	6,420
2000	0	0	3	142	55	5,302
2001	0	0	3	120	53	5,010
2002	0	0	0	0	48	4,400
2003	0	0	0	0	44	4,200
2004	0	0	0	0	50	4,700
2005	0	0	0	0	50	4,700
2006	0	0	0	0	52	4,840
2007	5	1,000	0	0	61	6,240
2008	5	1,000	0	0	57	5,780
2009	3	600	0	0	39	3,840
2010	0	0	0	0	43	4,000
2011	0	0	0	0	47	4,340
2012	0	0	0	0	46	4,240
2013	0	0	0	0	47	4,400
2014	0	0	0	0	48	4,440
2015	0	0	0	0	41	3,740
2016	0	0	0	0	40	3,700
2017	0	0	0	0	46	4,300
2018	0	0	0	0	42	3,900
2019	0	0	0	0	42	3,900
2020	0	0	0	0	48	4,260
Total	13	2,600	14	582	1,854	213,613

助成金実績一覧表

（単位：万円）

年号	研究奨励金		研究集会		日欧研究交流		海外出張助成	
	人数	助成額	人数	助成額	人数	助成金額	人数	助成金額
1987	18	1,800	8	400	0	0	0	0
1988	39	3,900	8	400	7	1,740	0	0
1989	42	4,200	8	400	9	2,260	0	0
1990	51	7,650	10	500	8	2,440	0	0
1991	55	11,000	11	550	9	2,710	9	250
1992	50	10,000	10	500	10	3,315	8	265
1993	50	10,000	10	500	11	3,511	9	300
1994	50	10,000	10	500	8	2,530	6	155
1995	50	6,500	10	500	7	2,020	6	170
1996	45	5,850	10	500	6	1,600	4	120
1997	41	4,920	10	500	6	1,610	2	55
1998	41	4,920	10	500	4	1,070	8	160
1999	41	4,920	10	500	4	710	8	160
2000	41	4,100	8	400	3	660	0	0
2001	41	4,100	7	350	2	440	0	0
2002	40	4,000	8	400	0	0	0	0
2003	40	4,000	4	200	0	0	0	0
2004	45	4,500	5	200	0	0	0	0
2005	45	4,500	5	200	0	0	0	0
2006	46	4,600	6	240	0	0	0	0
2007	50	5,000	6	240	0	0	0	0
2008	45	4,500	7	280	0	0	0	0
2009	30	3,000	6	240	0	0	0	0
2010	38	3,800	5	200	0	0	0	0
2011	41	4,100	6	240	0	0	0	0
2012	40	4,000	6	240	0	0	0	0
2013	42	4,200	5	200	0	0	0	0
2014	42	4,200	6	240	0	0	0	0
2015	35	3,500	6	240	0	0	0	0
2016	35	3,500	5	200	0	0	0	0
2017	41	4,100	5	200	0	0	0	0
2018	37	3,700	5	200	0	0	0	0
2019	37	3,700	5	200	0	0	0	0
2020	39	3,900	9	360	0	0	0	0
Total	1,347	163,060	236	10,760	94	26,616	60	1,635

助成金実績一覧表

（単位：万円）

年号	海外受入		特別助成		人数計	金額合計
	助成人数	助成金額	人数	助成金額		
1987	0	0	0	0	26	2,200
1988	0	0	0	0	54	6,040
1989	0	0	0	0	59	6,860
1990	0	0	0	0	69	10,590
1991	0	0	0	0	84	14,510
1992	0	0	0	0	78	14,080
1993	0	0	0	0	80	14,311
1994	0	0	2	110	76	13,295
1995	0	0	1	50	74	9,240
1996	0	0	0	0	65	8,070
1997	0	0	1	30	60	7,115
1998	0	0	0	0	63	6,650
1999	0	0	4	130	67	6,420
2000	0	0	3	142	55	5,302
2001	0	0	3	120	53	5,010
2002	0	0	0	0	48	4,400
2003	0	0	0	0	44	4,200
2004	0	0	0	0	50	4,700
2005	0	0	0	0	50	4,700
2006	0	0	0	0	52	4,840
2007	5	1,000	0	0	61	6,240
2008	5	1,000	0	0	57	5,780
2009	3	600	0	0	39	3,840
2010	0	0	0	0	43	4,000
2011	0	0	0	0	47	4,340
2012	0	0	0	0	46	4,240
2013	0	0	0	0	47	4,400
2014	0	0	0	0	48	4,440
2015	0	0	0	0	41	3,740
2016	0	0	0	0	40	3,700
2017	0	0	0	0	46	4,300
2018	0	0	0	0	42	3,900
2019	0	0	0	0	42	3,900
2020	0	0	0	0	48	4,260
Total	13	2,600	14	582	1,854	213,613

34th Financial Report

Balance Sheet

As of March 31, 2021

(Unit：JP Yen)

Account	Amount
Ⅰ Assets	
1. Current Assets	
Current Assets Total	21,599,548
2. Fixed Assets	
(1) Basic Fund	
Basic Fund Total	1,100,000,000
(2) Specific Assets	
Specific Assets Total	120,594
(3) Other Long - term Assets	
Other Long - term Assets Total	80,035,442
Fixed Assets Total	1,180,156,036
Assets Total	1,201,755,584
Ⅱ Liabilities	
1. Current Liabilities	
Current Liabilities Total	41,354,175
Liabilities Total	41,354,175
Ⅲ Equity（Net Assets）	
1. Designated Net Assets	
Designated Net Assets Total	1,000,120,594
（Amount Appropriating to basic Fund）	(1,000,000,000)
(Amount Appropriating to specific assets)	(120,494)
2.General Net Assets	160,280,815
（Amount Appropriating to）	(100,000,000)
Equity Total（Net Assets）	1,160,401,409
Liabilities & Equity Total	1,201,755,584

Statement of Net Assets

From April 1 st, 2020 to March 31, 2021

(Unit：JP Yen)

Account	Amount
Ⅰ General Net Assets Changes	
1. Ordinary income & Expenditure	
(1) Ordinary income	
Interest from basic fund	15,088,926
Donation	40,330,000
Other Income	560,827
Ordinary Income Total	55,979,753
(2) Ordinaty Expenditure	
Project Expense	50,367,712
Grant Expense	42,600,000
Novartis Research Grant	39,000,000
Research Meeting Grant	3,600,000
Administrative Expense	3,592,833
Ordinary Expenditure Total	53,960,545
Ordinary Balance without Appraisal Profit or Loss	2,019,208
2. Nonrecurring Profit & Loss	
Nonrecurring Balance of Current Period	0
General Net Assets Ending Balance	160,280,815
Ⅱ Designated Net Assets Changes	
Designated Net Assets Change	(330,000)
Designated Net Assets Ending Balance	1,000,120,594
Ⅲ Net Assets Balance Ending Balance	1,160,401,409

第34期（2020年度）財務報告

貸借対照表

2021年3月31日現在

（単位：円）

科　　目	金　額
Ⅰ資産の部	
1．流動資産	
流動資産合計	21,599,548
2．固定資産	
⑴ 基本財産	
基本財産合計	1,100,000,000
⑵ 特定資産	
特定資産合計	120,594
⑶ その他固定資産	
その他固定資産合計	80,035,442
固定資産合計	1,180,156,036
資産合計	1,201,755,584
Ⅱ負債の部	
1．流動負債	
流動負債合計	41,354,175
負債合計	41,354,175
Ⅲ正味財産の部	
1．指定正味財産	
指定正味財産合計	1,000,120,594
（うち基本財産への充当額）	(1,000,000,000)
（うち特定資産への充当額）	(120,494)
2．一般正味財産	160,280,815
（うち基本財産への充当額）	(100,000,000)
正味財産合計	1,160,401,409
負債及び正味財産合計	1,201,755,584

正味財産増減計算書

2020年4月1日から2021年3月31日まで

（単位：円）

科　　目	金　額
Ⅰ一般正味財産増減の部	
1．経常増減の部	
⑴ 経常収益	
基本財産運用益	15,088,926
受取寄付金	40,330,000
雑収益	560,827
経常収益　計	55,979,753
⑵ 経常費用	
事業費	50,367,712
支払助成金	42,600,000
ノバルティス研究奨励金	39,000,000
研究集会助成金	3,600,000
管理費	3,592,833
経常費用　計	53,960,545
当期経常増減額	2,019,208
2．経常外増減の部	
当期経常外増減額	0
一般正味財産期末残高	160,280,815
Ⅱ指定正味財産増減の部	
当期指定正味財産増減額	(330,000)
指定正味財産期末残高	1,000,120,594
Ⅲ正味財産期末残高	1,160,401,409

List of Trustees, Auditors, Councilors and Grant Selection Committee Members

[Board of Trustees] 5 trustees, 2 auditors As of July 1, 2021

Post	Name	Title
Chairman	Kuniaki Takata, Ph.D.	President, Gunma Prefectural Public University Corporation
Trustee	Sadayoshi Ito, M.D., Ph.D.	Special Administrator, Katta General Hospital Professor Emeritus, Tohoku University
	Akimichi Kaneko, M.D., Ph.D.	Professor Emeritus, Keio University
	Fujio Murakami, Ph.D.	Professor Emeritus, Osaka University
	Leo Lee	President, Novartis Pharma K.K.
Auditor	Tokuzo Nakajima, CPA	Representative, Tokuzo Nakajima CPA Firm
	Masanori Fuse	Financial Advisor, Novartis Pharma K.K.

[Board of Councilors] 10 councilors As of July 1, 2021

Post	Name	Title
Chairman	Takao Shimizu, M.D., Ph.D.	Project Head, National Center for Global Health and Medicine Professor Emeritus, University of Tokyo
Councilor	Masamitsu Iino, M.D., Ph.D.	Senior Professor, International Research Center for Neurointelligence, University of Tokyo Professor Emeritus, University of Tokyo
	Hiroyuki Kawashima, Ph.D	Former Professor, Niigata University
	Tsuneyoshi Kuroiwa, Ph.D.	Member of the Japan Academy; Professor Emeritus, University of Tokyo
	Masakatsu Shibasaki, Ph.D.	President, Microbial Chemistry Research Foundation Professor Emeritus, University of Tokyo
	Akihiko Nakano, Ph.D.	Deputy Director, RIKEN Center for Advanced Photonics Professor Emeritus, University of Tokyo
	Yoichi Nabeshima, M.D., Ph.D.	Trustee, Foundation for Biomedical Research and Innovation at Kobe Director, Institute of Biomedical Research and Innovation Professor Emeritus, Kyoto University
	Toyoshi Fujimoto, M.D., Ph.D.	Specially Appointed Professor, Juntendo University Professor Emeritus, Nagoya University
	Miwako Mori, Ph.D.	Professor Emeritus, Hokkaido University
	Tohru Hirose, Ph.D.	Head, Global Drug Development, Novartis Pharma K.K.

[Grantee Selection Committee] 20 members As of July. 1, 2021

Post	Name	Title
Chairman	Hiroshi Ito, M.D., Ph.D.	Professor, Keio University School of Medicine,
Member	Takashi Ohshima, Ph.D.	Professor, Kyushu University Graduate School of Pharmaceutical Sciences
	Toshiaki Ohteki, D.D.S., Ph.D.	Professor, Medical Research Institute, Tokyo Medical and Dental University
	Yasuyoshi Sakai, Ph.D.	Professor, Kyoto University Graduate School of Agriculture
	Taisuke Tomita, Ph.D.	Professor, University of Tokyo Graduate School of Pharmaceutical Sciences
	Fumiko Toyoshima, Ph.D.	Professor, Institute for Frontier Life and Medical Sciences, Kyoto University
	Tohru Minamino, M.D., Ph.D	Professor, Juntendo University Graduate School of Medicine
	Yasuhiro Yamada, M.D., Ph.D.	Professor, The Institute of Medical Science, University of Tokyo
	Masaki Ieda, M.D., Ph.D.	Professor, University of Tsukuba Faculty of Medicine
	Yasuteru Urano, Ph.D.	Professor, University of Tokyo Graduate School of Pharmaceutical Sciences
	Erina Kuranaga, Ph.D.	Professor, Tohoku University Graduate School of Life Sciences
	Mitinori Saito, M.D., Ph.D.	Professor, Kyoto University Institute for Advanced Study
	Fumitoshi Kakiuchi, Ph.D.	Professor, Keio University School of Fundamental Science and Technology
	Hiroshi Kawasaki, M.D., Ph.D.	Professor, Kanazawa University Faculty of Medicine
	Shoen Kume, Ph.D.	Professor, Tokyo Institute of Technology School of Life Science and Technology
	Kiyoshi Takeda, M.D., Ph.D.	Professor, Osaka University Graduate School of Medicine
	Kazuhiro Nakamura, Ph.D.	Professor, Nagoya University Graduate School of Medicine
	Tetsuya Higashiyama, Ph.D.	Professor, Nagoya University Institute of Transformative Bio-Molecules
	Sachiko Miyake, M.D., Ph.D.	Professor, Juntendo University Graduate School of Medicine
	Hozumi Motohashi, M.D., Ph.D.	Professor, Tohoku University Institute of Development, Aging and Cancer

公益財団法人ノバルティス科学振興財団

［理事・監事］

任期　2020年6月17日～ 2022年6月

＊2020年11月26日～ 2022年6月　　2021年7月17日現在（敬称略）

職 名	氏 名	現　　職
代表理事	高田　邦昭	群馬県公立大学法人 理事長
理 事	伊藤　貞嘉	公立刈田綜合病院 特別管理者 東北大学名誉教授
	金子　章道	慶應義塾大学名誉教授
	村上富士夫	大阪大学大学院生命機能研究科 招聘教授 大阪大学名誉教授
	レオ リー	ノバルティス ファーマ株式会社 代表取締役社長＊

任期　2020年6月17日～ 2024年6月

監 事	中嶋　德三	公認会計士 中嶋德三事務所
	布施　正則	ノバルティス ファーマ株式会社 企画管理本部ファイナンシャルアドバイザー

［評議員］

任期　2020年6月17日～ 2024年6月　　2021年7月1日現在（敬称略）

職 名	氏 名	現　　職
評議員長	清水　孝雄	国立国際医療研究センター プロジェクト長 東京大学名誉教授
評 議 員	飯野　正光	東京大学ニューロインテリジェンス国際研究機構 特任教授 東京大学名誉教授
	川島　博行	元新潟大学大学院医歯学総合研究科 教授
	黒岩　常祥	日本学士院会員 東京大学名誉教授
	柴崎　正勝	微生物化学研究会 理事長 微生物化学研究所長 東京大学名誉教授
	中野　明彦	理化学研究所 光量子工学研究センター 副センター長 東京大学名誉教授
	鍋島　陽一	神戸医療産業都市推進機構 先端医療研究センター長 京都大学名誉教授
	藤本　豊士	順天堂大学大学院医学研究科 特任教授 名古屋大学名誉教授
	森　美和子	北海道大学名誉教授
	廣瀬　　徹	ノバルティス ファーマ株式会社 取締役 グローバル医薬品開発本部長

［選考委員］

2021年7月1日現在（敬称略）

職 名	氏 名	現　　職
選考委員長	伊藤　裕	慶應義塾大学 医学部 教授
選考委員	大嶋 孝志	九州大学 大学院薬学研究院 教授
	樗木 俊聡	東京医科歯科大学 難治疾患研究所 教授
	阪井 康能	京都大学 大学院農学研究科 教授
	富田 泰輔	東京大学 大学院薬学系研究科 教授
	豊島 文子	京都大学 ウィルス・再生医科学研究所 教授
	南野　徹	順天堂大学 大学院医学研究科 教授
	山田 泰広	東京大学 医科学研究所 教授
	家田 真樹	筑波大学 医学医療系 教授
	浦野 泰照	東京大学 大学院薬学系研究科 教授
	倉永英里奈	東北大学 大学院生命科学研究科 教授
	斎藤 通紀	京都大学 高等研究院 教授
	垣内 史敏	慶應義塾大学 理工学部 教授
	河崎 洋志	金沢大学 医学系 教授
	粂　昭苑	東京工業大学 生命理工学院 教授
	竹田　潔	大阪大学 大学院医学系研究科 教授
	中村 和弘	名古屋大学 大学院医学系研究科 教授
	東山 哲也	名古屋大学トランスフォーマティブ生命分子研究所 教授
	三宅 幸子	順天堂大学 大学院医学研究科 教授
	本橋ほづみ	東北大学 加齢医学研究所 教授

事 務 局 便 り

寄付のお願い

当財団は、自然科学における創造的な研究の奨励等を行うことにより、学術の振興を図り、国民の健康と福祉の向上に寄与することを目的に公益事業を行っております。

当財団の事業は、基本財産の運用益並びに寄付金によって賄われており、財団では趣旨にご賛同いただける皆様からのご寄付を募っております。

当財団へのご寄付には、下記の税法上の優遇措置が適用されます。

優遇措置の概略

個人：年間寄付金の合計額もしくは年間所得の40％相当額のいずれか低い方から2千円を引いた金額が、所得税の寄付金控除額となります。

法人：支出した寄付金は、通常一般の寄付金の損金算入限度額とは別枠で、下記の範囲内で損金の算入できます。

（資本金等の額×当期の月数/12×0.375%＋所得の金額×6.25%）÷2

ご寄付は、随時受付けております。詳しくは、財団事務局までお問合せください。

（E-メール：foundation.japan@novartis.com）

事務局より

2021年度もお陰様で財団年報を発行する運びとなりました。2020年の初めより、新型コロナウイルス感染症の影響で、いろんなことが”非日常”となり、その環境に対応するのに苦労しておりましたが、2年も近く経ちますと、何が日常で何が非日常だったのかがだんだんと区別がつかなくなってきました。10月になり、ワクチンの効果がでてきたせいでしょうか感染者数が急激に減ってきました。考えてみれば、このmRNAワクチンも、多くの基礎研究が積み上げられた結果であることに思いを致しております。

このような日常の中でも、当財団の事業である研究奨励金助成・研究集会助成事業に対して多くの応募があり、その中から選ばれた研究に助成が行われ、それぞれに成果を上げられていることを嬉しく思います。

当財団は1987年9月の財団設立以来、助成件数は総数で1854件、総額21億円を超えるものとなりました。当財団は、自然科学の創造的研究への助成によって、日本の学術発展に寄与することを目指しており、助成を受けられた研究成果がすぐに応用につながらなくとも、将来、新分野につながることを夢見て、この事業を継続して参ります。

今まで助成事業が継続できていることも、偏に、助成事業にご理解・ご支援をいただいた方々、助成を受けられて研究を継続された皆様および財団関係者のお力添えの賜物であると、心より感謝申し上げます。引き続きご指導、ご支援の程よろしくお願い申し上げます。

事務局長　原　健記

公益財団法人 ノバルティス科学振興財団
〒105-6333 東京都港区虎ノ門1-23-1
虎ノ門ヒルズ森タワー
TEL：03-6899-2100
E-メール：foundation.japan@novartis.com
ホームページ：http://japanfoundation.novartis.org/